AN INTRODUCTION TO DISCRETE DIFFERENTIAL GEOMETRY

EDITOR SEONG-DEOG YANG

ANAM LECTURE NOTES
IN MATHEMATICS
VOLUME 2

DEPARTMENT OF MATHEMATICS
KOREA UNIVERSITY

An introduction to discrete differential geometry

Editor Seong-Deog Yang

Editor
Seong-Deog Yang
Department of Mathematics
Korea University
sdyang@korea.ac.kr

Mathematics Subject Classification (2020): 53-01
Edited and Published by Department of Mathematics, Korea University
Published in February, 2020
This book was typeset using TEX and memoir class.

Preface

The three articles in this volume 2 of the *Anam Lecture Notes in Mathematics* are the results of the authors' ongoing efforts to deliver the contents of discrete differential geometry, which is a field in its nascence, to a broader audience after they presented the materials at the "Introductory Workshop on Discrete Differential Geometry", held at Korea University, January 21-24, 2019.

Rooted in the integrability of differentiable objects in geometry, discrete differential geometry is of deep mathematical interest, and has gained interest from prominent mathematicians around the world. Furthermore, it is a field that readily bridges the gap between pure mathematics and applications due to its connection to architecture, computer graphics, and crystal structures, to name a few. Since the field is relatively new, it is often difficult to find well presented introductory texts or lectures on discrete differential geometry. The aim of this volume is to provide any researcher or student with well-designed introductory materials on the basics of discrete differential geometry. I hope that the materials will be accessible and (hopefully) interesting to audience of wide mathematical background, from undergraduate students to active researchers.

Finally, I want to express my many thanks to Joseph Cho, who has devoted his valuable time and energy in making the workshop successful and this volume possible.

Seoul, Republic of Korea — Seong-Deog Yang

February, 2020

Contents

Chapter 1

A first step to two topics in discretizations of surfaces in Euclidean space

Masashi Yasumoto
Osaka City University Advanced Mathematical Institute, 3-3-138, Sugimoto, Sumiyoshi-ku, Osaka, 558-8585, Japan
yasumoto@sci.osaka-cu.ac.jp

Abstract

A new research field "Discrete Differential Geometry" is rapidly developing from various perspectives. In this note we briefly introduce two classes of surfaces with special condition, and introduce a first step to discretization of surfaces based on integrable systems approaches.

1 Introduction

The study of surfaces is classical in differential geometry. In particular, since surfaces with special curvature condition have various connections with other research fields, they are central topics on this subject. Some comprehensive references are [14], [20], [21], [23] for example.

Furthermore, the research on integrable systems has various connections with other research fields. For example, as will be seen later, the compatibility condition

S.-D. Yang (ed.), *An introduction to discrete differential geometry.*
Anam Lecture Notes in Mathematics Volume 2

for surfaces with constant negative Gaussian curvature is the sine-Gordon equation

$$\omega_{uv} = \frac{1}{\rho^2} \sin \omega,$$

where ω ia a real-valued function depending on two real variables u, v, and ρ is nonzero real constant. The sine-Gordon equation is a famous nonlinear integrable (solvable) equation discovered by Bour [7], and it is known as the first integrable equation. Now the sine-Gordon has applications to other contexts (see [1] for example).

However, although a large amount of works on integrable systems has been investigated, there is no unifying definition of integrable systems. Many researchers attempt to give a unified framework of the theory of integrable systems, and some common features are found (see [18] for example). Over the last three decades, an approach to understand integrable systems from differential and discrete geometric perspectives has been launched. For example, as already mentioned, the sine-Gordon equation originates from a problem of surfaces with constant negative Gaussian curvature, and a procedure to obtain a new solution to the sine-Gordon equation comes from a geometric observation. This procedure is now called the Bäcklund transformation, and it is one of the integrable transformations in the context of integrable systems. Furthermore, as will be discussed in Subsection 3.5, a sequence of Bäcklund transformations produces a discrete geometric structure. Therefore, geometry behind integrable systems plays a pivotal role in the subject. There are several monographs in this subject, for example, see [6], [15], [19].

In this note we introduce the following two classes of surfaces with special geometric condition to understand two papers by Bobenko, Pinkall [4], [5]:

(1) Surfaces with constant negative Gaussian curvature in Euclidean 3-space $\mathbb{R}^3$. Such surfaces are called the *K-surfaces*.

(2) Surfaces parametrized by conformal curvature line coordinates. Such surfaces are called the *isothermic surfaces*.

The spirit of discrete differential geometry is scattered into these papers, and they are relatively accessible to geometers or those who are interested in this subject. This survey article is devoted to the preparation to read these articles.

This note consists of two parts. The first part is devoted to the theory of K-surfaces, that is based on the author's lectures for master students at Osaka City University in Japanese academic year 2017. The second part briefly introduces

a theory of isothermic surfaces, that is based on the author's mini-lectures at Summer School 2018 in Fukuoka "Geometric shape generation" held at Kyushu University (September 10-14, 2018) and at the introductory workshop on discrete differential geometry held at Korea University (January 21-24, 2019).

Acknowledgements

The author would like to thank Professors Miyuki Koiso and Seong-Deog Yang for giving him great opportunities to explain introductory topics on the study of discrete differential geometry. In particular, Professor Seong-Deog Yang gave the author a chance to write a survey article of these lectures. The author hopes that this article would be helpful for students and researchers interested in this subject. Also, the author is grateful to Professor Wayne Rossman and Dr. Joseph Cho for enjoyable conversations on the article. This work was partly supported by the Grant-in-Aid for JSPS Fellows: Grant Number 26-3154, 19J02034, JSPS Grant-in-Aid for Scientific Research on Innovative Areas "Discrete Geometric Analysis for Materials Design": Grant Number 18H04489, and Osaka City University Advanced Mathematical Institute (MEXT Joint Usage/Research Center on Mathematics and Theoretical Physics).

2 Ingredients from differential geometry of surfaces

In this section we overview basic notions of differential geometry of surfaces in the 3-dimensional Euclidean space. Throughout this paper, the 3-dimensional Euclidean space with standard Euclidean metric $\langle \cdot, \cdot \rangle$ and the Euclidean norm $\| \cdot \|$ is denoted by $\mathbb{R}^3$. Let

$$\begin{array}{rccc} f: & D\ (\subset \mathbb{R}^2) & \to & \mathbb{R}^3 \\ & \cup & & \cup \\ & (u,v) & \mapsto & f(u.v) \end{array}$$

be an immersion of C^∞, and let $\nu : D \to \mathbb{S}^2 := \{x \in \mathbb{R}^3 \mid \|x\| = 1\}$ be its unit normal vector field defined by

$$\nu = \frac{f_u(u,v) \times f_v(u,v)}{\|f_u(u,v) \times f_v(u,v)\|} \quad \left(f_*(u,v) := \frac{\partial f}{\partial *},\ * = u, v \right).$$

The first and second fundamental fomrs I_f, II_f are expressed by

$$I_f = Edu^2 + 2Fdudv + Gdv^2, \quad II_f = Ldu^2 + 2Mdudv + Ndv^2$$

and the first and second fundamental matrices I, II are defined by

$$\mathrm{I} = \begin{pmatrix} E & F \\ F & G \end{pmatrix}, \quad \mathrm{II} = \begin{pmatrix} L & M \\ M & N \end{pmatrix}$$

where the coefficients of the first and second fundamental forms are defined by

$$E = \|f_u(u,v)\|^2,\ F = \langle f_u(u,v), f_v(u,v)\rangle,\ G = \|f_u(u,v)\|^2,$$
$$L = \langle f_{uu}(u,v), \nu\rangle,\ M = \langle f_{uv}(u,v), \nu\rangle,\ N = \langle f_{vv}(u,v), \nu\rangle$$
$$\left(f_{**}(u,v) = \frac{\partial^2 f}{\partial * \partial \star},\ *, \star = u, v \right).$$

Defining $S := \mathrm{I}^{-1}\mathrm{II}$, we define Gaussian and mean curvatures K_f, H_f of f by

$$K_f = \det(S), \quad H_f = \frac{1}{2}\mathrm{trace}(S),$$

and the eigenvalues κ_1, κ_2 of S are called the principal curvatures of f.

To investigate K-surfaces in $\mathbb{R}^3$ in the next section, we introduce the following fundamental theorem, that is now called the "Theorema Egregium" of Gauss.

Theorem 2.1. *The Gaussian curvature K_f of an immersion f can be expressed by only the coefficients of the first fundamental forms E, F, G, and their partial derivatives.*

Although the proof of this theorem can be found in various references (for example, [14], [23]), as an introductory article, we give an outline of the proof. Using the coefficients of first and second fundamental forms, we can express

$$f_{uu} = \Gamma^1_{11} f_u + \Gamma^2_{11} f_v + L\nu,$$
$$f_{uv} = \Gamma^1_{12} f_u + \Gamma^2_{12} f_v + M\nu,$$
$$f_{vv} = \Gamma^1_{22} f_u + \Gamma^2_{22} f_v + N\nu,$$

where Γ^i_{jk} $(i.j,k = 1,2)$ are the Christoffel symbols. The following lemma is immediate:

Lemma 2.2. *Γ^i_{jk} can be expressed by E, F, G, and their partial derivatives.*

Proof. Here we only see Γ^1_{11} and Γ^2_{11}. By definition of the coefficients of the first fundamental form, we can easily show that

$$\langle f_{uu}, f_u\rangle = \frac{E_u}{2},\ \langle f_{uv}, f_v\rangle = \frac{E_v}{2},\ \langle f_{uv}, f_v\rangle = \frac{G_u}{2},\ \langle f_{vv}, f_v\rangle = \frac{G_v}{2},$$
$$\langle f_{uu}, f_v\rangle = F_u - \frac{E_v}{2},\ \langle f_{vv}, f_v\rangle = F_u - \frac{G_u}{2}.$$

Substituting $f_{uu} = \Gamma^1_{11} f_u + \Gamma^2_{11} f_v + L\nu$ into the above equations, we have

$$\begin{cases} E\Gamma^1_{11} + F\Gamma^2_{11} = \dfrac{E_u}{2} \\ F\Gamma^1_{11} + G\Gamma^2_{11} = F_u - \dfrac{E_v}{2} \end{cases} \iff \begin{pmatrix} E & F \\ F & G \end{pmatrix} \begin{pmatrix} \Gamma^1_{11} \\ \Gamma^2_{11} \end{pmatrix} = \begin{pmatrix} \dfrac{E_u}{2} \\ F_u - \dfrac{E_v}{2} \end{pmatrix}$$

Thus we show that Γ^1_{11} and Γ^2_{11} can be expressed by E, F, G, and their partial derivatives. The others can be shown similarly, proving the lemma. □

We go back to a proof of Theorem 2.1. Consider the following conditions

$$(f_{uu})_v = (f_{uv})_u, \quad (f_{uv})_v = (f_{vv})_u\ .$$

Then we have

$$\begin{aligned} (f_{uu})_v &= (\Gamma^1_{11} f_u + \Gamma^2_{11} f_v + L\nu)_v \\ &= \{(\Gamma^1_{11})_v + \Gamma^1_{11}\Gamma^1_{12} + \Gamma^2_{11}\Gamma^1_{22} - Ls_{12}\} f_u \\ &\quad + \{(\Gamma^2_{11})_v + \Gamma^1_{11}\Gamma^2_{11} + \Gamma^2_{11}\Gamma^2_{22} - Ls_{22}\} f_v \\ &\quad + (M\Gamma^1_{11} + N\Gamma^2_{11} + L_v)\nu, \end{aligned}$$

where s_{ij} $(i, j = 1, 2)$ are defined by $\begin{pmatrix} s_{11} & s_{12} \\ s_{21} & s_{22} \end{pmatrix} = \mathrm{I}^{-1}\mathrm{II} = S$. Similarly,

$$\begin{aligned} (f_{uv})_u &= \{(\Gamma^1_{12})_u + \Gamma^1_{11}\Gamma^1_{12} + \Gamma^1_{12}\Gamma^2_{12} - Ms_{11}\} f_u \\ &\quad + \{(\Gamma^2_{12})_u + \Gamma^2_{11}\Gamma^1_{12} + (\Gamma^2_{12})^2 - Ms_{21}\} f_v \\ &\quad + (L\Gamma^1_{12} + M\Gamma^2_{12} + M_u)\nu. \end{aligned}$$

Since f_u, f_v, and ν are linearly independent, we have

$$(\Gamma^2_{11})_v + \Gamma^1_{12}\Gamma^2_{11} + \Gamma^2_{11}\Gamma^2_{22} - Ls_{22} = (\Gamma^2_{12})_u + \Gamma^2_{11}\Gamma^1_{12} + (\Gamma^2_{12})^2 - Ms_{21}$$

Substituting s_{21} and s_{22} explicitly into the above equation, we have

$$-\frac{E(LN-M^2)}{EG-F^2} = (\Gamma^2_{12})_u - (\Gamma^2_{11})_v + \Gamma^2_{11}\Gamma^1_{12} + (\Gamma^2_{12})^2 - \Gamma^1_{11}\Gamma^2_{12} - \Gamma^2_{11}\Gamma^2_{22}$$

$$\Leftrightarrow K_f = -\frac{1}{E}\{(\Gamma^2_{12})_u - (\Gamma^2_{11})_v + \Gamma^2_{11}\Gamma^1_{12} + (\Gamma^2_{12})^2 - \Gamma^1_{11}\Gamma^2_{12} - \Gamma^2_{11}\Gamma^2_{22}\}. \tag{2.1}$$

By Lemma 2.2, we can show that K_f can be expressed by E, F, G, and their partial derivatives, proving the Theorema Egregium of Gauss. Equation (2.1) is called the Gauss equation. Furthermore, comparing the coefficients of ν, we have that

$$L_v - M_u = L\Gamma^1_{12} + M(\Gamma^2_{12} - \Gamma^1_{11}) - N\Gamma^2_{11}. \tag{2.2}$$

Similarly, computing $(f_{uv})_v = (f_{vv})_u$ and comparing the coefficients of ν, we have that

$$M_v - L_u = L\Gamma^1_{22} + M(\Gamma^2_{22} - \Gamma^1_{12}) - N\Gamma^2_{12}\ . \tag{2.3}$$

Equations (2.2), (2.3) are called the Codazzi (or Codazzi-Mainardi) equations.

3 K-surfaces in $\mathbb{R}^3$

In this subsection we discuss K-surfaces in $\mathbb{R}^3$. They are classical geometric objects of interest. For example, a famous result is that no complete regular K-surface can be isometrically immersed into $\mathbb{R}^3$. Details can be found in [14]. Furthermore, an interesting geometric property is that K-surfaces admit special coordinates called the asymptotic Chebyshev coordinates. Choosing such special coordinates often produces integrable equations, and there exists special geometry behind certain integrable equation. In this sense, analyzing certain integrable system is equivalent to investigating the corresponding geometry. The interaction between geometries and integrable systems is called "integrable geometry". Deeper adventure of integrable geometry can be found in [6], [15] for example.

3.1 Asymptotic Chebyshev nets

It is well-known that surfaces with negative Gaussian curvature admit the following special coordinates. Existence of such coordinates can be found in [23] for example.

Theorem 3.1. *If K_f is negative (not necessarily constant), there exist asymptotic coordinates (u, v) such that $L = N = 0$.*

Henceforth, we assume that K_f is negative and f is parametrized by asymptotic coordinates (u, v). Admitting asymptotic coordinates makes our arguments much simpler. We define $\rho : D \to \mathbb{R}_{>0} := \{r \in \mathbb{R} |\ r > 0\}$ by

$$K = -\frac{M^2}{EG - F^2} =: -\frac{1}{\rho^2},$$

and we define two functions $a, b : D \to \mathbb{R}_{>0}$ by $a^2 := E/\rho^2$, $b^2 := G/\rho^2$. Set the angle $\omega(u, v)$ between two asymptotes, then

$$\mathrm{I} = \begin{pmatrix} \rho^2 a^2 & \rho^2 ab\cos\omega \\ \rho^2 ab\cos\omega & \rho^2 b^2 \end{pmatrix}, \quad \mathrm{II} = \begin{pmatrix} 0 & \rho ab\sin\omega \\ \rho ab\sin\omega & 0 \end{pmatrix} .$$

The Gauss equation (2.1) becomes

$$\omega_{uv} + \frac{1}{2}\left(\frac{\rho_u b}{\rho a}\sin\omega\right)_u + \frac{1}{2}\left(\frac{\rho_v a}{\rho b}\sin\omega\right)_v - ab\sin\omega = 0 . \tag{3.1}$$

Furthermore, the Codazzi equations (2.2), (2.3) become

$$\begin{cases} a_v(u,v) + \dfrac{\rho_v(u,v)}{2\rho(u,v)}a(u,v) - \dfrac{\rho_u(u,v)}{2\rho(u,v)}b(u,v)\cos\omega(u,v) = 0 , \\ b_u(u,v) + \dfrac{\rho_u(u,v)}{2\rho(u,v)}b(u,v) - \dfrac{\rho_v(u,v)}{2\rho(u,v)}a(u,v)\cos\omega(u,v) = 0 . \end{cases} \tag{3.2}$$

Now we assume that K_f is negative constant. Then Equation (3.2) becomes

$$a_v(u,v) = 0, \quad b_u(u,v) = 0 ,$$

implying that $a(u,v) = a(u)$ and $b(u,v) = b(v)$. This result indicates that the norms of $f_u(u,v)$ and $f_v(u,v)$ depends only on u and v, respectively. Furthermore, Equation (3.1) becomes

$$\omega_{uv}(u,v) - a(u)b(v)\sin\omega(u,v) = 0 . \tag{3.3}$$

Therefore, under the following reparametrization

$$du' = \sqrt{E(u)}du, \quad dv' = \sqrt{G(v)}dv ,$$

Equation (3.3) can be reduced to the famous sine-Gordon equation

$$\omega_{u'v'} - \frac{1}{\rho^2}\sin\omega = 0\ . \tag{3.4}$$

In conclusion, we have the following theorem:

Theorem 3.2. *A surface f parametrized by asymptotic coordinates (u, v) is a K-surface if and only if the norms of f_u and f_v depends only on u and v, respectively. Such asymptotic coordinates are called asymptotic Chebyshev coordinates, and a surface admitting asymptotic Chebyshev coordinates is called a Chebyshev net. Furthermore, the compatibility condition for K-surfaces can be chosen as the sine-Gordon equation (3.4).*

As typified by this result, existence of special coordinates characterizes differential geometry of surfaces behind certain integrability. This enables us to investigate integrabilities using the corresponding geometries, and possibly enables us to analyze and discover common features appearing in the research of integrable systems, unifying with all the schemes of the integrable systems.

Note that, even if we replace a with λa and b with $\lambda^{-1}b$ at the same time for some constant $\lambda \in \mathbb{R}_{>0}$, Equation (3.4) remains unchanged. This implies that the sine-Gordon equation admits one-parameter family of its solutions. Henceforth, without loss of generality, we may assume that $(u, v) = (u', v')$. As an application of the fundamental theorem for surfaces, we can construct one-parameter family f^λ of a K-surface in $\mathbb{R}^3$ with first and second fundamental forms being

$$I_{f^\lambda} = \lambda^2\rho^2a^2du^2 + 2\rho^2ab\cos\omega dudv + \lambda^{-2}\rho^2b^2dv^2,\ \ II_{f^\lambda} = 2\rho ab\sin\omega dudv. \tag{3.5}$$

3.2 2×2 Lax pairs for K-surfaces

In this section we introduce 2×2 matrix representations for K-surfaces that are called 2×2 Lax pairs. A key idea is to identify $\mathbb{R}^4$ with the set of quaternions $\mathbb{H}$. Let us denote

$$\mathbb{H} := \left\{ x_0 + x_1\mathbf{i} + x_2\mathbf{j} + x_3\mathbf{k} \;\middle|\; \begin{array}{l} x_j \in \mathbb{R}\ (i = 0, 1, 2, 3) \\ \mathbf{i}^2 = \mathbf{j}^2 = \mathbf{k}^2 = -1,\ \mathbf{ij} = \mathbf{k},\ \mathbf{jk} = \mathbf{i},\ \mathbf{ki} = \mathbf{j} \end{array} \right\}.$$

For an element $a = a_0 + a_1\mathbf{i} + a_2\mathbf{j} + a_3\mathbf{k} \in \mathbb{H}$, we define

$$\overline{a} := a_0 - a_1\mathbf{i} - a_2\mathbf{j} - a_3\mathbf{k},\ \ |a| := \sqrt{a\overline{a}},$$
$$\mathrm{Re}(a) := a_0,\ \ \mathrm{Im}(a) := a_1\mathbf{i} + a_2\mathbf{j} + a_3\mathbf{k},$$

In particular, $\mathbb{R}^3$ can be indentified with the set of imaginary quaternions

$$\mathrm{Im}\mathbb{H} := \{x_1\mathbf{i} + x_2\mathbf{j} + x_3\mathbf{k} \in \mathbb{H} \mid x_i \in \mathbb{R}\ (i = 1, 2, 3)\}$$

by the following identification:

$$\begin{array}{ccc} \mathbb{R}^3 & \cong & \mathrm{Im}\mathbb{H} \\ \cup & & \cup \\ x = (x_1, x_2, x_3)^t & \leftrightarrow & \hat{x} = x_1\mathbf{i} + x_2\mathbf{j} + x_3\mathbf{k} \end{array}$$

Set $x, y \in \mathbb{R}^3$ and the corresponding imaginary quaternions $\hat{x}, \hat{y} \in \mathrm{Im}\mathbb{H}$, respectively. For simplicity, $\hat{x} \times \hat{y}$ is denoted by the imaginary quaternionic value corresponding to $x \times y \in \mathbb{R}^3$. Then we can easily show that

$$\hat{x}\hat{y} = \hat{x} \times \hat{y} - \langle x, y\rangle.$$

In particular, using the above relation, we have $\hat{y}\hat{x} = \overline{\hat{x}\hat{y}}$, implying

$$\langle x, y\rangle = -\frac{1}{2}(\hat{x}\hat{y} + \hat{y}\hat{x}).$$

If readers are interested in surface geometry in terms of quaternionic forms, the author recommends to read [9] for example.

Hereinafter we further consider the 2×2 matrix forms of each element in $\mathbb{R}^3 \cong \mathrm{Im}\mathbb{H}$ to derive a 2×2 Lax pairs for K-surfaces. In the context of integrable systems (or solitons), such matrix representations are important, since large amount of solvable nonlinear partial differential integrable equations can be expressed by the compatibility conditions for systems of linear matrix-valued (not necessarily 2×2) linear differential equations. For the remaining part of this subsection, we derive 2×2 Lax pairs for K-surfaces. In the previous subsection, we had already seen the sine-Gordon equation (3.4). We will see that such equations can be derived by the compatibility condition for the Lax pairs explicitly.

Let us consider the identification between $\mathbb{H}$ and certain set of 2×2 matrices by identifying

$$1 \leftrightarrow I, \quad \mathbf{i} \leftrightarrow \begin{pmatrix} 0 & -\sqrt{-1} \\ -\sqrt{-1} & 0 \end{pmatrix}, \quad \mathbf{j} \leftrightarrow \begin{pmatrix} 0 & -1 \\ 1 & 0 \end{pmatrix}, \quad \mathbf{k} \leftrightarrow \begin{pmatrix} -\sqrt{-1} & 0 \\ 0 & \sqrt{-1} \end{pmatrix}$$

with the standard matrix multiplication, where I is the 2×2 identity matrix. In fact, we can easily show that

$$\begin{pmatrix} 0 & -\sqrt{-1} \\ -\sqrt{-1} & 0 \end{pmatrix}^2 = \begin{pmatrix} 0 & -1 \\ 1 & 0 \end{pmatrix}^2 = \begin{pmatrix} -\sqrt{-1} & 0 \\ 0 & \sqrt{-1} \end{pmatrix}^2 = -I,$$

$$\mathbf{ij} \leftrightarrow \begin{pmatrix} 0 & -\sqrt{-1} \\ -\sqrt{-1} & 0 \end{pmatrix} \begin{pmatrix} 0 & -1 \\ 1 & 0 \end{pmatrix} = \begin{pmatrix} -\sqrt{-1} & 0 \\ 0 & \sqrt{-1} \end{pmatrix} \leftrightarrow \mathbf{k},$$

$$\mathbf{jk} \leftrightarrow \begin{pmatrix} 0 & -1 \\ 1 & 0 \end{pmatrix} \begin{pmatrix} -\sqrt{-1} & 0 \\ 0 & \sqrt{-1} \end{pmatrix} = \begin{pmatrix} 0 & -\sqrt{-1} \\ -\sqrt{-1} & 0 \end{pmatrix} \leftrightarrow \mathbf{i},$$

$$\mathbf{ki} \leftrightarrow \begin{pmatrix} -\sqrt{-1} & 0 \\ 0 & \sqrt{-1} \end{pmatrix} \begin{pmatrix} 0 & -\sqrt{-1} \\ -\sqrt{-1} & 0 \end{pmatrix} = \begin{pmatrix} 0 & -1 \\ 1 & 0 \end{pmatrix} \leftrightarrow \mathbf{j}.$$

These equalities can be regarded as the same properties as quaternions. Thus we can consider the following identification:

$$\begin{array}{ccccc} (x_1, x_2, x_3)^t & \leftrightarrow & x_1\mathbf{i} + x_2\mathbf{j} + x_3\mathbf{k} & \leftrightarrow & \begin{pmatrix} -\sqrt{-1}x_3 & -\sqrt{-1}x_1 - x_2 \\ -\sqrt{-1}x_1 + x_2 & \sqrt{-1}x_3 \end{pmatrix} \\ \| & & \| & & \| \\ x & & \hat{x} & & X \end{array}$$

Thus each element $x \in \mathbb{R}^3$ can be identified with the element in the Lie algebra $\mathfrak{su}_2$ of a Lie group

$$\mathrm{SU}_2 := \left\{ \begin{pmatrix} a & b \\ -\bar{b} & \bar{a} \end{pmatrix} \in \mathbb{SL}_2(\mathbb{C}) \,\middle|\, a\bar{a} + b\bar{b} = 1 \right\}.$$

Using the matrix forms, the inner product $\langle x, y \rangle$ of x, y is calculated by

$$\langle x, y \rangle = -\frac{1}{4}\mathrm{trace}(XY + YX) = -\frac{1}{2}\mathrm{trace}(XY),$$

where X and Y are matrix forms corresponding to x and y, respectively. The advantage to use the matrix forms is that we are able to treat rotations of $\mathbb{R}^3$. In fact, the following result does hold.

Theorem 3.3. *For any $x \in \mathbb{R}^3$ and its corresponding matrix $X \in \mathfrak{su}_2$, let Φ be an element in SU_2. Then $\Phi X \Phi^{-1}$ corresponds to a vector $Ax \in \mathbb{R}^3$ for some $A \in \mathrm{SO}_3(\mathbb{R})$.*

Proof. This result can be derived by a direct computation, In fact, setting

$$\Phi = \begin{pmatrix} a_1 + \sqrt{-1}a_2 & b_1 + \sqrt{-1}b_2 \\ -b_1 + \sqrt{-1}b_2 & a_1 - \sqrt{-1}a_2 \end{pmatrix} \in \mathrm{SU}_2,$$

we have

$$\Phi X \Phi^{-1} = \begin{pmatrix} -\sqrt{-1}\tilde{x}_3 & -\sqrt{-1}\tilde{x}_1 - \tilde{x}_2 \\ -\sqrt{-1}\tilde{x}_1 + \tilde{x}_2 & \sqrt{-1}\tilde{x}_3 \end{pmatrix}$$

where $(\tilde{x}_1, \tilde{x}_2, \tilde{x}_3)^t = Ax$ with

$$A = \begin{pmatrix} a_1^2 - a_2^2 - b_1^2 + b_2^2 & -2a_1a_2 - 2b_1b_2 & 2a_1b_1 - 2a_2b_2 \\ 2a_1a_2 - 2b_1b_2 & a_1^2 - a_2^2 - b_1^2 + b_2^2 & 2a_2b_1 + 2a_1b_2 \\ -2a_1b_1 - 2a_2b_2 & 2a_2b_1 - a_1b_2 & a_1^2 + a_2^2 - b_1^2 - b_2^2 \end{pmatrix} \in \mathrm{SO}_3(\mathbb{R}),$$

proving the proposition. □

Our mission to describe 2×2 Lax pairs for one parameter family f^λ of a K-surface $f = f^1$ with first and second fundamental forms satisfying Equation (3.5). Henceforth, we regard f^λ as an element in $\mathfrak{su}_2$. Since the angle between f_u^λ and f_v^λ is ω, we can define a matrix $\Phi^\lambda(u, v) = \Phi^\lambda \in \mathrm{SU}_2$ so that

$$\begin{aligned} f_u^\lambda &= \lambda\rho a \Phi^\lambda \left\{ \cos\frac{\omega}{2} \begin{pmatrix} 0 & -\sqrt{-1} \\ -\sqrt{-1} & 0 \end{pmatrix} - \sin\frac{\omega}{2} \begin{pmatrix} 0 & -1 \\ 1 & 0 \end{pmatrix} \right\} (\Phi^\lambda)^{-1} \\ &= \lambda\rho a \Phi^\lambda \begin{pmatrix} 0 & -\sqrt{-1}e^{\sqrt{-1}\omega/2} \\ -\sqrt{-1}e^{-\sqrt{-1}\omega/2} & 0 \end{pmatrix} (\Phi^\lambda)^{-1}, \end{aligned} \tag{3.6}$$

$$\begin{aligned} f_v^\lambda &= \lambda^{-1}\rho b \Phi^\lambda \left\{ \cos\frac{\omega}{2} \begin{pmatrix} 0 & -\sqrt{-1} \\ -\sqrt{-1} & 0 \end{pmatrix} + \sin\frac{\omega}{2} \begin{pmatrix} 0 & -1 \\ 1 & 0 \end{pmatrix} \right\} (\Phi^\lambda)^{-1} \\ &= \lambda^{-1}\rho b \Phi^\lambda \begin{pmatrix} 0 & -\sqrt{-1}e^{-\sqrt{-1}\omega/2} \\ -\sqrt{-1}e^{\sqrt{-1}\omega/2} & 0 \end{pmatrix} (\Phi^\lambda)^{-1}, \end{aligned} \tag{3.7}$$

$$\nu^\lambda = \Phi^\lambda \begin{pmatrix} -\sqrt{-1} & 0 \\ 0 & \sqrt{-1} \end{pmatrix} (\Phi^\lambda)^{-1}.$$

Here we set

$$U^\lambda = \begin{pmatrix} U_{11} & U_{12} \\ U_{21} & U_{22} \end{pmatrix} := (\Phi^\lambda)^{-1}\Phi_u^\lambda, \quad V^\lambda = \begin{pmatrix} V_{11} & V_{12} \\ V_{21} & V_{22} \end{pmatrix} := (\Phi^\lambda)^{-1}\Phi_v^\lambda \ .$$

Since $\Phi^\lambda \in \mathrm{SU}_2$, U^λ and Y^λ must be trace-free. So we have

$$U_{11} + U_{22} = V_{11} + U_{22} = 0.$$

The condition $\langle f_u^\lambda, \nu_u^\lambda\rangle = 0$ and the calculation

$$\begin{aligned}\nu_u^\lambda &= \Phi_u^\lambda \begin{pmatrix} -\sqrt{-1} & 0 \\ 0 & \sqrt{-1}\end{pmatrix}(\Phi^\lambda)^{-1} + \Phi^\lambda \begin{pmatrix} -\sqrt{-1} & 0 \\ 0 & \sqrt{-1}\end{pmatrix}((\Phi^\lambda)^{-1})_u \\ &= \Phi^\lambda \begin{pmatrix} 0 & 2\sqrt{-1}U_{12} \\ -2\sqrt{-1}U_{21} & 0\end{pmatrix}(\Phi^\lambda)^{-1}\end{aligned}$$

imply that $\langle f_u^\lambda, \nu_u^\lambda\rangle = -\frac{1}{2}\mathrm{trace}(f_u^\lambda \nu_u^\lambda) = \lambda\rho a\{e^{\sqrt{-1}\omega/2}U_{21} - e^{-\sqrt{-1}\omega/2}U_{12}\} = 0$. Similarly, we can calculate

$$\begin{aligned}\langle f_v^\lambda, \nu_v^\lambda\rangle &= \lambda^{-1}\rho b\{e^{-\sqrt{-1}\omega/2}V_{21} - e^{\sqrt{-1}\omega/2}V_{12}\} = 0, \\ \langle f_u^\lambda, \nu_v^\lambda\rangle &= \lambda\rho a\{e^{\sqrt{-1}\omega/2}V_{21} - e^{-\sqrt{-1}\omega/2}V_{12}\} = -\rho ab\sin\omega, \\ \langle f_v^\lambda, \nu_u^\lambda\rangle &= \lambda^{-1}\rho b\{e^{-\sqrt{-1}\omega/2}U_{21} - e^{-\sqrt{-1}\omega/2}U_{12}\} = -\rho ab\sin\omega.\end{aligned}$$

Combining these conditions and the compatibility condition $(\Phi_u^\lambda)_v = (\Phi_v^\lambda)_u$, we have the 2×2 Lax pairs for K-surfaces.

Theorem 3.4. *We have* $\Phi_u^\lambda = \Phi^\lambda U^\lambda$, $\Phi_v^\lambda = \Phi^\lambda V^\lambda$, *where*

$$\begin{aligned}U^\lambda &= \begin{pmatrix} \frac{\omega_u}{4} & -\frac{\sqrt{-1}}{2}\lambda a e^{\sqrt{-1}\omega/2} \\ -\frac{\sqrt{-1}}{2}\lambda a e^{-\sqrt{-1}\omega/2} & -\frac{\omega_u}{4}\end{pmatrix}, \\ V^\lambda &= \begin{pmatrix} -\frac{\omega_v}{4} & \frac{\sqrt{-1}}{2}\lambda^{-1} b e^{-\sqrt{-1}\omega/2} \\ \frac{\sqrt{-1}}{2}\lambda^{-1} b e^{\sqrt{-1}\omega/2} & \frac{\omega_v}{4}\end{pmatrix}.\end{aligned} \tag{3.8}$$

Furthermore, a celebrating discovery by Sym [22] produces K-surfaces in $\mathbb{R}^3$ from solutions to Lax pairs (3.8) for K-surfaces. This is an advantage to treat surfaces using the 2×2 matrix forms.

Theorem 3.5. *Let* Φ^λ *be a solution to Equation* (3.8). *Then a surface*

$$f^\lambda(u,v) = 2\lambda\rho\frac{\partial\Phi^\lambda}{\partial\lambda}\cdot(\Phi^\lambda)^{-1}$$

is a K-surface satisfying Equations (3.6), (3.7). *This formula is called the* Sym formula.

Proof. By computation, we have

$$\begin{aligned} f_u^\lambda &= 2\lambda\rho \left\{ \left(\frac{\partial \Phi^\lambda}{\partial \lambda} \right)_u \cdot (\Phi^\lambda)^{-1} + \frac{\partial \Phi^\lambda}{\partial \lambda} \cdot ((\Phi^\lambda)^{-1})_u \right\} \\ &= \lambda\rho a \Phi^\lambda \begin{pmatrix} 0 & -\sqrt{-1}e^{\sqrt{-1}\omega/2} \\ -\sqrt{-1}e^{-\sqrt{-1}\omega/2} & 0 \end{pmatrix} (\Phi^\lambda)^{-1}, \\ f_v^\lambda &= 2\lambda\rho\Phi^\lambda \frac{\partial V^\lambda}{\partial \lambda} (\Phi^\lambda)^{-1} \\ &= \lambda^{-1}\rho b \Phi^\lambda \begin{pmatrix} 0 & -\sqrt{-1}e^{-\sqrt{-1}\omega/2} \\ -\sqrt{-1}e^{\sqrt{-1}\omega/2} & 0 \end{pmatrix} (\Phi^\lambda)^{-1}, \end{aligned}$$

proving the theorem. □

3.3 Bäcklund transformations of sine-Gordon equation and K-surfaces

In this subsection we introduce an application of differential geometry of K-surfaces to producing new solutions to the sine-Gordon equation from a given solution. Now such a procedure is called the Bäcklund transformation. Recently, Bäcklund transformations for many integrable equations are fundamental tools in integrable systems. Here, let us emphasize that this first discovery of the Bäcklund transformations is highly inspiring the theory of integrable systems, and the machinery of Bäcklund transformations completely comes from differential geometry of K-surfaces.

Our problem is to construct new K-surface from a given K-surface. Let f be a K-surface with $K_f = -1/\rho^2$ parametrized by asymptotic Chebyshev coordinates. Then $\hat{f}$ is called a Bäcklund transform of f if it satisfies the following three conditions:

- Each vector $\hat{f} - f$ is tangent to both f and $\hat{f}$.
- $\|\hat{f} - f\| = r$.
- The angle between ν and $\hat{\nu}$ is constant θ, that is, $\langle \nu, \hat{\nu} \rangle = \cos\theta$.

First, we construct a Bäcklund transform $\hat{f}$ of f. Since f is a K-surface parametrized by asymptotic Chebyshev coordinates, the triad $\{A, B, C\}$ of

$$A := f_u,\ B := -f_u \times \nu = -\cot\omega f_u + \sec\omega f_v,\ C := \nu$$

forms an orthonormal basis. One can check that

$$\begin{pmatrix} A & B & C \end{pmatrix}_u = \begin{pmatrix} A & B & C \end{pmatrix} \begin{pmatrix} 0 & \omega_u & 0 \\ -\omega_u & 0 & -1/\rho \\ 0 & 1/\rho & 0 \end{pmatrix},$$

$$\begin{pmatrix} A & B & C \end{pmatrix}_v = \begin{pmatrix} A & B & C \end{pmatrix} \begin{pmatrix} 0 & 0 & -\sin\omega/\rho \\ 0 & 0 & -\cos\omega/\rho \\ \sin\omega/\rho & -\cos\omega/\rho & 0 \end{pmatrix}.$$

With these conditions, set $\hat{f} := f + r(\cos\phi A + \sin\phi B)$. Then

$$\hat{f}_u = \{1 - r(\phi_u - \omega_u)\sin\phi\}A + r(\phi_u - \omega_u)\cos\phi B + \frac{r}{\rho}\sin\phi C,$$
$$\hat{f}_v = (\cos\omega - r\phi_v \sin\phi)A + (\sin\omega + r\phi_v\cos\phi)B + \frac{r}{\rho}\sin(\omega - \phi)C.$$

Requiring the condition $\|\hat{f}_u\| = \|\hat{f}_v\| = 1$ and setting

$$\beta = \frac{\rho}{r}\left(1 \pm \sqrt{1 - \frac{r^2}{\rho^2}}\right) = \frac{r}{\rho}\left(1 \mp \sqrt{1 - \frac{r^2}{\rho^2}}\right)^{-1},$$

we have

$$\begin{cases} \phi_u = \omega_u + \dfrac{\beta}{\rho}\sin\phi, \\ \phi_v = \dfrac{1}{\beta\rho}\sin(\phi - \omega). \end{cases} \tag{3.9}$$

Using these expressions, we have

$$I_{\hat{f}} = du^2 + 2\cos(2\phi - \omega)dudv + dv^2.$$

Furthermore, since the unit normal vector field $\hat{\nu}$ of $\hat{f}$ is expressed as

$$\hat{\nu} = -\frac{r}{\rho}\sin\phi A + \frac{r}{\rho}\cos\phi B + \left(1 - \frac{r\beta}{\rho}\right)C,$$

we have

$$II_{\hat{f}} = \frac{2}{\rho}\sin(2\phi - \omega)dudv.$$

Hence the resulting surface $\hat{f}$ is a K-surface with $K_{\hat{f}} = -\dfrac{1}{\rho^2}$, and we can check that the $\hat{f}$ satisfies the condition of Bäcklund transforms, that is,

$$\langle \hat{f} - f, \nu \rangle = \langle \hat{f} - f, \hat{\nu} \rangle = 0, \ \|\hat{f} - f\| = r, \ \langle \nu, \hat{\nu} \rangle = 1 - \frac{r\beta}{\rho}.$$

Finally, we rewrite Equation (3.9). Setting $\hat{\omega} := 2\phi - \omega$, we can check that $\hat{\omega}$ satisfies

$$\hat{\omega}_{uv} = \frac{1}{\rho^2} \sin \hat{\omega}.$$

And Equation (3.9) can be written as

$$(\mathbb{B}_\beta) \qquad \begin{cases} \left(\dfrac{\hat{\omega} - \omega}{2} \right)_u = \dfrac{\beta}{\rho} \sin \left(\dfrac{\hat{\omega} + \omega}{2} \right), \\ \left(\dfrac{\hat{\omega} + \omega}{2} \right)_v = \dfrac{1}{\beta\rho} \sin \left(\dfrac{\hat{\omega} - \omega}{2} \right). \end{cases}$$

Equation $(\mathbb{B}_\beta)$ is called the β-Bäcklund transformation, and we write $\hat{\omega} = \mathbb{B}_\beta(\omega)$. As already mentioned before, Bäcklund transformations produce new solutions to the sine-Gordon equation.

3.4 Bianchi permutability of Bäcklund transformations for the sine-Gordon equation

Here we introduce a permutability of Bäcklund transformations for the sine-Gordon equation, that is called the Bianchi permutability. The Bianchi permutability produces the fourth solution from a given solution and two distinct Bäcklund transforms of the given solution, that can be regarded as a nonlinear version of the superposition principle.

Theorem 3.6 (Bianchi Permutability)**.** *Let ω be a solution to the sine-Gordon equation (3.4), and let ω_1, ω_2 be two Bäcklund transforms given by*

$$\omega_1 := \mathbb{B}_{\beta_1}\omega, \quad \omega_2 := \mathbb{B}_{\beta_2}\omega.$$

Then there exists the fourth solution ω_{12} such that it is a β_2-Bäcklund tarnsform of ω_1 and is a β_1-Bäcklund tarnsform of ω_2 as well, that is,

$$\omega_{12} = \mathbb{B}_{\beta_2}\mathbb{B}_{\beta_1}\omega = \mathbb{B}_{\beta_1}\mathbb{B}_{\beta_2}\omega.$$

The Bianchi permutability indicates that the Bäcklund tarnsformations for the sine-Gordon equation (3.4) commutes and solutions to Equation (3.4) can be obtained diagramatically (see Figure 3.1).

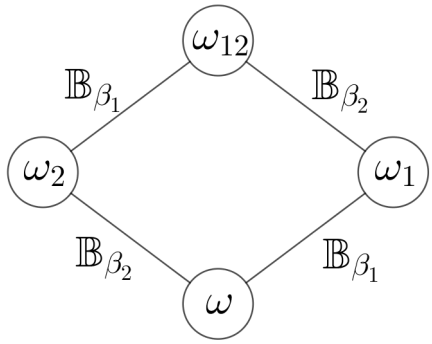

Figure 3.1: Bianchi permutability of the sine-Gordon equation

Here we prove the Bianchi permutability of the Bäcklund tarnsformations for the sine-Gordon equation (3.4). Let ω_{12} (resp. ω_{21}) be a β_2-Bäcklund transform (resp. β_1-Bäcklund transform) of ω_1 (resp. ω_2). By definition of Bäcklund tarnsformations, we have

$$(\omega_1)_u = \omega_u + \frac{2\beta_1}{\rho}\sin\left(\frac{\omega+\omega_1}{2}\right), \qquad (\omega_2)_u = \omega_u + \frac{2\beta_2}{\rho}\sin\left(\frac{\omega+\omega_1}{2}\right),$$
$$(\omega_{12})_u = (\omega_1)_u + \frac{2\beta_2}{\rho}\sin\left(\frac{\omega_1+\omega_{12}}{2}\right), (\omega_{21})_u = (\omega_2)_u + \frac{2\beta_1}{\rho}\sin\left(\frac{\omega_2+\omega_{21}}{2}\right).$$

Here we assume that $\omega_{12} = \omega_{21}$. Deforming the above equations, we have

$$\begin{aligned}
&\beta_1\left\{\sin\left(\frac{\omega+\omega_1}{2}\right) - \sin\left(\frac{\omega_2+\omega_{12}}{2}\right)\right\} \\
&\quad - \beta_2\left\{\sin\left(\frac{\omega+\omega_2}{2}\right) - \sin\left(\frac{\omega_1+\omega_{12}}{2}\right)\right\} = 0. \\
&\qquad \Longleftrightarrow 2\beta_1\cos\left(\frac{\omega+\omega_1+\omega_2+\omega_{12}}{4}\right)\sin\left(\frac{\omega+\omega_1-\omega_2-\omega_{12}}{4}\right) \\
&\qquad\qquad - 2\beta_2\cos\left(\frac{\omega+\omega_1+\omega_2+\omega_{12}}{4}\right)\sin\left(\frac{\omega+\omega_2-\omega_1-\omega_{12}}{4}\right) = 0.
\end{aligned}$$

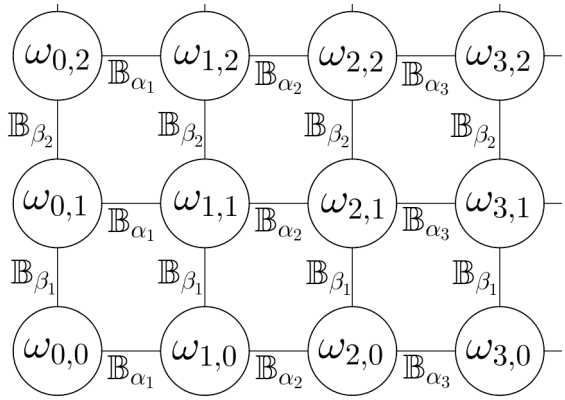

Figure 3.2: Bianchi lattice arising from Bianchi permutbilities of the sine-Gordon equation

Therefore, we have

$$\tan\left(\frac{\omega_{12}-\omega}{4}\right)=\frac{\beta_2+\beta_1}{\beta_2-\beta_1}\tan\left(\frac{\omega_2-\omega_1}{4}\right)$$
$$\Longrightarrow \omega_{12}=\omega+4\tan^{-1}\left(\frac{\beta_2+\beta_1}{\beta_2-\beta_1}\tan\left(\frac{\omega_2-\omega_1}{4}\right)\right).$$

Here we iterate Bianchi permutabilities as follows: Let ω be a solution to the sine-Gordon equation (3.4). Now we add the subscript $(0,0)$ to ω, and define the following sequence given by the following system

$$\omega_{(i,j)}=\mathbb{B}_{\alpha_i}\omega_{(i-1,j)},\ \omega_{(i,j)}=\mathbb{B}_{\beta_j}\omega_{(i,j-1)}\quad(\alpha_i,\beta_j\in\mathbb{R},\ (i,j)\in\mathbb{Z}^2) \tag{3.10}$$

so that the Bianchi permutabilities $\mathbb{B}_{\beta_j}\mathbb{B}_{\alpha_i}=\mathbb{B}_{\alpha_i}\mathbb{B}_{\beta_j}$ hold. For a fixed $(u,v)\in D$, $\omega_{(m,n)}$ can be regarded as a map from $\mathbb{Z}^2$ to $\mathbb{R}$. The lattice associated is called the Bianchi lattice (Figure 3.2).

Furthermore, by a similar argument, we can show the following theorem, that can be regarded as a higher dimensional version of the Bianchi permutability theorem.

Theorem 3.7 (Bianchi Cube)**.** *Let ω be a solution to Equation (3.4), let ω_i be β_i-Bäcklund transforms of ω $(i=1,2,3)$, and set $\omega_{ij}=\mathbb{B}_i\mathbb{B}_j\omega=\mathbb{B}_j\mathbb{B}_i\omega$*

$(i, j = 1, 2, 3)$. *Then there exists* ω_{123} *such that*

$$\omega_{123} = \mathbb{B}_3\omega_{12} = \mathbb{B}_2\omega_{13} = \mathbb{B}_1\omega_{23} \ .$$

The proof can be given in a similar way to the proof of the Bianchi permutability, so here we omit it. In conclusion, we can create a cube labelled with $\omega, \omega_1, \omega_2, \omega_3, \omega_{12}, \omega_{13}, \omega_{23}, \omega_{123}$ (Figure 3.3), and this can be regarded as a map from $\mathbb{Z}^3$ to $\mathbb{R}$. This cube is called the Bianchi cube.

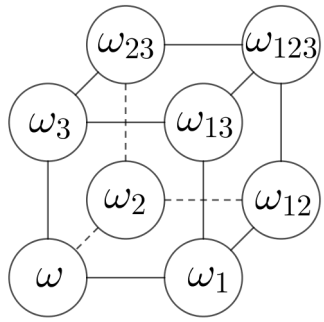

Figure 3.3: Bianchi lattice arising from Bianchi permutbilities of the sine-Gordon equation

Note that Bäcklund transformations are found in many nonlinear intergrable partial differential equations. A central topic on the study of integrable systems is to find Bäcklund transformations for nonlinear integrable equations.

3.5 Discrete geometric structure in Bianchi permutability

In this subsection we observe discrete geometric properties arising from the Bianchi permutability of Bäcklund transformations for the sine-Gordon equation. In the previous subsection, we saw that Bäcklund transformations produce the Bianchi lattice or cube.

As already mentioned, Bäcklund transformations produce new K-surfaces from a given K-surface. So it is natural to expect that there is a simple geometric relation between the original K-surface and its Bäcklund transforms. In fact, by construction of Bäcklund transforms, we have

$$\hat{f} - f = r\left\{\cos\left(\frac{\omega + \hat{\omega}}{2}\right)A + \sin\left(\frac{\omega + \hat{\omega}}{2}\right)B\right\}.$$

From this, we can show the following identity:

$$\hat{f} - f = \rho(\hat{\nu} \times \nu). \tag{3.11}$$

Applying Equation (3.11) to the Bianchi lattice, we have the following theorem.

Theorem 3.8. *Let f be a K-surface, and let f_1, f_2 be Bäcklund transforms of f given by $\omega_1 = \mathbb{B}_{\beta_1}$, $\omega_2 = \mathbb{B}_{\beta_2}\omega$, respectively. Then there exists the fourth surface f_{12} given by ω_{12}, and a quadrilateral (f, f_1, f_2, f_{12}) is a bent parallelogram, that is,*

$$\|f_1 - f\| = \|f_{12} - f_2\|, \quad \|f_2 - f\| = \|f_{12} - f_1\|, \tag{3.12}$$

but (f, f_1, f_2, f_{12}) is not necessarily coplanar. Furthermore, if we write a surface $f_{m,n}$ corresponding to $\omega_{m,n}$, the five points $f_{m,n}, f_{m+1,n}, f_{m,n+1}, f_{m-1,n}, f_{m,n-1}$ are coplanar.

Iterating the above procedure, we obtain a discrete surface $f_{m,n} : \mathbb{Z}^2 \to \mathbb{R}^3$ satisfying Theorem 3.8. Furthermore, we are also able to apply Theorem 3.8 to the Bianchi cube, we have a discrete map $f_{\ell,m,n} : \mathbb{Z}^3 \to \mathbb{R}^3$ such that the restriction of $f_{\ell,m,n}$ to the $\mathbb{Z}^2 \times \{0\}$, $\mathbb{Z} \times \{0\} \times \mathbb{Z}$, and $\{0\} \times \mathbb{Z}^2$ gives a Bianchi lattice of a K-surface.

Thus, a magic of the Bianchi permutbility can be easily understood by discrete geometric properties. In fact, at each point of f, f itself and four vertices adjacent to f are coplanar, and each quadrilateral (f, f_1, f_{12}, f_2) becomes a bent parallelogram. As typified by the seminal work by Bobenko, Pinkall [5], finding such discrete geometric structures and describing a discrete surface theory preserving such discrete discrete geometric structures (equivalently, discrete integrabilities) play pivotal roles in the study of discrete differential geometry.

4 Isothermic surfaces in $\mathbb{R}^3$

Stepping away from K-surfaces, in this section, we introduce isothermic surfaces in $\mathbb{R}^3$. To avoid confusion for readers, let us mention the terminology "isothermic". A similar terminology "isothermal" is used in a similar context. Isothermal immersions are the same as conformal immersions. On the other hand, isothermic surfaces are surfaces admitting conformal curvature line coordinates, that is, $f : D \to \mathbb{R}^3$ is an *isothermic surface* if it satisfies

$$I_f = E(du^2 + dv^2), \quad II_f = Ldu^2 + N^2dv^2.$$

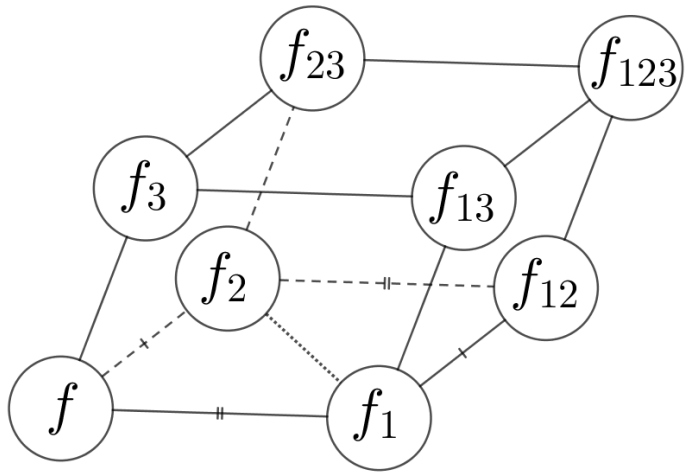

Figure 3.4: Bianchi cube of a K-surface. Each quadrilateral becomes a bent parallelogram, and it satisfies the same edge length condition.

We call such coordinates the isothermic coordinates. Such surfaces were at first discussed by Bour [7]. An important geometric property was given by Cayley [11], saying any isothermic surface is divisible into "infinitesimal" squares by their curvature lines. We will discuss this property in Subsection 4.4.

In contrast to the fact that any surface admits conformal coordinates or curvature line coordinates[1] (see [23] for example), all the surfaces do not necessarily admit isothermic coordinates. So we are interested in what surfaces are included in the class of isothermic surfaces.

When considering isothermic surfaces, it is convenient to use the complex coordinate $z = u + \sqrt{-1}v$. Here we use the following symbols

$$\frac{\partial f}{\partial z} = f_z := \frac{1}{2}\left(f_u - \sqrt{-1}f_v\right), \quad \frac{\partial f}{\partial \bar{z}} = f_{\bar{z}} := \frac{1}{2}\left(f_u + \sqrt{-1}f_v\right).$$
$$dz := du + \sqrt{-1}dv, \quad d\bar{z} := du - \sqrt{-1}dv.$$

A complex-valued function $G = G(z, \bar{z})$ is holomorphic if $G_{\bar{z}} = 0$, that is, $G = G(z)$. Let us begin with the following fact (see [3]):

[1] In this case we exclude umbilic points. Umbilic points are points where two principal curvatures of f coincide.

Proposition 4.1. *Let f be a conformal immersion satisfying $I_f = E(du^2 + dv^2)$. Then f is isothermic if and only if the coefficient of Hopf differential*

$$Q(u,v) = Q(z,\bar{z}) := \langle f_{zz}, \nu \rangle = \frac{1}{4}(L - N - 2\sqrt{-1}M)$$

can be chosen as a real-valued function. More generally, a surface is isothermic if and only if there exists a holomorphic quadratic differential $h(z)dz^2$ such that

$$Q(z,\bar{z}) = h(z)R(z,\bar{z}),$$

where $R(z,\bar{z})$ is a real-valued function.

The proof is immediate. In fact, defining a new complex coordinate w by

$$dw = \sqrt{h(z)}dz,$$

we have an isothermic immersion. Thus, to show the isothermicity, we only have to check that the corresponding Hopf differential satisfies the above condition. Here we see several examples of isothermic surfaces.

Example 4.2. Away from singular points (points where $\operatorname{rank}(df) < 2$), every surface of revolution is isothermic. In this case we only have to reparametrize a profile curve so that a surface becomes isothermic. Similarly, every quadric is isothermic.

Example 4.3. Away from umbilic points, every minimal and surface with nonzero constant mean curvature (CMC surfaces, for short) is isothermic. In fact, if we start from a conformal minimal or CMC immersion into $\mathbb{R}^3$, we know that the corresponding Hopf differential becomes holomorphic.

Other classes of isothermic surfaces are introduced in [3]. As typified by these examples, isohermic surfaces contain important classes of surfaces.

4.1 Möbius invariance of isothermicities

Isothermic surfaces have the following property that is essential when describing a discretization of isothermic surfaces.

Theorem 4.4. *Let f be an isothermic surface, and $M : \mathbb{R}^3 \to \mathbb{R}^3$ be a Möbius transformation of $\mathbb{R}^3$. Then $M \circ f$ is also isothermic.*

The above result implies that isothermicity is preserved under Möbius transformation. The Möbius transformation of $\mathbb{R}^3$ consists of translations, dilations, rotations, and inversions. Here we outline the proof of Theorem 4.4. If M is a translation, dilation, or rotation, the proof is immediate. So we only consider only the case that M is an inversion, that is, we consider

$$M \circ f = \frac{f}{\|f\|^2}.$$

Then we can easily check that

$$(M \circ f)_u = \frac{\|f\|^2 f_u - 2\langle f, f_u\rangle f}{\|f\|^4}, \quad (M \circ f)_v = \frac{\|f\|^2 f_v - 2\langle f, f_v\rangle f}{\|f\|^4},$$

implying that $I_{M\circ f} = \|f\|^{-4} I_f$. Futhermore, the remaining task is to show that $(M \circ f)_{uv} \in \operatorname{span}\{(M \circ f)_u, (M \circ f)_v\}$. A direct computation show that

$$(M \circ f)_{uv} = -\frac{4\langle f, f_v\rangle}{\|f\|^2}(M \circ f)_u + \frac{2\langle f, f_v\rangle f_u - 2\langle f, f_u\rangle f_v - 2\langle f, f_{uv}\rangle f + \|f\|^2 f_{uv}}{\|f\|^4}.$$

Since f is isothermic, f_{uv} can be expressed as $f_{uv} = c_1 f_u + c_2 f_2$ for some $c_1, c_2 \in \mathbb{R}$. Substituting f_{uv} into the above equation, we have

$$(M \circ f)_{uv} = \left(c_1 - \frac{2\langle f, f_v\rangle}{\|f\|^2}\right)(M \circ f)_u + \left(c_2 - \frac{2\langle f, f_u\rangle}{\|f\|^2}\right)(M \circ f)_v,$$

proving the theorem.

More generally, we are able to extend this result to 3-dimensional spaces that are conformal to $\mathbb{R}^3$ (for example, spherical 3-space and hyperbolic 3-space), leading us to the natural idea to describe a unified description of isothermic surfaces in conformal geometry. An elementary introduction to surface theory in conformal geometry is introduced by Cho-Rossman's article in this volume.

4.2 Cross ratio of four points in space

As shown in Theorem 4.4, isothermicity is Möbius invariant. We further discuss a characterization of isothermic surfaces in $\mathbb{R}^3$ in terms of Möbius invariant flavors. For this, we introduce a notion of cross ratio of four points in space. In this subsection, we identify each element in $\mathbb{R}^3$ with element in $\mathfrak{su}_2$ (see Subsection 3.2).

Definition 4.5. Let A, B, C, D be points in $\mathbb{R}^3 \cong \mathfrak{su}_2$. Then a pair $\{q, \bar{q}\}$ ($q \in \mathbb{C}$) of the eigenvalues of the following matrix

$$Q(A, B, C, D) := (A - B) \cdot (B - C)^{-1} \cdot (C - D) \cdot (D - A)^{-1}$$

is called the cross ratio of A, B, C, D.

Henceforce, we write exactly one of the eigenvalues q as $q := cr(A, B, C, D)$, and we call $cr(A, B, C, D)$ the cross ratio of A, B, C, D. This is a generalization of the standard cross ratio of four points on the complex plane. An important fact is that the cross ratio of four points in space is also Möbius invariant. Furthermore, the following proposition holds.

Proposition 4.6. *Let A, B, C, D be points in $\mathbb{R}^3$, and let $cr(A, B, C, D)$ be the cross ratio of A, B, C, D. Then $cr(A, B, C, D)$ is nonzero real if and if A, B, C, D are concircular or they lie on a line.*

The proof can be directly shown. Here we only see a sketch of the proof. Since A, B, C, D are points in $\mathbb{R}^3$, there exists a sphere passing through these four points. By Möbius transformations, this sphere can be regarded as $\mathbb{S}^2$, and A, B, C, D can be projected to $\mathbb{C}$. Thus Proposition 4.6 can be shown directly from the standard cross ratio property.

4.3 Christoffel transformations for isothermic surfaces

Here we introduce a geometric integrable transformation for isothermic surfaces called the Christoffel transformation.

Definition 4.7. Let $f : D \to \mathbb{R}^3$ be an isothermic surface. Then there exists an isothermic surfaces $f^* : D \to \mathbb{R}^3$ such that

$$f^*_u = \frac{f_u}{\|f_u\|^2}, \quad f^*_v = -\frac{f_v}{\|f_v\|^2} \quad \left(\Leftrightarrow df^* = \frac{f_u}{\|f_u\|^2} du - \frac{f_v}{\|f_v\|^2} dv\right)$$

holds. The new surface f^* is called a Christoffel transform of f. We write $f^* := \mathcal{C}f$, and $\mathcal{C}$ is called the Christoffel transformation.

The original definition of Christoffel transforms is as follows: Let f be an isothermic surface in $\mathbb{R}^3$. Then f^* is a Christoffel transform of f if

- f^* is defined on the same domain as f,

- f^* has the same conformal structure as f,
- f and f^* have parallel tangent planes with opposite orientations at corresponding points.

On the other hand, we can show that Christoffel transforms in Definition 4.7 satisfy the above conditions, if f^* exists. Furthermore, any Christoffel transform of an isothermic surface can be expressed as in Definition 4.7 and df^* can be also expressed as

$$df^* = \rho(d\nu + H_f df),$$

where $\rho = \rho(u, v)$ is a non zero real-valued function, and $(f^*)^* = f$. Here we use Definition 4.7 as the definition of Christoffel transforms. Details can be found in [15], [12] for example.

The existence of the Christoffel transform of an isothermic surface can be easily shown. In fact, we only have to check the compatibility condition $(f^*_u)_v = (f^*_v)_u$. On the other hand, the converse also holds.

Theorem 4.8. *Isothermicity of a surface is equivalent to the existence of the Christoffel transform.*

As already mentioned, showing one direction is immediate. On the other hand, showing the other direction, that is, it is not trivial to show the existence of isothermic coordinates under the assumption of the existence of the Christoffel transform. Here we only see a sketch of the proof:

- Assume that f is parametrized by curvature line coordinates.
- By the above assumption, the Codazzi equations (2.2), (2.3) can be simplified as

$$2(\kappa_1)_u = \frac{G_u}{G}(\kappa_1 - \kappa_2), \quad 2(\kappa_2)_v = \frac{E_v}{E}(\kappa_2 - \kappa_1), \tag{4.1}$$

  where κ_1, κ_2 are principal curvatures of f.
- Using the existence of the Christoffel transforms, and $\rho_{uv} = \rho_{vu}$, and Equations (4.1), finally we have

$$\left(\log \frac{E}{G}\right)_{uv} = 0,$$

implying that there exist positive real-valued function $a = a(u)$ and $b = b(v)$ depending only on u and v, respectively, so that

$$(a(u))^2 E = (b(v))^2 G.$$

4.4 Characterizing isothermic surfaces using cross ratio

Here we characterize isothermic surfaces using the cross ratio in space. As already shown in Theorem 4.4, isothermicity is preserved under Möbius transformation. Furthermore, cross ratio in space is also preserved under Möbius transformations. So it is natural to expect that there is certain relation between isothermic surfaces and the cross ratio.

First we see an equivalent condition for surfaces to be isothermic. Away from umbilic points, we can choose curvature line coordinates (u, v), that is, the first and second fundamental forms satisfy

$$I_f = Edu^2 + Gdv^2, \quad II_f = Ldu^2 + Ndv^2.$$

Then we can stretch the curvature line coordinates $(\tilde{u}, \tilde{v}) := (\tilde{u}(u), \tilde{v}(v))$, where $\tilde{u} = \tilde{u}(u)$ and $\tilde{v} = \tilde{v}(v)$ depend only on u and v, respectively, and $\tilde{u}$ and $\tilde{v}$ are strictly monotone functions on u and v, respectively. One can easily check that $(\tilde{u}, \tilde{v})$ are also curvature line coordinates. Then the surface f is isothermic if and only if there exists curvature line coordinates $(\tilde{u}, \tilde{v})$ so that they are also isothermic coordinates, that is, $\|f_{\tilde{u}}\|^2 = \|f_{\tilde{v}}\|^2$. By direct computation, we have

$$\left(\frac{du}{d\tilde{u}}\right)^2 E = \left(\frac{dv}{d\tilde{v}}\right)^2 G \;\Leftrightarrow\; \frac{E}{G} = \frac{\alpha(u)}{\beta(v)} \quad \left(\alpha(u) = \left(\frac{d\tilde{u}}{du}\right)^2,\ \beta(v) = \left(\frac{d\tilde{v}}{dv}\right)^2\right).$$

As already mentioned, Cayley found that any isothermic surface is divisible into "infinitesimal" squares by their curvature lines. Here we characterize this property using the cross ratio. Let f be an isothermic surface. Now we consider the cross ratio of the four points $f(u, v), f(u + \epsilon, v), f(u + \epsilon, v + \epsilon), f(u, v + \epsilon)$ for some ϵ

that is sufficiently close to 0. By the Taylor expansion, we have

$$\begin{aligned} f(u+\epsilon, v) &= f(u,v) + \frac{\epsilon}{1!} f_u(u,v) + \frac{\epsilon^2}{2!} f_{uu}(u,v) + \mathcal{O}(\epsilon^3), \\ f(u+\epsilon, v+\epsilon) &= f(u,v) + \frac{\epsilon}{1!}(f_u(u,v) + f_v(u,v)) \\ &\quad + \frac{\epsilon^2}{2!}(f_{uu}(u,v) + 2f_{uv}(u,v) + f_{vv}(u,v)) + \mathcal{O}(\epsilon^3), \\ f(u, v+\epsilon) &= f(u,v) + \frac{\epsilon}{1!} f_v(u,v) + \frac{\epsilon^2}{2!} f_{vv}(u,v) + \mathcal{O}(\epsilon^3). \end{aligned}$$

Using them, we can check that

$$\lim_{\epsilon \to 0} cr(f(u,v), f(u+\epsilon, v), f(u+\epsilon, v+\epsilon), f(u, v+\epsilon)) = -\frac{E}{G}.$$

In particular, isothermicity can be characterized as follows:

Theorem 4.9. *Let f be a surface parametrized by curvature line coordinates (u, v). Then f is an isothermic surface if and only if*

$$\lim_{\epsilon \to 0} cr(f(u,v), f(u+\epsilon, v), f(u+\epsilon, v+\epsilon), f(u, v+\epsilon)) = -\frac{\alpha(u)}{\beta(v)},$$

where $\alpha(u)$ and $\beta(v)$ are positive real-valued functions depending only on u and v, respectively.

4.5 Application of Christoffel transformations for isothermic surfaces

In the previous subsection, we briefly discussed Christoffel transformations of isothermic surfaces. Here we apply Christoffel transformations to isothermic minimal surfaces in $\mathbb{R}^3$. As already mentioned, away from umbilic points, any minimal surface is isothermic. Furthermore, the following property is known.

Theorem 4.10. *Let f be an isothermic surface in $\mathbb{R}^3$. Then f is an isothermic minimal surface if and only if f^* can be chosen as the Gauss map ν of f.*

In this article, we omit the proof of Theorem 4.10. Details can be found in [15] for example. Using this fact, we derive a Weierstrass representation for isothermic minimal surfaces in $\mathbb{R}^3$. Choose a holomorphic function $g = g(z)$, and take the

inverse image of the stereographic projection

$$\mathbb{C} \ni g \mapsto \nu := \left(\frac{2\mathrm{Re}(g)}{1+|g|^2}, \frac{2\mathrm{Im}(g)}{1+|g|^2}, \frac{-1+|g|^2}{1+|g|^2} \right)^t \in \mathbb{S}^2 \subset \mathbb{R}^3.$$

Since g is holomorphic, ν is also isothermic, and

$$\|\nu_u\|^2 = \frac{4|g_u|^2}{(1+|g|^2)^2} = \frac{4|g_v|^2}{(1+|g|^2)^2} = \|\nu_v\|^2.$$

Taking the Christoffel transform of ν, we have

$$f_u = \frac{\nu_u}{\|\nu_u\|^2} = \frac{1}{2}\mathrm{Re}\left(\frac{1+g^2}{g_u}, \frac{\sqrt{-1}(1-g^2)}{g_u}, \frac{2g}{g_u} \right)^t,$$
$$f_v = -\frac{\nu_v}{\|\nu_v\|^2} = -\frac{1}{2}\mathrm{Re}\left(\frac{1+g^2}{g_v}, \frac{\sqrt{-1}(1-g^2)}{g_v}, \frac{2g}{g_v} \right)^t.$$

Finally we can derive a Weierstrass representation for isothermic minimal surfaces:

Theorem 4.11. *Any isothermic minimal surface f can be described by*

$$f = \mathrm{Re}\left(\int \left(\frac{1+g^2}{g'}, \frac{\sqrt{-1}(1-g^2)}{g'}, \frac{2g}{g'} \right)^t dz \right) \quad (z = u + \sqrt{-1}v,\ g' = g_z),$$

where g is a holomorphic function.

4.6 Darboux transformations of isothermic surfaces

In this subsection we introduce another famous integrable transformation called the Darboux transformation. Similarly to the case of Bäcklund transformation for K-surfaces (see Section 3), Darboux [13] discovered a new geometric transformation for isothermic surfaces, and Bianchi [2] showed that the Bianchi permutability of Darboux transformations also holds. First we start from the original definition of Darboux transforms and transformations. Let f be an isothermic surface. Then $\hat{f}$ is called the Darboux transform of f if

- there exists a sphere congruence enveloped by the original surface f and the transform $\hat{f}$,
- the correspondence, given by the sphere congruence, from the original surface to the other enveloping surface, preserves curvature lines, and

- this correspondence preserves conformality, that is, f and $\hat{f}$ are conformally equivalent.

Writing $\hat{f} := \mathcal{D}f$, we call $\mathcal{D}$ the Darboux transformation of f.

After about 100 years passed since Darboux transformations for isothermic surfaces were defined, a great discovery was given by Hertrich-Jeromin, Pedit [17] using the quaternionic calculus. This implies that the definition of Darboux transformations for isothermic surfaces is equivalent to the following property, that we adopt as the definition of Darboux transformtions for isothermic surfaces:

Definition 4.12 (and Theorem)**.** Let f be an isothermic surface in $\mathbb{R} \cong \mathrm{Im}\mathbb{H}$, and let f^* be its Christoffel transform. Then $\hat{f}^\lambda$ $(\lambda \in \mathbb{R} \setminus \{0\})$ is the λ-Darboux transform of f if $\hat{f}^\lambda$ satisfies

$$d\hat{f} = \lambda(\hat{f} - f)df^*(\hat{f} - f),$$

and we write $\hat{f}^\lambda := \mathcal{D}_\lambda f$.

In the next subsection, this description enables us to show the Bianchi permutability of Darboux transformations. Here we calculate the Christoffel transform $(\hat{f}^\lambda)^*$ of $\hat{f}^\lambda$. By definition, we have

$$\begin{aligned} d(\hat{f}^\lambda) = \lambda(\hat{f}^\lambda - f)df^*(\hat{f}^\lambda - f) \\ \iff (\hat{f}^\lambda)_u du + (\hat{f}^\lambda)_v dv = \lambda(\hat{f}^\lambda - f)\left(\frac{f_u}{\|f_u\|^2}du - \frac{f_v}{\|f_v\|^2}dv\right)(\hat{f}^\lambda - f). \end{aligned}$$

Thus $(\hat{f}^\lambda)^*$ satisfies

$$\begin{aligned} ((\hat{f}^\lambda)^*)_u &= \left\{\lambda(\hat{f}^\lambda - f)\frac{f_u}{\|f_u\|^2}(\hat{f}^\lambda - f)\right\} \Big/ \left\|\lambda(\hat{f}^\lambda - f)\frac{f_u}{\|f_u\|^2}(\hat{f}^\lambda - f)\right\|^2 \\ &= \lambda^{-1}\frac{(\hat{f}^\lambda - f)f_u(\hat{f}^\lambda - f)}{\|\hat{f}^\lambda - f\|^4} = \lambda_i^{-1}(\hat{f}^\lambda - f)^{-1}f_u(\hat{f}^\lambda - f)^{-1}. \end{aligned}$$

Similarly, we have $((\hat{f}^\lambda)^*)_v = \lambda^{-1}(\hat{f}^\lambda - f)^{-1} f_v (\hat{f}^\lambda - f)^{-1}$. So we have

$$\begin{aligned} d(\hat{f}^\lambda)^* &= \lambda^{-1}(\hat{f}^\lambda - f)^{-1} df (\hat{f}^\lambda - f)^{-1} \\ &= \lambda^{-1}(\hat{f}^\lambda - f)^{-1}(d\hat{f}^\lambda - d\hat{f}^\lambda + df)(\hat{f}^\lambda - f)^{-1} \\ &= \lambda^{-1}(\hat{f}^\lambda - f)^{-1}\{d\hat{f}^\lambda + (\hat{f}^\lambda - f)\cdot d(\hat{f}^\lambda - f)\cdot(\hat{f}^\lambda - f)\}(\hat{f}^\lambda - f)^{-1} \\ &= \lambda^{-1}\{(\hat{f}^\lambda - f)^{-1} d\hat{f}^\lambda (\hat{f}^\lambda - f)^{-1} + d(\hat{f}^\lambda - f)^{-1}\} \\ &= df^* + \lambda^{-1} d(\hat{f}^\lambda - f)^{-1}. \end{aligned}$$

Setting

$$(\hat{f}^\lambda)^* := f^* + \frac{1}{\lambda}(\hat{f}^\lambda - f)^{-1}, \tag{4.2}$$

we can check that $(\hat{f}^\lambda)^*$ is the Christoffel transform of $\hat{f}^\lambda$.

4.7 Bianchi permutability of Christoffel and Darboux transformations

In the previous subsection, we derived the Christoffel transform of the Darboux transform of an isothermic surface f. From this, we can easily show the following permutability.

Theorem 4.13. *Let f be an isothermic surface in $\mathbb{R}^3$, let f^* be its Christoffel transform, and let $\hat{f}^\lambda$ be the λ-Darboux transform of f. Then there exists a surface $(\hat{f}^\lambda)^*$ in Equation (4.2) so that it is the Darboux transform of f^*, and the Christoffel transform of $\hat{f}$ as well, that is,*

$$(\hat{f}^\lambda)^* = \mathcal{D}_\lambda \mathcal{C} f = \mathcal{C}\mathcal{D}_\lambda f$$

holds.

The half of this theorem was already proven. In fact, we showed that $(\hat{f}^\lambda)^*$ in Equation (4.2) is the Christoffel transform of $\hat{f}^\lambda$. The remaining task is to show that it is the λ-Darboux transform of f^*. By Equation (4.2), we have

$$\begin{aligned} d(\hat{f}^\lambda)^* &= \lambda^{-1}(\hat{f}^\lambda - f)^{-1} df (\hat{f}^\lambda - f)^{-1} \\ &= \lambda^{-1}\cdot\lambda((\hat{f}^\lambda)^* - f^*)\cdot d(f^*)^*\cdot\lambda((\hat{f}^\lambda)^* - f^*) \\ &= \lambda((\hat{f}^\lambda)^* - f^*) d(f^*)^* ((\hat{f}^\lambda)^* - f^*), \end{aligned}$$

proving the theorem. Thus, like the Bianchi permutability of the sine-Gordon equation, a diagram in Figure 4.1 holds.

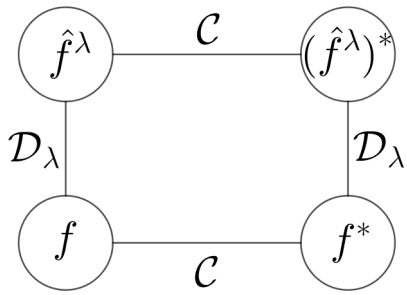

Figure 4.1: Bianchi permutability of Christoffel and Darboux transformations for isothermic surfaces

4.8 Bianchi permutability of Darboux transformations

In this subsection we introduce Bianchi permutability of Darboux transfomations for isothermic surfaces. The Bianchi permutability for Darboux transformations states the following:

Theorem 4.14. *Let f be an isothermic surface in $\mathbb{R}^3 \cong \mathrm{Im}\mathbb{H}$, and let $\hat{f}_i = \mathcal{D}_i f$ $(i = 1, 2)$ be λ_i-Darboux transforms of f. Then there exists $\hat{f}_{12}$ so that it is the λ_2-Darboux transform of $\hat{f}_1$, and λ_1-Darboux transform of $\hat{f}_2$ as well, that is,*

$$\hat{f}_{12} = \mathcal{D}_2\mathcal{D}_1 f = \mathcal{D}_1\mathcal{D}_2 f.$$

holds. Furthermore, $\hat{f}_{12}$ satisfies

$$cr(f, \hat{f}_1, \hat{f}_{12}, \hat{f}_2) = \frac{\lambda_2}{\lambda_1}. \tag{4.3}$$

Proof. First we check that $\hat{f}_{12}$ given by Equation (4.3) is the λ_1-Darboux transform of $\hat{f}_2$ under the assumption that $\hat{f}_{12}$ is the λ_2-Darboux transform of $\hat{f}_1$. We will check later that this assumption does hold. By definition, we have

$$\begin{aligned} d\hat{f}_{12} &= \lambda_2(\hat{f}_{12} - \hat{f}_1)d\hat{f}_1^*(\hat{f}_{12} - \hat{f}_1) \\ &= \frac{\lambda_2}{\lambda_1}(\hat{f}_{12} - \hat{f}_1)(\hat{f}_1 - f)^{-1}df(\hat{f}_1 - f)^{-1}(\hat{f}_{12} - \hat{f}_1) \end{aligned}$$

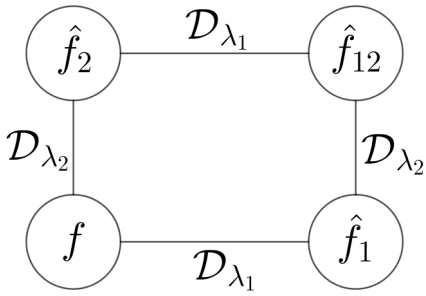

Figure 4.2: Bianchi permutability of Darboux transformations for isothermic surfaces

Since $cr(f, \hat{f}_1, \hat{f}_{12}, \hat{f}_2) = \lambda_2/\lambda_2$ and $\hat{f}_1 - f, \hat{f}_2 - f \in \mathrm{Im}\mathbb{H}$, we have

$$(\hat{f}_1 - f)^{-1}(\hat{f}_{12} - \hat{f}_1) = \frac{\lambda_1}{\lambda_2}(\hat{f}_2 - f)^{-1}(\hat{f}_{12} - \hat{f}_2).$$

So we have

$$\begin{aligned} d\hat{f}_{12} &= \frac{\lambda_2}{\lambda_1}\left\{\frac{\lambda_2}{\lambda_1}(\hat{f}_2 - f)(\hat{f}_{12} - \hat{f}_2)^{-1}\right\}^{-1} df \frac{\lambda_1}{\lambda_2}(\hat{f}_2 - f)^{-1}(\hat{f}_{12} - \hat{f}_2) \\ &= \frac{\lambda_1}{\lambda_2}(\hat{f}_{12} - \hat{f}_2)(\hat{f}_2 - f)^{-1} df (\hat{f}_2 - f)^{-1}(\hat{f}_{12} - \hat{f}_2) \\ &= \lambda_1(\hat{f}_{12} - \hat{f}_2) d\hat{f}_2^*(\hat{f}_{12} - \hat{f}_2). \end{aligned}$$

Thus $\hat{f}_{12}^*$ is the λ_1-Darboux transform of $\hat{f}_2$. The remaining task is to show that $\hat{f}_{12}^*$ is the λ_2-Darboux transform of $\hat{f}_1$. Choosing $\hat{f}_{12}$ so that $cr(f, \hat{f}_1, \hat{f}_{12}, \hat{f}_2) = \lambda_2/\lambda_1$, that is,

$$\begin{aligned} \hat{f}_{12} &= \left\{\lambda_2 \hat{f}_1(\hat{f}_1 - f)^{-1} - \lambda_1 \hat{f}_2(\hat{f}_2 - f)^{-1}\right\}\left\{\lambda_2(\hat{f}_1 - f)^{-1} - \lambda_1(\hat{f}_2 - f)^{-1}\right\}^{-1} \\ &= (\lambda_2 - \lambda_1)\left\{\lambda_2(\hat{f}_1 - f)^{-1} - \lambda_1(\hat{f}_2 - f)^{-1}\right\}^{-1} + f. \end{aligned}$$

By the above equation,

$$\begin{aligned} d\hat{f}_{12} &= (\lambda_2 - \lambda_1)\left[d\left\{\lambda_2(\hat{f}_1 - f)^{-1} - \lambda_1(\hat{f}_2 - f)^{-1}\right\}^{-1}\right] + df \\ &= -(\lambda_2 - \lambda_1)c_1 d\left\{\lambda_2(\hat{f}_1 - f)^{-1} - \lambda_1(\hat{f}_2 - f)^{-1}\right\} c_1 + df, \end{aligned}$$

$$= -(\lambda_2-\lambda_1)c_1\Big\{\lambda_2(\hat{f}_1-f)^{-1}df(\hat{f}_1-f)^{-1} - \lambda_1(\hat{f}_2-f)^{-1}df(\hat{f}_2-f)^{-1}\Big\}c_1 + df,$$

where

$$c_1 = \Big\{\lambda_2(\hat{f}_1-f)^{-1} - \lambda_1(\hat{f}_2-f)^{-1}\Big\}^{-1} = (\lambda_2-\lambda_1)^{-1}(\hat{f}_{12}-f).$$

The computation is straightforward but tedious. So we do not write explicit computations here. Deforming these equations, finally we can check that $\hat{f}_{12}^*$ is the λ_2-Darboux transform of $\hat{f}_1$, that is,

$$d\hat{f}_{12} = \lambda_2(\hat{f}_{12}-\hat{f}_1)d\hat{f}_1^*(\hat{f}_{12}-\hat{f}_1),$$

proving the theorem. □

Similarly, like in the case of Bäcklund transformations for the sine-Gordon equation, iterating the Bianchi permutability, we can show the following theorem.

Theorem 4.15. *Let f be an isothermic surface, and let $\hat{f}_i := \mathcal{D}_{\lambda_i} f$ $(i = 1, 2, 3)$ be λ_i-Darboux transforms of f. Then there exists the point $\hat{f}_{123}$ so that*

$$\hat{f}_{123} = \mathcal{D}_{\lambda_1}\mathcal{D}_{\lambda_2}\mathcal{D}_{\lambda_3} f = \mathcal{D}_{\lambda_2}\mathcal{D}_{\lambda_1}\mathcal{D}_{\lambda_3} f = \mathcal{D}_{\lambda_3}\mathcal{D}_{\lambda_1}\mathcal{D}_{\lambda_2} f \ ,$$

that is, for any permutation $\sigma : \{1, 2, 3\} \to \{1, 2, 3\}$,

$$\mathcal{D}_{\lambda_1}\mathcal{D}_{\lambda_2}\mathcal{D}_{\lambda_3} = \mathcal{D}_{\lambda_{\sigma(1)}}\mathcal{D}_{\lambda_{\sigma(2)}}\mathcal{D}_{\lambda_{\sigma(3)}}$$

holds (see Figure 4.3).

Finally, we state a discrete geoemtric structure arising from the Bianchi permutability of Darboux transformations for isothermic surfaces. Let f be an isothermic surface, and let $\hat{f}_i$ $(i = 1, 2)$ be λ_i-Darboux transforms of f. By Theorem 4.14, there exists $\hat{f}_{12} = \mathcal{D}_1\mathcal{D}_2 f = \mathcal{D}_2\mathcal{D}_1 f$ so that it satisfies Equation (4.3). This implies that four points $f, \hat{f}_1, \hat{f}_{12}, \hat{f}_2$ are concircular. Thus we know that the Bianchi permutability, an discrete integrable structure, is given by the cross ratio, and it arises a discrete geometric structure[2]. Furthermore, as already mentioned in Subsections 4.1, 4.4, isothermicity is Möbius invariant, and it is characterized by the infinitesimal cross ratio (i.e. the limit of the cross ratio).

[2]In this case the discrete geometric structure is the concircularity of four points.

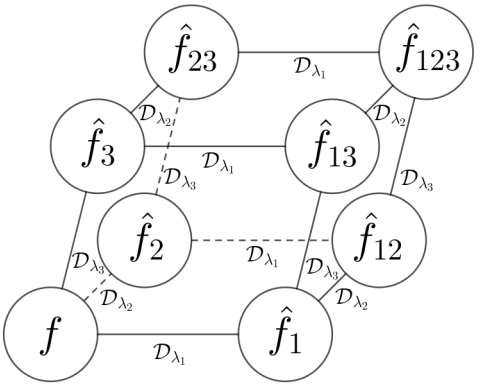

Figure 4.3: Bianchi cube of Darboux transformations for isothermic surfaces

Focusing on these points, Bobenko, Pinkall [4] described a theory of discrete isothermic surfaces preserving the discrete integrable structure (i.e. cross ratio). Soon after, Hertrich-Jeromin, Hoffmann, Pinkall [16] introduced a discrete version of Darboux transforms of isothermic surfaces. The discrete theory preserves the discrete integrabilities introduced in Subsections 4.7, 4.8, and produces higher dimensional discrete symmetries. Such a higher dimensional discrete symmetry is now called the "multidimensional consistency" in the book [6].

More generally, as already mentioned before, due to Möbius invariance of isothermicity, it is natural to consider isothermic surfaces in conformal geometry. In fact, [10], [15], and so on, described discrete isothermic surfaces in Möbius geometry, including discrete isothermic surfaces in 3-dimensional spherical and hyperbolic spaces. Furthermore, a new machinery using the one-parameter family of flat connections was invented to discuss discrete isothermic surfaces or more general discrete surfaces in more general spaces. Using the notion of the flat connections, the aforementioned proofs of the Bianchi permutabilities and permutabilities of more general transformations are simplified and unified. If the readers are interested in this direction, the author would like to recommend to read further references, for example, [8], [10], [12],[15].

References

[1] A. Barone, F. Esposito, C. J. Magee, and A. C. Scott. Theory and applications of the sine-gordon equation. *Riv. Nuovo Cimento* **1**(2): 227–267, 1971. DOI: 10.1007/BF02820622.

[2] L. Bianchi. Ricerche sulle superficie isoterme e sulla deformazione delle quadriche. *Ann. Mat. Pura Appl.* **11**(1): 93–157, 1905. DOI: 10.1007/BF02419963.

[3] A. I. Bobenko and U. Eitner. *Painlevé equations in the differential geometry of surfaces*. Vol. 1753. Lecture Notes in Math. Berlin: Springer-Verlag, 2000. vi+120. DOI: 10.1007/b76883.

[4] A. I. Bobenko and U. Pinkall. Discrete isothermic surfaces. *J. Reine Angew. Math.* **475**: 187–208, 1996. DOI: 10.1515/crll.1996.475.187.

[5] A. I. Bobenko and U. Pinkall. Discrete surfaces with constant negative Gaussian curvature and the Hirota equation. *J. Differential Geom.* **43**(3): 527–611, 1996.

[6] A. I. Bobenko and Y. B. Suris. *Discrete differential geometry*. Graduate Studies in Mathematics 98. Providence, RI: American Mathematical Society, 2008. xxiv+404.

[7] E. Bour. Théorie de la déformation des surfaces. *J. Éc. Impériale Polytech.* **39**: 1–148, 1862.

[8] F. E. Burstall. Isothermic surfaces: conformal geometry, Clifford algebras and integrable systems. In: *Integrable systems, geometry, and topology*. C.-L. Terng (Ed.). Vol. 36. AMS/IP Stud. Adv. Math. Providence, RI: Amer. Math. Soc., 2006, 1–82.

[9] F. E. Burstall, D. Ferus, K. Leschke, F. Pedit, and U. Pinkall. *Conformal geometry of surfaces in S^4 and quaternions*. Vol. 1772. Lecture Notes in Mathematics. Berlin: Springer-Verlag, 2002. viii+89. DOI: 10.1007/b82935.

[10] F. E. Burstall, U. Hertrich-Jeromin, and W. Rossman. Discrete linear Weingarten surfaces. *Nagoya Math. J.* **231**: 55–88, 2018. DOI: 10.1017/nmj.2017.11.

[11] A. Cayley. On the surfaces divisible into squares by their curves of curvature. *Proc. Lond. Math. Soc.* **4**: 120–121, 1871. DOI: 10.1112/plms/s1-4.1.120.

[12] J. Cho, K. Naokawa, Y. Ogata, M. Pember, W. Rossman, and M. Yasumoto. Discretization of isothermic surfaces in Lie sphere geometry. In progress.

[13] G. Darboux. Sur les surfaces isothermiques. *C. R. Acad. Sci. Paris* **128**: 1299–1305, 1899.

[14] L. P. Eisenhart. *A treatise on the differential geometry of curves and surfaces*. Boston: Ginn and Company, 1909.

[15] U. Hertrich-Jeromin. *Introduction to Möbius differential geometry*. Vol. 300. London Mathematical Society Lecture Note Series. Cambridge: Cambridge University Press, 2003. xii+413.

[16] U. Hertrich-Jeromin, T. Hoffmann, and U. Pinkall. A discrete version of the Darboux transform for isothermic surfaces. In: *Discrete integrable geometry and physics (Vienna, 1996)*. A. I. Bobenko and R. Seiler (Eds.). Vol. 16. Oxford Lecture Ser. Math. Appl. New York: Oxford Univ. Press, 1999, 59–81.

[17] U. Hertrich-Jeromin and F. Pedit. Remarks on the Darboux transform of isothermic surfaces. *Doc. Math.* **2**: 313–333, 1997.

[18] N. J. Hitchin, G. B. Segal, and R. S. Ward. *Integrable systems*. Vol. 4. Oxford Graduate Texts in Mathematics. New York: The Clarendon Press, Oxford University Press, 1999. x+136.

[19] T. Hoffmann. *Discrete differential geometry of curves and surfaces*. Vol. 18. COE Lecture Note. Fukuoka: Kyushu University, Faculty of Mathematics, 2009. 78 pp.

[20] J. C. C. Nitsche. *Lectures on minimal surfaces*. Trans. by J. M. Feinberg. Vol. 1. Cambridge: Cambridge University Press, 1989. xxvi+563.

[21] R. Osserman. *A survey of minimal surfaces*. Second edition. New York: Dover Publications, Inc., 1986. vi+207.

[22] A. Sym. Soliton surfaces and their applications (soliton geometry from spectral problems). In: *Geometric aspects of the Einstein equations and integrable systems (Scheveningen, 1984)*. R. Martini (Ed.). Vol. 239. Lecture Notes in Phys. Berlin: Springer, 1985, 154–231. DOI: 10.1007/3-540-16039-6_6.

[23] M. Umehara and K. Yamada. *Differential geometry of curves and surfaces*. Trans. by W. Rossman. Singapore: World Sci. Publishing, 2017.

Chapter 2

Discrete isothermicity in Möbius subgeometries

Joseph Cho, Wayne Rossman
Graduate School of Science, Kobe University, Kobe 657-0834, Japan
joseph.cho@berkeley.edu, wayne@math.kobe-u.ac.jp

Abstract

We give an elementary description of Möbius geometry using a Minkowski space model, primarily in low dimensions with comments about generalizing to higher dimensions. We then give an application to the discretization of isothermic surfaces in three dimensional spaceforms.

1 Introduction

In this article, we give an elementary description of how an understanding of Möbius transformations, which are maps between n-dimensional spaceforms preserving the collection of spheres of all dimensions less than n, is assisted by use of Minkowski spaces.

The arguments are essentially the same regardless of dimension of the spaceforms and the subsuming Minkowski spaces, and in fact the story can extend beyond Minkowski spaces, as we touch upon when we introduce $\mathbb{R}^{p,q}$ spaces. So we do not wish to hide the uniformity of arguments across all dimensions, and in fact we wish to highlight that as we move from 2-dimensional spaceforms to 3-dimensional ones.

S.-D. Yang (ed.), *An introduction to discrete differential geometry.*
Anam Lecture Notes in Mathematics Volume 2

However, there are some advantages to initially restricting to 2-dimensional and 3-dimensional spaceforms for new entrants to this topic. Two obvious reasons are that those low dimensional spaces are more familiar to many than the higher dimensional counterparts, and the vectors and matrices involved are not so complicated even when written in dirty detail in terms of choices of coordinate systems. A third less immediate reason is that the case of 2-dimensional spaceforms can take advantage of the fact that 2-dimensional Euclidean space can be identified with the set of complex numbers, resulting in a very elementary way of describing Möbius transformations that does not exist in higher dimensions - fractional linear transformations, which almost every undergraduate student of mathematics has been exposed to.

This theory has applications to a number of subjects within differential geometry, and, as one example, we touch upon isothermic surfaces. We use the theory here to show how one can naturally discretize that notion of isothermic surfaces.

Finally, we end with selected recommendations for further reading in this field.

2 Möbius geometry of circles

In this section, we review the notion of Möbius geometry of circles using the Minkowski model, and see how the Euclidean plane, the 2-sphere, and the hyperbolic plane are subgeometries of Möbius geometry.

2.1 Ambient spaces

We first review the ambient spaces appearing in this section. In fact, we view the 2-sphere and the hyperbolic plane as existing inside Euclidean 3-space and Minkowski 3-space, respectively; therefore, we first describe those spaces.

2.1.1 Euclidean 2-plane

Let $\mathbb{R}^2$ denote the usual 2-dimensional Euclidean plane, that is,

$$\mathbb{R}^2 = \{(x_1, x_2)^t : x_1, x_2 \in \mathbb{R}\}$$

with metric $g_{\mathbb{R}^2}$

$$g_{\mathbb{R}^2} = \mathrm{d}x_1^2 + \mathrm{d}x_2^2.$$

Therefore, the inner product $\langle \cdot, \cdot \rangle_2$ is given by

$$\langle x, y \rangle_2 = x_1 y_1 + x_2 y_2$$

for any $x = (x_1, x_2)^t, y = (y_1, y_2)^t \in \mathbb{R}^2$.

The set of isometries of $\mathbb{R}^2$ is a group under the composition operation, generated by

(1) translations,

(2) reflections across lines containing the origin, and

(3) rotations fixing the origin.

Here, translations are maps

$$(x_1, x_2)^t \mapsto (x_1, x_2)^t + (t_1, t_2)^t,$$

for some $t_1, t_2 \in \mathbb{R}$, while rotations and reflections can be described via

$$\begin{pmatrix} x_1 \\ x_2 \end{pmatrix} \mapsto \begin{pmatrix} \cos\theta & \sin\theta \\ \mp\sin\theta & \pm\cos\theta \end{pmatrix} \begin{pmatrix} x_1 \\ x_2 \end{pmatrix}$$

for some $\theta \in \mathbb{R}$. Note that for all $\theta \in \mathbb{R}$, the matrices

$$\begin{pmatrix} \cos\theta & \sin\theta \\ \mp\sin\theta & \pm\cos\theta \end{pmatrix} \in \mathrm{O}(2) \tag{2.1}$$

for

$$\mathrm{O}(2) = \{A \in M_{2\times 2} : A^t A = I_2\},$$

where $M_{n\times n}$ denotes the set of all $n \times n$ matrices, and I_n denotes the $n \times n$ identity matrix.

Exercise 2.1. Verify that every matrix $A \in \mathrm{O}(2)$ is of the form given in (2.1).

2.1.2 Euclidean 3-space

Similar to the Euclidean plane, let $\mathbb{R}^3$ denote the Euclidean 3-space, in other words,

$$\mathbb{R}^3 = \{(x_1, x_2, x_3)^t : x_1, x_2, x_3 \in \mathbb{R}\}$$

with metric $g_{\mathbb{R}^3}$

$$g_{\mathbb{R}^3} = \mathrm{d}x_1^2 + \mathrm{d}x_2^2 + \mathrm{d}x_3^2.$$

The corresponding inner product $\langle \cdot, \cdot \rangle_3$ is now given by

$$\langle x, y \rangle_3 = x_1 y_1 + x_2 y_2 + x_3 y_3$$

for any $x = (x_1, x_2, x_3)^t, y = (y_1, y_2, y_3)^t \in \mathbb{R}^3$.

The set of isometries of $\mathbb{R}^3$ is again a group under the composition operation, generated by

(1) translations,

(2) reflections across planes containing the origin, and

(3) rotations fixing the origin.

Here, the reflections and rotations are described via

$$\begin{pmatrix} x_1 \\ x_2 \\ x_3 \end{pmatrix} \mapsto A \begin{pmatrix} x_1 \\ x_2 \\ x_3 \end{pmatrix}$$

where $A \in \mathrm{O}(3) = \{A \in M_{3\times 3} : A^t A = I_3\}$.

Exercise 2.2. Show that the following matrices are in O(3).

- $\begin{pmatrix} 1 & 0 & 0 \\ 0 & \cos\theta & \sin\theta \\ 0 & \mp\sin\theta & \pm\cos\theta \end{pmatrix}$
- $\begin{pmatrix} \cos\theta & 0 & \sin\theta \\ 0 & 1 & 0 \\ \mp\sin\theta & 0 & \pm\cos\theta \end{pmatrix}$
- $\begin{pmatrix} \cos\theta & \sin\theta & 0 \\ \mp\sin\theta & \pm\cos\theta & 0 \\ 0 & 0 & 1 \end{pmatrix}$

Exercise 2.3. Let $x, y \in \mathbb{R}^3$ and $A \in \mathrm{O}(3)$. Using the fact that $\langle x, y \rangle_3 = x^t y$, show that $\langle Ax, Ay \rangle_3 = \langle x, y \rangle_3$.

2.1.3 Minkowski 3-space

Now let $\mathbb{R}^{2,1}$ denote the Minkowski 3-space of signature $(- + +)$, that is,

$$\mathbb{R}^{2,1} = \{(x_0, x_1, x_2)^t : x_0, x_1, x_2 \in \mathbb{R}\}$$

with non-Euclidean metric $g_{\mathbb{R}^3}$

$$g_{\mathbb{R}^{2,1}} = -\,\mathrm{d}x_0^2 + \mathrm{d}x_1^2 + \mathrm{d}x_2^2.$$

Therefore, the corresponding (indefinite) inner product $\langle\cdot,\cdot\rangle_{2,1}$ is now given by

$$\langle x, y\rangle_{2,1} = -x_0y_0 + x_1y_1 + x_2y_2$$

for any $x = (x_0, x_1, x_2)^t, y = (y_0, y_1, y_2)^t \in \mathbb{R}^{2,1}$. The definition of inner product leads to the *causality* of a given vector: a non-zero vector $x \in \mathbb{R}^{2,1}$ is called

- *spacelike*, if $\langle x, x\rangle > 0$,
- *lightlike*, if $\langle x, x\rangle = 0$, and
- *timelike*, if $\langle x, x\rangle < 0$.

The isometries of $\mathbb{R}^{2,1}$ that fix the origin can be described as

$$\begin{pmatrix} x_1 \\ x_2 \\ x_3 \end{pmatrix} \mapsto A \begin{pmatrix} x_1 \\ x_2 \\ x_3 \end{pmatrix}$$

for

$$A \in \mathrm{O}(2,1) = \{A \in M_{3\times 3} : A^t I_{2,1} A = I_{2,1}\}$$

where

$$I_{2,1} = \begin{pmatrix} -1 & 0 & 0 \\ 0 & 1 & 0 \\ 0 & 0 & 1 \end{pmatrix}.$$

Note that the signatures of the diagonal terms of $I_{2,1}$ correspond to the signatures of the metric $g_{2,1}$.

Exercise 2.4. Show that the following matrices are in $\mathrm{O}(2,1)$.

- $\begin{pmatrix} \cosh\varphi & 0 & \sinh\varphi \\ 0 & 1 & 0 \\ \sinh\varphi & 0 & \cosh\varphi \end{pmatrix}$
- $\begin{pmatrix} \cosh\varphi & \sinh\varphi & 0 \\ \sinh\varphi & \cosh\varphi & 0 \\ 0 & 0 & 1 \end{pmatrix}$

Exercise 2.5. For $A \in \mathrm{O}(2,1)$ such that

$$A = \begin{pmatrix} 1 & 0 & 0 \\ 0 & & \\ 0 & & B \end{pmatrix},$$

show that $B \in \mathrm{O}(2)$.

2.1.4 General description of Euclidean spaces and Minkowski spaces

The descriptions of the above spaces are similar, and we can in fact describe these spaces uniformly as follows. Let $\mathbb{R}^{p,q}$ denote a space with $p+q$ dimension:

$$\mathbb{R}^{p,q} = \{(x_1, \ldots, x_q, x_{q+1}, \ldots, x_{q+p})^t : x_i \in \mathbb{R}\}$$

with (non-Euclidean) metric

$$g_{p,q} = -\left(\sum_{i=1}^{q} \mathrm{d}x_i^2\right) + \sum_{i=q+1}^{q+p} \mathrm{d}x_i^2.$$

Then, the corresponding (indefinite) inner product $\langle \cdot, \cdot \rangle_{p,q}$ is now given by

$$\langle x, y \rangle_{p,q} = -\left(\sum_{i=1}^{q} x_i y_i\right) + \sum_{i=q+1}^{q+p} x_i y_i.$$

for any $x = (x_1, \ldots, x_{p+q})^t, y = (y_1, \ldots, y_{p+q})^t \in \mathbb{R}^{p,q}$.

The isometries of $\mathbb{R}^{p,q}$ that fix the origin can be described as

$$\begin{pmatrix} x_1 \\ \vdots \\ x_q \\ x_{q+1} \\ \vdots \\ x_{q+p} \end{pmatrix} \mapsto A \begin{pmatrix} x_1 \\ \vdots \\ x_q \\ x_{q+1} \\ \vdots \\ x_{q+p} \end{pmatrix}$$

for

$$A \in \mathrm{O}(p,q) = \{A \in M_{(p+q)\times(p+q)} : A^t I_{p,q} A = I_{p,q}\}$$

where $I_{p,q}$ is the diagonal matrix of the form

$$\begin{array}{c} \overbrace{}^{q}\ \overbrace{}^{p} \\ \left.\begin{array}{c}\\\\\\\end{array}\right\{q \\ \left.\begin{array}{c}\\\\\\\end{array}\right\{p \end{array} \begin{pmatrix} -1 & & & & & & \\ & \ddots & & & & & \\ & & -1 & & & & \\ & & & 1 & & & \\ & & & & \ddots & & \\ & & & & & 1 & \end{pmatrix}.$$

Note that the signatures of the diagonal terms again correspond to the signatures of the metric $g_{p,q}$.

We say that such $\mathbb{R}^{p,q}$ is a ($(p+q)$-dimensional) pseudo-Euclidean space of signature (p,q). In particular, if $p = n$ and $q = 0$, we call $\mathbb{R}^n$ the Euclidean n-space; if $p = n-1$ and $q = 1$, we call $\mathbb{R}^{n-1,1}$ the Minkowski n-space.

Now that the notions of Euclidean spaces and Minkowski spaces are defined, we may introduce spaces with non-vanishing constant (sectional) curvature.

2.1.5 2-sphere

Let the 2-sphere $\mathbb{S}^2$ be defined as

$$\mathbb{S}^2 := \{x \in \mathbb{R}^3 : \langle x, x\rangle_3 = 1\},$$

where its metric $g_{\mathbb{S}^2}$ is defined by restricting the metric of the ambient space $\mathbb{R}^3$ to the 2-dimensional tangent spaces of $\mathbb{S}^2$. One of the ways to understand the metric endowed on the 2-sphere is to use the stereographic projection.

In these notes, we use the stereographic projection from the north pole $(0,0,1)^t$, denoted by $\sigma : \mathbb{S}^2 \setminus \{(0,0,1)^t\} \to \{(x_1,x_2,0)^t \in \mathbb{R}^3\} \cong \mathbb{R}^2$, where

$$\sigma((x_1,x_2,x_3)^t) = \frac{1}{1-x_3}\,(x_1,x_2)^t\,.$$

Geometrically, $\sigma(p)$ is determined by finding the intersection between the x_1x_2-plane and the line through the north pole and the point p. Stereographic projection is a bijection, with its inverse σ^{-1} defined as

$$\sigma^{-1}((x_1,x_2)^t) = \frac{1}{1+x_1^2+x_2^2}(2x_1,2x_2,x_1^2+x_2^2-1)^t. \tag{2.2}$$

Viewing σ^{-1} as a coordinate patch for $\mathbb{S}^2$, we can now compute the metric $g_{\mathbb{S}^2}$ as follows: calculating that

$$\partial_1\sigma^{-1} = \frac{\partial}{\partial x_1}\sigma^{-1} = \frac{1}{(1+x_1^2+x_2^2)^2}\left(-2x_1^2+2x_2^2+2, -4x_1x_2, 4x_1\right)$$
$$\partial_2\sigma^{-1} = \frac{\partial}{\partial x_2}\sigma^{-1} = \frac{1}{(1+x_1^2+x_2^2)^2}\left(-4x_1x_2, 2x_1^2-2x_2^2+2, 4x_2\right),$$

we have that

$$\begin{aligned} g_{\mathbb{S}^2} &= \langle\partial_1\sigma^{-1}, \partial_1\sigma^{-1}\rangle_3\,\mathrm{d}x_1^2 + 2\langle\partial_1\sigma^{-1}, \partial_2\sigma^{-1}\rangle_3\,\mathrm{d}x_1\,\mathrm{d}x_2 \\ &\qquad + \langle\partial_2\sigma^{-1}, \partial_2\sigma^{-1}\rangle_3\,\mathrm{d}x_2^2 \\ &= \frac{4}{(1+x_1^2+x_2^2)^2}(\mathrm{d}x_1^2+\mathrm{d}x_2^2). \end{aligned}$$

The isometries of $\mathbb{S}^2$ are the reflections and rotations of $\mathbb{R}^3$ fixing the origin. Thus the isometry group of $\mathbb{S}^2$ is represented by $\mathrm{O}(3)$.

Circles of $\mathbb{S}^2$ are "planar slices" of $\mathbb{S}^2$, which we formulate as follows: recall that any point $(x_1, x_2, x_3)^t$ in a plane in $\mathbb{R}^3$ can be described via the equation

$$m_1x_1 + m_2x_2 + m_3x_3 = q \tag{2.3}$$

for some $m_1, m_2, m_3, q \in \mathbb{R}$. Rewriting the above equation, we have

$$\langle x, m\rangle_3 = q$$

for $m = (m_1, m_2, m_3)^t$ and $x = (x_1, x_2, x_3)^t$. Therefore, we may consider circles in the 2-sphere as

$$\tilde{C}_{\mathbb{S}^2}[m, q] := \{x \in \mathbb{S}^2 \subset \mathbb{R}^3 : \langle x, m\rangle_3 = q\},$$

provided that the set is non-empty, a condition we can characterize as follows.

Lemma 2.6. *$\tilde{C}_{\mathbb{S}^2}[m, q]$ is non-empty (and includes more than one point) if and only if $\langle m, m\rangle_3 > q^2$.*

Proof. Let a plane $\mathcal{P}$ be defined from (2.3) via some $m \in \mathbb{R}^3$ and $q \in \mathbb{R}$. $\mathcal{P}$ and $\mathbb{S}^2$ intersect transversally if and only if the squared distance between $\mathcal{P}$ and the origin is less than 1, i.e.

$$\frac{q^2}{\langle m, m\rangle_3} < 1,$$

giving us the desired conclusion. □

2.1.6 Hyperbolic 2-plane

Denoting the hyperbolic 2-plane as $\mathbb{H}^2$, we first introduce the Minkowski model of the hyperbolic plane. For the Minkowski 3-space $\mathbb{R}^{2,1}$, let $\mathbb{H}^2$ be defined via

$$\mathbb{H}^2 := \{x = (x_0, x_1, x_2)^t \in \mathbb{R}^{2,1} : \langle x, x\rangle_{2,1} = -1, x_0 > 0\},$$

the upper sheet of the two-sheeted hyperboloid in Minkowski 3-space. Similar to the 2-sphere case, the metric $g_{\mathbb{H}^2}$ is defined by restricting the metric of the ambient space $\mathbb{R}^{2,1}$ to the 2-dimensional tangent spaces of $\mathbb{H}^2$, which we will calculate using the Poincaré disk model.

From the Minkowski model, define a stereographic projection into the Poincaré disk model via

$$\tau((x_0, x_1, x_2)^t) = \frac{1}{1+x_0}(x_1, x_2).$$

One immediately sees that since for any $x = (x_0, x_1, x_2)^t$, we have $x_1^2 + x_2^2 = x_0^2 - 1$,

$$\left\langle \frac{1}{1+x_0}(x_1, x_2), \frac{1}{1+x_0}(x_1, x_2) \right\rangle_2 = \frac{1}{(1+x_0)^2}(x_1^2 + x_2^2) < \frac{x_0^2 - 1}{x_0^2 + 1} < 1;$$

hence we can see the Poincaré disk model as the unit disk in the Euclidean plane. We call the unit circle in the Poincaré disk model, the *ideal boundary*.

Viewing

$$\tau^{-1}((x_1, x_2)^t) = \frac{1}{1 - x_1^2 - x_2^2}(1 + x_1^2 + x_2^2, 2x_1, 2x_2)^t \tag{2.4}$$

as a coordinate patch for $\mathbb{H}^3$, we can compute the metric $g_{\mathbb{H}^2}$ similarly to the case of the 2-sphere, and obtain that

$$\begin{aligned} g_{\mathbb{H}^2} &= \langle \partial_1\tau^{-1}, \partial_1\tau^{-1}\rangle_{2,1}\,\mathrm{d}x_1^2 + 2\langle \partial_1\tau^{-1}, \partial_2\tau^{-1}\rangle_{2,1}\,\mathrm{d}x_1\,\mathrm{d}x_2 \\ &\qquad + \langle \partial_2\tau^{-1}, \partial_2\tau^{-1}\rangle_{2,1}\,\mathrm{d}x_2^2 \\ &= \frac{4}{(1 - x_1^2 - x_2^2)^2}(\mathrm{d}x_1^2 + \mathrm{d}x_2^2). \end{aligned}$$

Again, the isometries of $\mathbb{H}^2$ are the reflections and rotations of $\mathbb{R}^{2,1}$ fixing the origin, telling us that the isometry group of $\mathbb{H}^2$ is represented by $\mathrm{O}(2,1)$.

Exercise 2.7. Show that each isometry group for $\mathbb{R}^2$, $\mathbb{S}^2$ and $\mathbb{H}^2$ is 3-dimensional. (Hint: for the $\mathbb{R}^3$ case, count the dimensions for translations and isometries fixing the origin separately.)

Circles in $\mathbb{H}^2$ are given similarly to those in $\mathbb{S}^2$, as "planar slices": given a vector $m = (m_0, m_1, m_2)^t \in \mathbb{R}^{2,1}$ and $q \in \mathbb{R}$, we let

$$\tilde{C}_{\mathbb{H}^2}[m, q] := \{x \in \mathbb{H}^2 : \langle x, m\rangle_{2,1} = q\}$$

be a circle. Circles in $\mathbb{H}^2$ come in three different types, which can be characterized via m as follows:

- *Bounded circles* arise when $\langle m, m\rangle_{2,1} < 0$. These appear as genuine circles within the Poincaré disk model.
- *Horocircles* appear when $\langle m, m\rangle_{2,1} = 0$. These appear as circles tangent to the ideal boundary in the Poincaré disk model.
- *Unbounded circles* arise when $\langle m, m\rangle_{2,1} > 0$, and appear as arcs of circles that intersect the ideal boundary transversally in the Poincaré disk model.

Exercise 2.8. Show that $\tilde{C}_{\mathbb{H}^2}[m, q]$ is non-empty (and includes more than one point) if and only if $\langle m, m\rangle_{2,1} + q^2 > 0$. (Hint: for the case of bounded circles, use an argument similar to that used for the proof of Lemma 2.6.)

2.2 Minkowski model of Möbius geometry

Let $\mathbb{R}^{3,1}$ be a Minkowski 4-space with signature $(-+++)$ as in Section 2.1.4, i.e. the space is equipped with inner product

$$\langle X, Y\rangle_{3,1} = -x_0y_0 + x_1y_1 + x_2y_2 + x_3y_3$$

for some $X = (x_0, x_1, x_2, x_3)^t, Y = (y_0, y_1, y_2, y_3)^t \in \mathbb{R}^{3,1}$. The 3-dimensional lightcone $\mathcal{L}^3$ is

$$\mathcal{L}^3 = \{X \in \mathbb{R}^{3,1} : \langle X, X\rangle_{3,1} = 0\}.$$

To make 2-dimensional spaceforms, choose $\mathfrak{q}_\kappa \in \mathbb{R}^{3,1}$ with $\langle \mathfrak{q}_\kappa, \mathfrak{q}_\kappa\rangle_{3,1} = -\kappa$, and define

$$M^2_\kappa = \{X \in \mathcal{L}^3 : \langle X, \mathfrak{q}_\kappa\rangle_{3,1} = -1\}.$$

Here, we call $\mathfrak{q}_\kappa$ the *spaceform vector*. By applying a suitable transformation in $\mathrm{O}(3, 1)$, we may assume without loss of generality that

$$\mathfrak{q}_\kappa = \left(\tfrac{1}{2}(\kappa + 1), \tfrac{1}{2}(\kappa - 1), 0, 0\right)^t. \tag{2.5}$$

Denoting $\mathcal{R}^2_\kappa = \left(\mathbb{R}^2 \cup \{\infty\}\right) \setminus \left\{x : \langle x, x\rangle_2 = -\frac{1}{\kappa}\right\}$, we have the following lemma.

Lemma 2.9. *The map* $\psi_\kappa : \mathcal{R}^2_\kappa \to M^2_\kappa$ *defined by*

$$\psi_\kappa(x) = \frac{1}{1+\kappa\langle x,x\rangle_2}\begin{pmatrix} 1+\langle x,x\rangle_2 \\ 1-\langle x,x\rangle_2 \\ 2x \end{pmatrix} \tag{2.6}$$

is a bijection for any choice of κ.

Exercise 2.10. Prove Lemma 2.9 by showing that $\phi_\kappa = \psi_\kappa^{-1}$ if $\phi_\kappa : M^2_\kappa \to \mathcal{R}^2_\kappa$ is defined as

$$\phi_\kappa(Y) = \phi_\kappa((y_0,y_1,y_2,y_3)^t) = \frac{1}{y_0+y_1}(y_2,y_3). \tag{2.7}$$

To find the metric endowed on M^2_κ, as done for the 2-sphere and the hyperbolic 2-plane cases, we view ψ as a coordinate patch for M^2_κ and compute the metric: By calculation, we find that for $x = (x_1,x_2)^t$,

$$\begin{aligned} \partial_1\psi_\kappa &= -\tfrac{2}{(1+\kappa\langle x,x\rangle_2)^2}\left((\kappa-1)x_1,(\kappa+1)x_1,\kappa x_1^2-\kappa x_2^2-1,2\kappa x_1x_2\right) \\ \partial_2\psi_\kappa &= -\tfrac{2}{(1+\kappa\langle x,x\rangle_2)^2}\left((\kappa-1)x_2,(\kappa+1)x_2,2\kappa x_1x_2,\kappa x_1^2-\kappa x_2^2+1\right). \end{aligned} \tag{2.8}$$

Therefore, we see that

$$\begin{aligned} g_{M^2_\kappa} &= \langle\partial_1\psi_\kappa,\partial_1\psi_\kappa\rangle_{3,1}\,\mathrm{d}x_1^2 + 2\langle\partial_1\psi_\kappa,\partial_1\psi_\kappa\rangle_{3,1}\,\mathrm{d}x_1\,\mathrm{d}x_2 \\ &\qquad + \langle\partial_1\psi_\kappa,\partial_1\psi_\kappa\rangle_{3,1}\,\mathrm{d}x_2^2 \\ &= \frac{4}{(1+\kappa(x_1^2+x_2^2))^2}(\mathrm{d}x_1^2+\mathrm{d}x_2^2). \end{aligned} \tag{2.9}$$

The form of the metric $g_{M^2_\kappa}$ suggests that we have the following important theorem, confirmed in many standard textbooks in differential geometry:

Theorem 2.11. M^2_κ *has constant (sectional) curvature* κ.

2.3 2-dimensional spaceforms as Möbius subgeometries

We now explain how we can view the 2-dimensional spaceforms as subgeometries of Möbius geometry.

First, take the 2-sphere $\mathbb{S}^2$. Since for any $(x_1,x_2,x_3) \in \mathbb{S}^2 \subset \mathbb{R}^3$, we have that

$$x_1^2+x_2^2+x_3^2 = 1,$$

we see that

$$0 = -1 + x_1^2 + x_2^2 + x_3^2 = \langle (1, x_1, x_2, x_3)^t, (1, x_1, x_2, x_3)^t \rangle_{3,1}.$$

Therefore,

$$(1, x_1, x_2, x_3)^t \in \mathcal{L}^3$$

for any $(x_1, x_2, x_3)^t \in \mathbb{S}^2$. Furthermore, for $\mathfrak{q}_1 = (1, 0, 0, 0)^t$,

$$\langle (1, x_1, x_2, x_3)^t, q_1 \rangle_{3,1} = -1,$$

telling us that

$$(1, x_1, x_2, x_3)^t \in M_1^2.$$

A simple reversal of the argument gives us a natural bijection between $\mathbb{S}^2$ and M_1^2.

Exercise 2.12. Further convince yourself of this correspondence between $\mathbb{S}^2$ and M_1^2 by calculating ψ_1, where ψ_κ is as in (2.6), and comparing this with σ^{-1} as in (2.2).

Similarly, for any point $(x_0, x_1, x_2)^t \in \mathbb{H}^2 \subset \mathbb{R}^{2,1}$ in the hyperbolic 2-plane,

$$-x_0^2 + x_1^2 + x_2^2 = -1.$$

Hence,

$$0 = -x_0^2 + 1 + x_1^2 + x_2^2 = \langle (x_0, 1, x_1, x_2)^t, (x_0, 1, x_1, x_2)^t \rangle_{3,1},$$

telling us that

$$(x_0, 1, x_1, x_2) \in \mathcal{L}^3$$

for any $(x_0, x_1, x_2)^t \in \mathbb{H}^2$. Then it is easy to check that

$$(x_0, 1, x_1, x_2) \in M_{-1}^2,$$

since

$$\langle (x_0, 1, x_1, x_2), \mathfrak{q}_{-1} \rangle_{3,1} = \langle (x_0, 1, x_1, x_2), (0, -1, 0, 0) \rangle_{3,1} = -1.$$

Therefore, we again have a natural bijection between $\mathbb{H}^2$ and M_{-1}^2.

Exercise 2.13. Further convince yourself of the correspondence between $\mathbb{H}^2$ and M_{-1}^2 by calculating ψ_{-1}, where ψ_κ is as in (2.6), and comparing this with τ^{-1} as in (2.4).

Lifting the Euclidean 2-plane $\mathbb{R}^2$ into the lightcone $\mathcal{L}^3$ requires a bit more thought: in addition to

$$\mathfrak{q}_0 = \left(\tfrac{1}{2}, -\tfrac{1}{2}, 0, 0\right)^t,$$

we define $\mathfrak{o} := (1, 1, 0, 0)^t \in \mathbb{R}^{3,1}$ so that

$$\mathfrak{q}_0, \mathfrak{o} \in \mathcal{L}^3 \quad \text{and} \quad \langle \mathfrak{q}_0, \mathfrak{o} \rangle_{3,1} = -1.$$

Now, for any $x = (x_1, x_2)^t \in \mathbb{R}^2$, view $x = (0, 0, x_1, x_2) \in \mathbb{R}^{3,1}$, and define

$$X := 2x + \mathfrak{o} + \frac{1}{2}\langle 2x, 2x \rangle_{3,1} \mathfrak{q}_0.$$

It is a straightforward calculation to see that

$$X = \begin{pmatrix} 0 \\ 0 \\ 2x_1 \\ 2x_2 \end{pmatrix} + \begin{pmatrix} 1 \\ 1 \\ 0 \\ 0 \end{pmatrix} + \frac{1}{2}\langle 2x, 2x \rangle_2 \begin{pmatrix} \frac{1}{2} \\ -\frac{1}{2} \\ 0 \\ 0 \end{pmatrix} = \begin{pmatrix} 1 + \langle x, x \rangle_2 \\ 1 - \langle x, x \rangle_2 \\ 2x_1 \\ 2x_2 \end{pmatrix} = \phi_0(x).$$

Remark 2.14. Note that M_0^2 obtained via (2.6) has metric 4 times the usual metric of $\mathbb{R}^2$ via (2.9). This is so that when $\kappa \neq 0$, we have the usual expression of the metric of spaceforms with nonzero sectional curvature. To remedy this for the $\mathbb{R}^2$ case, we may do as follows: Instead of normalizing $\mathfrak{q}_\kappa$ as in (2.5), we let

$$\mathfrak{q} = (1, -1, 0, 0)^t,$$

and for $M = \{X \in \mathcal{L}^3 : \langle X, \mathfrak{q} \rangle = -1\}$, we can calculate that

$$M = \left\{ \begin{pmatrix} \frac{1}{2}(1 + \langle x, x \rangle_2) \\ \frac{1}{2}(1 + \langle x, x \rangle_2) \\ x_1 \\ x_2 \end{pmatrix} : x = \begin{pmatrix} x_1 \\ x_2 \end{pmatrix} \in \mathbb{R}^2 \right\}.$$

Therefore, choosing $\mathfrak{o} = \frac{1}{2}(1, 1, 0, 0, 0)^t$ so that

$$\mathfrak{q}, \mathfrak{o} \in \mathcal{L}^3 \quad \text{and} \quad \langle \mathfrak{q}_0, \mathfrak{o} \rangle_{3,1} = -1, \tag{2.10}$$

we find that $\psi : \mathbb{R}^2 \to M$ defined via

$$\psi(x) = x + \mathfrak{o} + \frac{1}{2}\langle x, x \rangle_{3,1} \mathfrak{q} \tag{2.11}$$

where we view $x = (0, 0, x_1, x_2) \in \mathbb{R}^{3,1}$, gives us a bijection between $\mathbb{R}^2$ and M. Using ψ as a coordinate patch for M, one can check that

$$g_M = \mathrm{d}x_1^2 + \mathrm{d}x_2^2.$$

In fact, one does not need to choose $\mathfrak{o}$ and $\mathfrak{q}$ as given: Choosing any $\mathfrak{o}$ and $\mathfrak{q}$ so that (2.10) holds, we see that

$$\mathrm{span}\{\mathfrak{o}, \mathfrak{q}\} \cong \mathbb{R}^{1,1}$$

implying that

$$\mathrm{span}\{\mathfrak{o}, \mathfrak{q}\}^\perp \cong \mathbb{R}^2$$

with ψ as defined in (2.11) giving us a bijection between $\mathrm{span}\{\mathfrak{o}, \mathfrak{q}\}^\perp \cong \mathbb{R}^2$ and M.

2.4 Conformal 2-sphere

We wish to see that the 2-dimensional spaceforms we are interested in can be identified as the *conformal 2-sphere*. Recall that $\psi_\kappa : \mathcal{R}^2_\kappa \to M^2_\kappa$ was defined in (2.6) as

$$\psi_\kappa(x) = \frac{1}{1 + \kappa\langle x, x\rangle_2} \begin{pmatrix} 1 + \langle x, x\rangle_2 \\ 1 - \langle x, x\rangle_2 \\ 2x \end{pmatrix}.$$

Also, we note that the metric calculated for M^2_κ in (2.9) for different values of κ were all conformally equivalent. Seeing that any point $(x_1, x_2) \in \mathcal{R}^2_\kappa$ is mapped onto a lightlike line

$$\mathrm{span}\{(1 + \langle x, x\rangle_2, 1 - \langle x, x\rangle_2, 2x_1, 2x_2)^t\}$$

via ψ_κ for all values of κ, we can consider the (2-dimensional) projective lightcone $\mathbb{P}(\mathcal{L}^3)$, defined as

$$\mathbb{P}(\mathcal{L}^3) = \{\mathrm{span}\{X\} : X \in \mathcal{L}^3\},$$

as a model for unifying all the 2-dimensional spaceforms with constant sectional curvatures, since each line in $\mathbb{P}(\mathcal{L}^3)$ determines at most one point in any given 2-dimensional spaceform, determined by the choice of κ. We call this the *conformal 2-sphere*.

2.5 Circles in the conformal 2-sphere

Recall that circles in $\mathbb{S}^2$ were defined as

$$\tilde{C}_{\mathbb{S}^2}[m,q] = \{x \in \mathbb{S}^2 : \langle x, m\rangle_3 = q\},$$

where we have $\langle m, m\rangle_3 > q^2$ from Lemma 2.6. If we consider

$$C := (q, m_1, m_2, m_3)^t \in \mathbb{R}^{3,1},$$

then $x = (x_1, x_2, x_3)^t \in \tilde{C}_{\mathbb{S}^2}[m,q]$ if and only if

$$\langle (1, x_1, x_2, x_3), S\rangle_{3,1} = 0,$$

where C is spacelike, since $\langle C, C\rangle_{3,1} = \langle m, m\rangle_3 - q^2 > 0$.

Motivated by this we define circles $\tilde{C}$ in Mobius geometry for some κ using a spacelike vector $C \in \mathbb{R}^{3,1}$ as

$$\tilde{C} := \{X \in M^2_\kappa : \langle X, C\rangle_{3,1} = 0\}. \tag{2.12}$$

The scaling of C does not matter, and we will always assume that $\langle C, C\rangle_{3,1} = 1$.

We have already seen that such a definition is coherent with circles in $\mathbb{S}^2$; therefore, since stereographic projection preserves circles, we can deduce the above definition gives the "correct circles" in any 2-dimensional spaceform M^2_κ. In the next example, we calculate this directly for $M^2_0 \cong \mathbb{R}^2$.

Example 2.15. For some spacelike unit vector $C = (c_0, c_1, c_2, c_3)^t \in \mathbb{R}^{3,1}$, let $X \in \tilde{C}$, for $\kappa = 0$. Since $X \in M^2_0$, we write

$$X = (1 + \langle x, x\rangle_2, 1 - \langle x, x\rangle_2, 2x_1, 2x_2)^t$$

for some $x = (x_1, x_2)^t$. Then $\langle X, C\rangle_{3,1} = 0$ tells us that for $c = (c_2, c_3)^t$,

$$\begin{aligned} 0 &= -c_0(1 + \langle x, x\rangle_2) + c_1(1 - \langle x, x\rangle_2) + 2\langle x, c\rangle_2 \\ &= -c_0 - c_0\langle x, x\rangle_2 + c_1 - c_1\langle x, x\rangle_2 + 2\langle x, c\rangle_2 \\ &= 2\langle x, c\rangle_2 - (c_0 + c_1)\langle x, x\rangle_2 - c_0 + c_1. \end{aligned}$$

If $c_0 + c_1 = 0$, then the above equation tells us that $\tilde{C}$ projects to a line. Now, assuming $c_0 + c_1 \neq 0$, we have that

$$\begin{aligned}\left\langle x - \frac{c}{c_0+c_1}, x - \frac{c}{c_0+c_1} \right\rangle_2 \\ &= \langle x, x\rangle_2 - 2\frac{\langle x, c\rangle_2}{c_0+c_1} + \frac{\langle c, c\rangle_2}{(c_0+c_1)^2} \\ &= \frac{1}{c_0+c_1}\left((c_0+c_1)\langle x, x\rangle_2 - 2\langle x, c\rangle_2 + \frac{\langle c, c\rangle_2}{c_0+c_1}\right) \\ &= \frac{1}{c_0+c_1}\left(-c_0 + c_1 + \frac{\langle c, c\rangle_2}{c_0+c_1}\right) \\ &= \frac{-c_0^2 + c_1^2 + \langle c, c\rangle_2}{(c_0+c_1)^2} = \frac{1}{(c_0+c_1)^2},\end{aligned}$$

telling us that $\tilde{C}$ projects to a circle in $\mathbb{R}^2$.

Exercise 2.16. Use Exercise 2.8 to show that the circles defined in (2.12) give the correct circles as described in Section 2.1.6. (Hint: set $C = (m_0, q, m_1, m_2)$.)

Therefore, in Möbius geometry, the set of circles becomes the set of all unit spacelike vectors, also known as de Sitter 3-space $\mathbb{S}^{3,1}$, that is,

$$\mathbb{S}^{3,1} := \{C \in \mathbb{R}^{3,1} : \langle C, C\rangle_{3,1} = 1\}.$$

2.6 Möbius transformations

Identifying $\mathbb{R}^2 \cong \mathbb{C}$, via $\mathbb{R}^2 \ni (x_1, x_2)^t \sim x_1 + \sqrt{-1}x_2 \in \mathbb{C}$, we recall that all Möbius transformations of the complex plane are given by linear fractional transformations, that is,

$$z \mapsto \frac{az+b}{cz+d},$$

for some $a, b, c, d \in \mathbb{C}$ such that $ad - bc \neq 0$. In this section, we first investigate how these transformations are given in the Möbius geometry as $\mathrm{O}(3,1)$ matrices, and convince ourselves that the group of Möbius transformations is $\mathrm{O}(3,1)$ in the Minkowski model.

To see this, using the following five functions

$$f_1(z) = z + \frac{d}{c}, \quad f_2(z) = \bar{z}, \quad f_3(z) = \frac{1}{\bar{z}},$$
$$f_4(z) = \frac{bc-ad}{c^2}z, \quad f_5(z) = z + \frac{a}{c},$$

where $\bar{z}$ denotes the usual complex conjugation, we first break down the linear fractional transformation as

$$f_5 \circ f_4 \circ f_3 \circ f_2 \circ f_1(z) = \frac{az+b}{cz+d}. \tag{2.13}$$

Exercise 2.17. Verify (2.13).

Therefore, a Möbius transformation of the complex plane can be given as a composition of homothety, rotation, translation, conjugation, and inversion. We now show that these operations can be described as $\mathrm{O}(3,1)$ acting on the projective lightcone $\mathbb{P}(\mathcal{L}^3)$ as follows: First, using the identification $\mathbb{C} \cong \mathbb{R}^2 \cong M_0^2$, we lift a point $z = x_1 + \sqrt{-1}x_2 \sim (x_1, x_2)^t = x$ to the null line

$$L = \mathrm{span}\{(1 + \langle x, x\rangle_2, 1 - \langle x, x\rangle_2, 2x^t)^t\} \in \mathbb{P}(\mathcal{L}^3).$$

Then, for some $A \in \mathrm{O}(3,1)$, we have that $AL \in \mathbb{P}(\mathcal{L}^3)$, which we can project back into $\mathbb{R}^2 \cong \mathbb{C}$ using the condition that a vector in the null line AL must make inner product -1 with $\mathfrak{q}_0$.

- To describe conjugation in Möbius geometry, let

$$A_1 = \begin{pmatrix} 1 & 0 & 0 & 0 \\ 0 & 1 & 0 & 0 \\ 0 & 0 & 1 & 0 \\ 0 & 0 & 0 & -1 \end{pmatrix} \in \mathrm{O}(3,1).$$

  Then

$$A_1 L = \mathrm{span}\{(1 + \langle x, x\rangle_2, 1 - \langle x, x\rangle_2, 2x_1, -2x_2)^t\}.$$

  To find the vector in $A_1 L$ that is in M_0^2, we solve

$$\langle t(1 + \langle x, x\rangle_2, 1 - \langle x, x\rangle_2, 2x_1, -2x_2)^t, \mathfrak{q}_0\rangle_{3,1} = -1$$

  for t, which tells us that $t = 1$. Projecting this vector back using ϕ_κ defined in (2.7), we obtain

$$\phi_\kappa((1 + \langle x, x\rangle_2, 1 - \langle x, x\rangle_2, 2x_1, -2x_2)^t) = (x_1, -x_2).$$

  Hence A_1 corresponds to the map

$$z \sim (x_1, x_2)^t \mapsto (x_1, -x_2)^t \sim \bar{z},$$

  which is a conjugation.

- For homothety, we let

$$A_2 = \begin{pmatrix} \cosh(\log(r)) & -\sinh(\log(r)) & 0 & 0 \\ -\sinh(\log(r)) & \cosh(\log(r)) & 0 & 0 \\ 0 & 0 & 1 & 0 \\ 0 & 0 & 0 & 1 \end{pmatrix} \in \mathrm{O}(3,1)$$

for some $r \in \mathbb{R}$, giving us

$$A_2 L = \left(\frac{1}{r} + r\langle x, x\rangle_2, \frac{1}{r} - r\langle x, x\rangle_2, 2x^t \right)^t.$$

Again, to find the correct scaling, we solve

$$\left\langle t \left(\frac{1}{r} + r\langle x, x\rangle_2, \frac{1}{r} - r\langle x, x\rangle_2, 2x^t \right)^t, \mathfrak{q}_0 \right\rangle_{3,1} = -1$$

for t, and we have that $t = r$. Projecting this vector via ϕ_κ then tells us that A_2 corresponds to the map

$$z \sim (x_1, x_2)^t \mapsto (rx_1, rx_2)^t \sim rz,$$

for $r \in \mathbb{R}$, a homothety.

- In a similar way, we can show that

$$A_3 = \begin{pmatrix} 1 & 0 & 0 & 0 \\ 0 & 1 & 0 & 0 \\ 0 & 0 & \cos\theta & -\sin\theta \\ 0 & 0 & \sin\theta & \cos\theta \end{pmatrix} \in \mathrm{O}(3,1).$$

corresponds to a map

$$z \sim (x_1, x_2)^t \mapsto (x_1\cos\theta - x_2\sin\theta, x_1\sin\theta + x_2\cos\theta)^t \sim e^{\sqrt{-1}\theta} z,$$

a rotation. We leave showing this correspondence as an exercise.

- Also, we have that

$$A_4 = \begin{pmatrix} 1 & 0 & 0 & 0 \\ 0 & -1 & 0 & 0 \\ 0 & 0 & 1 & 0 \\ 0 & 0 & 0 & 1 \end{pmatrix} \in \mathrm{O}(3,1)$$

corresponds to a map

$$z \sim (x_1, x_2)^t \mapsto \frac{1}{x_1^2 + x_2^2}(x_1, x_2)^t \sim \frac{1}{\bar{z}},$$

an inversion. We leave the verification of this correspondence as an exercise.

- Finally, for

$$A_5 = \begin{pmatrix} 1 + \frac{1}{2}\langle y, y\rangle_2 & \frac{1}{2}\langle y, y\rangle_2 & y_1 & y_2 \\ -\frac{1}{2}\langle y, y\rangle_2 & 1 - \frac{1}{2}\langle y, y\rangle_2 & -y_1 & -y_2 \\ y_1 & y_1 & 1 & 0 \\ y_2 & y_2 & 0 & 1 \end{pmatrix} \in \mathrm{O}(3,1),$$

where $y = (y_1, y_2)^t$, we have that A_5 corresponds to the map

$$z \sim (x_1, x_2)^t \mapsto (x_1 + y_1, x_2 + y_2)^t \sim z + z_0$$

for $z_0 = y_1 + \sqrt{-1}y_2$, a translation. We also leave the checking of this correspondence as an exercise.

Exercise 2.18. Show that the matrices A_3, A_4, and A_5 correspond to a rotation, an inversion, and a translation, respectively.

The fact that the group of Möbius transformations are now described as $\mathrm{O}(3,1)$ acting on $\mathbb{P}(\mathcal{L}^3)$ is one of the advantages of using the Minkowski model to unify the different 2-dimensional spaceforms as a conformal 2-sphere. An easy consequence of representing Möbius transformations as $\mathrm{O}(3,1)$ comes from the previous observation that the space of spheres are represented by de Sitter 3-space $\mathbb{S}^{3,1}$:

Theorem 2.19. *Möbius transformations preserve circles.*

3 Möbius geometry of spheres

We now add a dimension and consider the Möbius geometry of spheres. The basics of Möbius geometry of spheres can be described analogously to that of circles as we only need to add a dimension to most of the arguments. Therefore, we leave most of the proofs in this section as an exercise. (For hints, we ask the readers to refer to the analogous proofs in the section regarding Möbius geometry of circles.)

3.1 3-sphere and hyperbolic 3-space

We first introduce two 3-dimensional spaceforms with nonzero constant sectional curvature.

3.1.1 3-sphere

Let $\mathbb{R}^4$ denote the Euclidean 4-space with inner product $\langle \cdot, \cdot \rangle_4$. The 3-sphere $\mathbb{S}^3$ is defined as

$$\mathbb{S}^3 = \{x \in \mathbb{R}^4 : \langle x, x \rangle_4 = 1\}.$$

To calculate the metric, we use the stereographic projection from the north pole $(0, 0, 0, 1)^t$, denoted by

$$\sigma : \mathbb{S}^2 \setminus \{(0, 0, 0, 1)^t\} \to \{(x_1, x_2, x_3, 0)^t \in \mathbb{R}^4\} \cong \mathbb{R}^3,$$

where

$$\sigma((x_1, x_2, x_3, x_4)^t) = \frac{1}{1 - x_4} (x_1, x_2, x_3)^t .$$

Stereographic projection is a bijection, with its inverse σ^{-1} defined as

$$\sigma^{-1}((x_1, x_2, x_3)^t) = \tfrac{1}{1+x_1^2+x_2^2+x_3^2}(2x_1, 2x_2, 2x_3, x_1^2 + x_2^2 + x_3^2 - 1)^t.$$

Exercise 3.1. Using σ^{-1} as a coordinate patch for $\mathbb{S}^3$, show that the metric $g_{\mathbb{S}^3}$ is equal to

$$g_{\mathbb{S}^3} = \frac{4}{(1 + x_1^2 + x_2^2 + x_3^2)^2}(\mathrm{d}x_1^2 + \mathrm{d}x_2^2 + \mathrm{d}x_3^2).$$

As in the 2-dimensional case, the isometry group of $\mathbb{S}^3$ is $\mathrm{O}(4)$.

The spheres of $\mathbb{S}^3$ are again given by "planar slices" of $\mathbb{S}^3$ in $\mathbb{R}^4$: For some $m \in \mathbb{R}^4$ and $q \in \mathbb{R}$, spheres $\tilde{S}_{\mathbb{S}^3}[m, q]$ are defined as

$$\tilde{S}_{\mathbb{S}^3}[m, q] := \{x \in \mathbb{S}^3 : \langle x, m \rangle_4 = q\},$$

provided that the set is non-empty (and includes more than one point).

Exercise 3.2. Show that $\tilde{S}_{\mathbb{S}^3}[m, q]$ is non-empty (and includes more than one point) if and only if $\langle m, m \rangle_4 - q^2 > 0$.

3.1.2 Hyperbolic 3-space

Similar to the 2-dimensional case, we define hyperbolic 3-space using Minkowski 4-space $\mathbb{R}^{3,1}$, equipped with indefinite inner product $\langle\cdot,\cdot\rangle_{3,1}$. Then two copies of hyperbolic 3-space are obtained via

$$\mathbb{H}^3 := \{x \in \mathbb{R}^{3,1} : \langle x, x\rangle_{3,1} = -1\}.$$

The Poincaré ball model is given by the stereographic projection τ from the north pole, defined as

$$\tau((x_0, x_1, x_2, x_3)^t) = \frac{1}{1+x_0}(x_1, x_2, x_3).$$

Exercise 3.3. Check that for $x = (x_0, x_1, x_2, x_3)^t \in \mathbb{H}^3$,

(1) $\big\langle \tau(x), \tau(x)\big\rangle_3 < 1$ if and only if $x_0 > 0$, and

(2) $\big\langle \tau(x), \tau(x)\big\rangle_3 > 1$ if and only if $x_0 < 0$.

As in the 2-dimensional case, we call the Euclidean unit sphere in the Poincaré ball model the *ideal boundary*, and the isometry group of $\mathbb{H}^3$ is $\mathrm{O}(3,1)$.

Exercise 3.4. Show that each isometry group of $\mathbb{R}^3$, $\mathbb{S}^3$ and $\mathbb{H}^3$ is 6-dimensional.

Exercise 3.5. Viewing

$$\tau^{-1}((x_1, x_2, x_3)^t) = \tfrac{1}{1-x_1^2-x_2^2-x_3^2}(1 + x_1^2 + x_2^2 + x_3^2, 2x_1, 2x_2, 2x_3)^t$$

as a coordinate patch for $\mathbb{H}^3$, verify that

$$g_{\mathbb{H}^3} = \frac{4}{(1 - x_1^2 - x_2^2 - x_3^2)^2}(\mathrm{d}x_1^2 + \mathrm{d}x_2^2 + \mathrm{d}x_3^2).$$

Spheres in $\mathbb{R}^{3,1}$ are again given as intersections between a plane and $\mathbb{H}^3$. Therefore, we view spheres $\tilde{S}_{\mathbb{H}^2}[m, q]$ as

$$\tilde{S}_{\mathbb{H}^3}[m, q] = \{x \in \mathbb{H}^2 : \langle x, m\rangle_{3,1} = q\}$$

for some $m \in \mathbb{R}^3$ and $q \in \mathbb{R}$. Once again, we have three types of spheres in the hyperbolic 3-space, characterized by m:

- *Bounded spheres* arise when $\langle m, m\rangle_{3,1} < 0$. In the Poincaré ball model, these spheres are represented as Euclidean spheres not intersecting the ideal boundary.

- *Horospheres* appear when $\langle m, m\rangle_{3,1} = 0$. These spheres become spheres tangent to the ideal boundary in the Poincaré ball model.
- *Unbounded spheres* arise when $\langle m, m\rangle_{3,1} > 0$. In the Poincaré ball model, these spheres appear as Euclidean spheres intersecting the ideal boundary transversally.

Exercise 3.6. Show that $\tilde{S}_{\mathbb{H}^3}[m, q]$ is non-empty (and includes more than one point) if and only if $\langle m, m\rangle_{3,1} + q^2 > 0$.

3.2 Minkowski 5-space

We now introduce the Minkowski model of Möbius geometry of spheres. Let $\mathbb{R}^{4,1}$ be the Minkowski 5-space, equipped with the indefinite inner product $\langle \cdot, \cdot \rangle$ such that

$$\langle X, Y\rangle = -x_0y_0 + x_1y_1 + x_2y_2 + x_3y_3 + x_4y_4$$

for $X = (x_0, x_1, x_2, x_3, x_4)^t, Y = (y_0, y_1, y_2, y_3, y_4)^t \in \mathbb{R}^{4,1}$.

From the 4-dimensional lightcone

$$\mathcal{L} = \{X \in \mathbb{R}^{4.1} : \langle X, X\rangle = 0\},$$

we define the 3-dimensional spaceforms M_κ as

$$M_\kappa = \{X \in \mathcal{L} : \langle X, \mathfrak{q}_\kappa\rangle = -1\}$$

for some $\mathfrak{q}_\kappa \in \mathbb{R}^{4,1}$ such that $\langle \mathfrak{q}_\kappa, \mathfrak{q}_\kappa\rangle = -\kappa$.

After normalizing

$$\mathfrak{q}_\kappa = \left(\frac{1}{2}(\kappa + 1), \frac{1}{2}(\kappa - 1), 0, 0, 0\right)^t$$

by applying a suitable transformation $\mathrm{O}(4, 1)$, we have the following bijection for $\mathcal{R}_\kappa = \left(\mathbb{R}^3 \cup \{\infty\}\right) \setminus \left\{x : \langle x, x\rangle_3 = -\frac{1}{\kappa}\right\}$:

Lemma 3.7. *The map $\psi_\kappa : \mathcal{R}_\kappa \to M_\kappa$ defined by*

$$\psi_\kappa(x) = \frac{1}{1 + \kappa\langle x, x\rangle_2} \begin{pmatrix} 1 + \langle x, x\rangle_2 \\ 1 - \langle x, x\rangle_2 \\ 2x \end{pmatrix} \tag{3.1}$$

is a bijection for any choice of κ.

Exercise 3.8. Prove Lemma 3.7 by showing that $\phi_\kappa : M_\kappa \to \mathcal{R}_\kappa$ defined via

$$\phi_\kappa(X) = \frac{1}{x_0 + x_1}(x_2, x_3, x_4)^t \tag{3.2}$$

for $X = (x_0, x_1, x_2, x_3, x_4)^t$ satisfies $\psi_\kappa^{-1} = \phi_\kappa$.

We leave computing the metric of M_κ to an exercise.

Exercise 3.9. We compute the metric of M_κ as follows:

(1) Show that the tangent space of M_κ at X is

$$T_X M_\kappa = \left\{ \mathcal{T}_a = \tfrac{2}{(1+\kappa\langle x,x\rangle_3)^2} \begin{pmatrix} -(\kappa-1)\langle x,a\rangle_3 \\ -(\kappa+1)\langle x,a\rangle_3 \\ a + \kappa\langle x,x\rangle_3 a - 2\kappa\langle x,a\rangle_3 x \end{pmatrix} \right\} \tag{3.3}$$

for $a \in \mathcal{R}_\kappa$. (Hint: consider a curve $x(t) : (-\epsilon, \epsilon) \to \mathcal{R}_\kappa$ such that $X(0) = X$ for $X(t) := \psi_\kappa(x(t)) : (-\epsilon, \epsilon) \to M_\kappa$, and show that

$$X'(t) = \mathcal{T}_{x'},$$

where $'$ denotes differentiation with respect to t.)

(2) Verify

$$\langle \mathcal{T}_a, \mathcal{T}_b \rangle = \frac{4}{(1 + \kappa\langle x, x\rangle_3)^2}\langle a, b\rangle_3. \tag{3.4}$$

Exercise 3.10. We can also compute the metric of M_κ via the method analogous to the one used to show (2.9), by viewing ψ_κ as a coordinate chart: Compute $\partial_1\psi_\kappa$, $\partial_2\psi_\kappa$, and $\partial_3\psi_\kappa$ as in (2.8), and verify that

$$g_{M_\kappa} = \frac{4}{(1 + \kappa\langle x, x\rangle_3)^2}(\mathrm{d}x_1^2 + \mathrm{d}x_2^2 + \mathrm{d}x_3^2). \tag{3.5}$$

The form of the metric for M_κ gives us the following theorem:

Theorem 3.11. *M_κ has sectional curvature κ.*

3.3 Möbius subgeometries

We now explain how the 3-dimensional spaceforms with constant sectional curvatures are represented by M_κ, by looking at concrete examples. In particular, in the next example and exercises, we see how the Euclidean 3-space $\mathbb{R}^3$, the 3-sphere $\mathbb{S}^3$, and the hyperbolic 3-space $\mathbb{H}^3$ are obtained via M_κ for $\kappa = 0, 1, -1$, respectively.

Example 3.12. Let $\kappa = 1$, giving us that $\mathfrak{q}_\kappa = (1,0,0,0,0)^t$. Setting $X = (x_0, x_1, x_2, x_3, x_4)^t$, then $X \in M_1$ if and only if

$$-1 = \langle X, \mathfrak{q} \rangle = -x_0,$$

and

$$0 = \langle X, X \rangle = -1 + x_1^2 + x_2^2 + x_3^2 + x_4^2.$$

Therefore, $X = (1, x^t)^t \in M_1$ for $x = (x_1, x_2, x_3, x_4)$ if and only if

$$\langle x, x \rangle_4 = 1,$$

and we see that $x \in \mathbb{S}^3$.

Exercise 3.13. Show that $M_{-1} \cong \mathbb{H}^3$.

Exercise 3.14. For $\mathfrak{o}, \mathfrak{q} \in \mathcal{L}$ such that $\langle \mathfrak{o}, \mathfrak{q} \rangle = -1$, let M_0 be defined by

$$M_0 := \{X \in \mathcal{L} : \langle X, \mathfrak{q} \rangle = -1\}.$$

(1) Show that $\operatorname{span}\{\mathfrak{o}, \mathfrak{q}\} \cong \mathbb{R}^{1,1}$, and hence deduce that $\operatorname{span}\{\mathfrak{o}, \mathfrak{q}\}^\perp \cong \mathbb{R}^3$.

(2) Show that $\phi : \operatorname{span}\{\mathfrak{o}, \mathfrak{q}\}^\perp \to M_0$ is a bijection if

$$\phi(x) = x + \mathfrak{o} + \frac{1}{2}\langle x, x \rangle \mathfrak{q},$$

with inverse

$$\psi(X) = X - \mathfrak{o} + \langle X, \mathfrak{o} \rangle \mathfrak{q},$$

telling us that $M_0 \cong \mathbb{R}^3$.

As the metric (3.5) suggests, all 3-dimensional spaceforms M_κ are conformally equivalent. Observing that for any value of κ, ψ_κ maps any point $x \in \mathcal{R}_\kappa$ to a lightlike line defined by

$$\operatorname{span}\{1 + \langle x, x \rangle_3, 1 - \langle x, x \rangle_3, 2x^t)^t\},$$

we identify all the different spaceforms M_κ with the projective lightcone $\mathbb{P}(\mathcal{L})$, where

$$\mathbb{P}(\mathcal{L}) := \{\text{span}\{X\} : X \in \mathcal{L}\} = \{\text{null lines in } \mathbb{R}^{4,1}\}.$$

We call the 3-dimensional projective lightcone the *conformal 3-sphere*.

3.4 Spheres in Möbius geometry

Analogous to the circles case in Section 2.5, we define spheres $\tilde{S}$ in M_κ as

$$\tilde{S} := \{X \in M_\kappa : \langle X, S\rangle = 0\}$$

for some spacelike vector $S \in \mathbb{R}^{4,1}$. The scaling of S does not matter; hence, we will always assume that $\langle S, S\rangle = 1$.

In the next exercises, we verify that the above definition of spheres in M_κ is consistent with the definition of spheres in the 3-sphere, hyperbolic 3-space, and Euclidean 3-space.

Exercise 3.15. For a spacelike vector $S := (q, m_1, m_2, m_3, m_4)^t \in \mathbb{R}^{4,1}$, let $X \in M_1$, that is, $\langle X, \mathfrak{q}_1\rangle = -1$.

(1) Show that for $x = (x_1, x_2, x_3, x_4)^t \in \mathbb{S}^3$, $X = (1, x)^t$.

(2) Using Exercise 3.2, verify that $X = (1, x)^t \in \tilde{S}$ if and only if $x \in \tilde{S}_{\mathbb{S}^3}[m, q]$ for $m = (m_1, m_2, m_3, m_4)^t$.

Exercise 3.16. For a spacelike vector $S := (m_0, q, m_1, m_2, m_3)^t \in \mathbb{R}^{4,1}$, let $X \in M_{-1}$, i.e. $\langle X, \mathfrak{q}_{-1}\rangle = -1$.

(1) Show that for $x = (x_0, x_1, x_2, x_3)^t \in \mathbb{H}^3$, $X = (x_0, 1, x_1, x_2, x_3)^t$.

(2) Using Exercise 3.6, verify that $X \in \tilde{S}$ if and only if $x \in \tilde{S}_{\mathbb{S}^3}[m, q]$ for $m = (m_0, m_1, m_2, m_3)^t$.

Exercise 3.17. Let $S = (s_0, s_1, s_2, s_3, s_4)^t$ be a spacelike vector with $s_0 + s_1 \neq 0$, and $X \in M_0$. Using Example 2.15 as a hint, show that $X \in \tilde{S}$ if and only if $x = \phi_\kappa(X)$ satisfies

$$\left\langle x - \frac{s}{s_0 + s_1}, x - \frac{s}{s_0 + s_1} \right\rangle_2 = \frac{1}{(s_0 + s_1)^2},$$

where $s = (s_2, s_3, s_4)^t$.

Hence, the space of spheres is represented by the de Sitter 4-space $\mathbb{S}^{3,1}$ defined as

$$\mathbb{S}^{3,1} := \{S \in \mathbb{R}^{4,1} : \langle S, S\rangle = 1\}.$$

Remark 3.18. Using the definition of spheres, we can show that four distinct points in some spaceform always determine a sphere. Let x_1, x_2, x_3, x_4 be distinct points in some 3-dimensional spaceform with constant sectional curvature κ, and let $X_1, X_2, X_3, X_4 \in M_\kappa \subset \mathcal{L}$ be their lifts, respectively. Since X_1, X_2, X_3, and X_4 are all lightlike, we have that $\operatorname{span}\{X_1, X_2, X_3, X_4\}$ must have indefinite metric. Hence, we can choose a unit spacelike vector $S \in \mathbb{R}^{4,1}$ such that

$$S \notin \operatorname{span}\{X_1, X_2, X_3, X_4\} \quad \text{and} \quad S \perp \operatorname{span}\{X_1, X_2, X_3, X_4\}.$$

Then, we have that

$$X_1, X_2, X_3, X_4 \in \tilde{S} = \{X \in M_\kappa : \langle X, S\rangle = 0\},$$

telling us that X_1, X_2, X_3, X_4 are all in spheres determined by S.

Exercise 3.19. Let x_1, x_2, x_3, x_4 be generically-placed distinct points in some 3-dimensional spaceform with constant sectional curvature κ, and furthermore let $X_1, X_2, X_3, X_4 \in M_\kappa \subset \mathcal{L}$ be their lifts, respectively. Show that x_1, x_2, x_3, x_4 are concircular if and only if X_1, X_2, X_3, X_4 are linearly dependent.

3.5 Möbius transformations

Möbius transformations map the conformal 3-sphere to the conformal 3-sphere, such that spheres get mapped to spheres. Since the space of spheres is $\mathbb{S}^{3,1}$, we can immediately deduce that $\mathrm{O}(4,1)$ acts on the projective lightcone $\mathbb{P}(\mathcal{L})$ by the usual matrix multiplication, and maps spheres to spheres. Therefore, we see that Möbius transformations are represented by the Lie group $\mathrm{O}(4,1)$.

On the other hand, it is a well-known fact that Möbius transformations in $\mathbb{R}^3 \cup \{\infty\}$ are generated by reflection, homothety, rotation, translation, and inversion. In this section, we present a few examples of these Möbius transformations of $\mathbb{R}^3 \cup \{\infty\}$ in terms of $\mathrm{O}(4,1)$ matrices. In the next examples, let us take a point $x = (x_1, x_2, x_3)^t \in \mathbb{R}^3$ and its lift into the projective lightcone $\operatorname{span}\{X\} = \operatorname{span}\{(1 + \langle x, x\rangle_3, 1 - \langle x, x\rangle_3, 2x^t)^t\} \in \mathbb{P}(\mathcal{L})$.

Example 3.20. If we define

$$A_1 := \begin{pmatrix} 1 & 0 & 0 & 0 & 0 \\ 0 & 1 & 0 & 0 & 0 \\ 0 & 0 & -1 & 0 & 0 \\ 0 & 0 & 0 & 1 & 0 \\ 0 & 0 & 0 & 0 & 1 \end{pmatrix} \in \mathrm{O}(4,1),$$

then we have that

$$\begin{aligned} \operatorname{span}\{A_1 X\} &= \operatorname{span}\{(1+\langle x,x\rangle_3, 1-\langle x,x\rangle_3, -2x_1, 2x_2, 2x_3)^t\} \\ &= \{t(1+\langle x,x\rangle_3, 1-\langle x,x\rangle_3, -2x_1, 2x_2, 2x_3)^t : t \in \mathbb{R}\} \\ &\in \mathbb{P}(\mathcal{L}). \end{aligned}$$

To project this back down to $M_0 \cong \mathbb{R}^3$, we calculate that for $t = 1$,

$$\langle tA_1 X, \mathfrak{q}_0 \rangle = -1.$$

Then using ϕ_κ as defined in (3.2), we see that $A_1 X$ is projected as $(-x_1, x_2, x_3)^t \in \mathbb{R}^3$, telling us that A_1 is a reflection with respect to the x_2x_3-plane.

Example 3.21. Defining

$$A_2 := \begin{pmatrix} 1 & 0 & 0 & 0 & 0 \\ 0 & -1 & 0 & 0 & 0 \\ 0 & 0 & 1 & 0 & 0 \\ 0 & 0 & 0 & 1 & 0 \\ 0 & 0 & 0 & 0 & 1 \end{pmatrix} \in \mathrm{O}(4,1),$$

we have that

$$\operatorname{span}\{A_2 X\} = \{t(1+\langle x,x\rangle_3, -1+\langle x,x\rangle_3, 2x^t)^t : t \in \mathbb{R}\}.$$

Then we can verify that for $t = \frac{1}{\langle x,x\rangle_3}$, $\langle tA_2 X, \mathfrak{q}_0 \rangle = -1$. Projecting this down, we see that A_2 corresponds to the map

$$x \mapsto \frac{1}{\langle x,x\rangle_3} x,$$

an inversion.

Exercise 3.22. Show that for

$$A_3 := \begin{pmatrix} 1 & 0 & 0 & 0 & 0 \\ 0 & 1 & 0 & 0 & 0 \\ 0 & 0 & \cos\theta & -\sin\theta & 0 \\ 0 & 0 & \sin\theta & \cos\theta & 0 \\ 0 & 0 & 0 & 0 & 1 \end{pmatrix} \in \mathrm{O}(4,1),$$

A_3 acting on the projective lightcone $\mathbb{P}(\mathcal{L})$ is equivalent a rotation in $\mathbb{R}^3 \cong M_0$ with respect to the x_3-axis, that is,

$$(x_1, x_2, x_3)^t \mapsto (x_1\cos\theta - x_2\sin\theta, x_1\sin\theta + x_2\cos\theta, x_3)^t.$$

Exercise 3.23. Show that for

$$A_4 := \begin{pmatrix} \cosh(\log r) & -\sinh(\log r) & 0 & 0 & 0 \\ -\sinh(\log r) & \cosh(\log r) & 0 & 0 & 0 \\ 0 & 0 & 1 & 0 & 0 \\ 0 & 0 & 0 & 1 & 0 \\ 0 & 0 & 0 & 0 & 1 \end{pmatrix} \in \mathrm{O}(4,1),$$

A_4 acting on the projective lightcone $\mathbb{P}(\mathcal{L})$ is equivalent a homothety in $\mathbb{R}^3 \cong M_0$ with homothety factor $r > 0$, that is,

$$x \mapsto rx.$$

Exercise 3.24. For $y = (y_1, y_2, y_3)^t \in \mathbb{R}^3$, let A_5 be defined via

$$A_5 := \begin{pmatrix} 1 + \frac{1}{2}\langle y, y\rangle_3 & \frac{1}{2}\langle y, y\rangle_3 & y_1 & y_2 & y_3 \\ -\frac{1}{2}\langle y, y\rangle_3 & 1 - \frac{1}{2}\langle y, y\rangle_3 & -y_1 & -y_2 & -y_3 \\ y_1 & y_1 & 1 & 0 & 0 \\ y_2 & y_2 & 0 & 1 & 0 \\ y_3 & y_3 & 0 & 0 & 1 \end{pmatrix} \in \mathrm{O}(4,1).$$

Show that A_5 acting on the projective lightcone $\mathbb{P}(\mathcal{L})$ is equivalent a translation in $\mathbb{R}^3 \cong M_0$ by y, that is,

$$x \mapsto x + y.$$

3.6 Cross-ratios

Cross-ratios are projectively invariant, and their natural treatment comes from the context of projective geometry. The fact that we have a projective model of Möbius geometry alludes to the fact that cross-ratios are Möbius invariant, since Möbius transformations are projective transformations. However, in these notes, we show the Möbius invariance the cross-ratios with the tools we have at hand.

Let $X_1, X_2, X_3, X_4 \in \mathcal{L}$, and define the *cross-ratio* of the four points to be

$$\operatorname{cr}(X_1, X_2, X_3, X_4) := \frac{s_{12}s_{34} + s_{14}s_{23} - s_{13}s_{24} \pm \sqrt{\mathcal{E}}}{2s_{14}s_{23}} \tag{3.6}$$

where $s_{ij} = \langle X_i, X_j \rangle$, and

$$\mathcal{E} = s_{12}^2 s_{34}^2 + s_{13}^2 s_{24}^2 + s_{14}^2 s_{23}^2 - 2s_{13}s_{14}s_{23}s_{24} - 2s_{12}s_{14}s_{23}s_{34} - 2s_{12}s_{13}s_{24}s_{34} \leq 0.$$

Note that this definition is well-defined only up to complex conjugation; however, as in [2], we will refer to the cross-ratios as if they are a complex number, and we ask the readers to remember that the either member of the complex conjugate pair can be the cross-ratio of given four points.

First, we check that this definition coincides with the cross-ratio of four-points in the complex plane $\mathbb{C}$. Recall that for $z_1, z_2, z_3, z_4 \in \mathbb{C}$, we have that the cross-ratios of four points z_1, z_2, z_3, z_4 are defined as

$$\operatorname{cr}(z_1, z_2, z_3, z_4) = \frac{z_1 - z_2}{z_2 - z_3}\frac{z_3 - z_4}{z_4 - z_1}.$$

Using the correspondence $\mathbb{C} \cong \mathbb{R}^2 \subset \mathbb{R}^3 \cong M_0$ via

$$\begin{aligned} \mathbb{C} \ni x_1 + \sqrt{-1}x_2 &\sim x = (x_1, x_2, 0)^t \in \mathbb{R}^3 \\ &\sim X = (1 + \langle x, x \rangle_3, 1 - \langle x, x \rangle_3, 2x^t)^t \in M_0, \end{aligned}$$

we can directly calculate and verify the following lemma:

Lemma 3.25. *For $z_1, z_2, z_3, z_4 \in \mathbb{C}$ and corresponding $X_1, X_2, X_3, X_4 \in M_0$, we have that*

$$\operatorname{cr}(z_1, z_2, z_3, z_4) = \operatorname{cr}(X_1, X_2, X_3, X_4).$$

The form of the cross-ratio defined in (3.6) tells us two things: first, since the expression is written completely in terms of the inner product of lightlike vectors

in $\mathbb{R}^{4,1}$, applying any Möbius transformation to the four lightlike vectors will not change the value under consideration, that is, for any $A \in \mathrm{O}(4,1)$,

$$\mathrm{cr}(X_1, X_2, X_3, X_4) = \mathrm{cr}(AX_1, AX_2, AX_3, AX_4),$$

giving us the Möbius invariance of cross-ratios.

Furthermore, scaling $X_1, X_2, X_3, X_4 \in \mathcal{L}$ by $\alpha_1, \alpha_2, \alpha_3, \alpha_4 \in \mathbb{R}$, respectively, does not change the value of the cross-ratio, i.e.

$$\mathrm{cr}(X_1, X_2, X_3, X_4) = \mathrm{cr}(\alpha_1 X_1, \alpha_2 X_2, \alpha_3 X_3, \alpha_4 X_4).$$

Therefore, cross-ratios are notions that are well-defined not only for four points in each choice of spaceform, but also for four points in the conformal 3-sphere $\mathbb{P}(\mathcal{L})$ (or four null lines in $\mathcal{L}$). This is the projective invariance of cross-ratios. We recommend the readers to examine a more formal discussion of cross-ratios through many textbooks on projective geometry; for example, [36] has insightful description of projective geometry and cross-ratios.

Remark 3.26. Let $x_1, x_2, x_3, x_4 \in \mathbb{R}^3$ with lifts $X_1, X_2, X_3, X_4 \in M_0$. One can also calculate the cross-ratio of these four points in the following way: Since four points always determine a sphere (see Remark 3.18), we can find a Möbius transformation mapping the sphere to a plane in $\mathbb{R}^3$. Identifying the plane with the complex plane, x_1, x_2, x_3, x_4 can be identified with $z_1, z_2, z_3, z_4 \in \mathbb{C}$, respectively. Then the Möbius invariance of cross-ratios and Lemma 3.25 guarantees us that

$$\mathrm{cr}(X_1, X_2, X_3, X_4) = \frac{z_1 - z_2}{z_2 - z_3}\frac{z_3 - z_4}{z_4 - z_1} = \mathrm{cr}(z_1, z_2, z_3, z_4).$$

Exercise 3.27. Show that $X_1, X_2, X_3, X_4 \in \mathbb{P}(\mathcal{L})$ are concircular if and only if $\mathrm{cr}(X_1, X_2, X_3, X_4) \in \mathbb{R}$. (Hint: One way to show this is to use the fact that the cross-ratio is real if and only if $\mathcal{E} = 0$. One could also show this for four points in the complex plane, and use Remark 3.26.)

Remark 3.28. Let $x_1, x_2, x_3, x_4 \in \mathbb{R}^3$ with lifts $X_1, X_2, X_3, X_4 \in M_0$. Then we have the identification

$$\begin{aligned}\mathbb{R}^3 \ni x = (a,b,c)^t &\sim h = ai + bj + ck \in \operatorname{Im}\mathbb{H} \\ &\sim A = \begin{pmatrix} \sqrt{-1}c & a + \sqrt{-1}b \\ -a + \sqrt{-1}b & -\sqrt{-1}c \end{pmatrix} \in \mathfrak{su}(2),\end{aligned}$$

where $\mathbb{H}$ denotes the set of quaternions, and $\mathfrak{su}(2)$ is the Lie algebra associated with the special unitary group SU(2). Then using quaternionic multiplication and inverse, one can compute that

$$\mathrm{cr}(X_1, X_2, X_3, X_4) = (h_1 - h_2)(h_2 - h_3)^{-1}(h_3 - h_4)(h_4 - h_1)^{-1},$$

or using the usual matrix multiplication and inverse, one has that

$$\mathrm{cr}(X_1, X_2, X_3, X_4) = (A_1 - A_2)(A_2 - A_3)^{-1}(A_3 - A_4)(A_4 - A_1)^{-1}.$$

4 Isothermic surfaces

In this section, we introduce isothermic surfaces within the context of conformal geometry.

4.1 Surface theory

We briefly review the surface theory in three dimensional spaceforms. In the following discussions and throughout these notes, let $\Sigma \subset \mathbb{R}^2$ be a simply-connected domain.

4.1.1 Surfaces in Euclidean space

Let $x : \Sigma \to \mathbb{R}^3$ be a smooth surface with normal $n : \Sigma \to \mathbb{S}^2$, that is,

$$n = \frac{x_u \times x_v}{\sqrt{\langle x_u \times x_v, x_u \times x_v \rangle_3}},$$

where $x_u = \frac{\partial}{\partial u} x$ denotes the partial derivative of x with respect to u. The *first fundamental form* of a surface x is

$$\mathrm{I} = \begin{pmatrix} \langle x_u, x_u \rangle_3 & \langle x_u, x_v \rangle_3 \\ \langle x_v, x_u \rangle_3 & \langle x_v, x_v \rangle_3 \end{pmatrix} =: \begin{pmatrix} g_{11} & g_{12} \\ g_{21} & g_{22} \end{pmatrix}, \tag{4.1}$$

while the *second fundamental form* is

$$\mathrm{II} = \begin{pmatrix} \langle x_{uu}, n \rangle_3 & \langle x_{uv}, n \rangle_3 \\ \langle x_{vu}, n \rangle_3 & \langle x_{vv}, n \rangle_3 \end{pmatrix} =: \begin{pmatrix} b_{11} & b_{12} \\ b_{21} & b_{22} \end{pmatrix}. \tag{4.2}$$

We can calculate that for $n_u = ax_u + cx_v$ and $n_v = bx_u + dx_v$,

$$\begin{aligned}\mathrm{II} &= -\begin{pmatrix}\langle n_u, x_u\rangle_3 & \langle n_v, x_u\rangle_3 \\ \langle n_u, x_v\rangle_3 & \langle n_v, x_v\rangle_3\end{pmatrix} = \begin{pmatrix}ag_{11} + cg_{12} & bg_{11} + dg_{12} \\ ag_{12} + cg_{22} & bg_{12} + dg_{22}\end{pmatrix} \\ &= -\mathrm{I}\begin{pmatrix}a & b \\ c & d\end{pmatrix},\end{aligned}$$

where we used the fact that $g_{12} = g_{21}$. Therefore, we have

$$\begin{pmatrix}a & b \\ c & d\end{pmatrix} = -\mathrm{I}^{-1}\mathrm{II}.$$

The eigenvectors of $\mathrm{I}^{-1}\mathrm{II}$ tell us directions where n bends straightest, i.e. principal curvature directions, and the eigenvalues give us the principal curvatures.

Exercise 4.1. Calculate the first and second fundamental form of the following surfaces in the Euclidean space:

(1) the plane, given by $x(u, v) = (u, v, 0)^t$,

(2) circular cylinder, given by $x(u, v) = (\cos u, \sin u, v)^t$, and

(3) catenoid, given by $x(u, v) = (2\cosh v \cos u, 2\cosh v \sin u, 2v)^t$.

4.1.2 Surfaces in the 3-sphere

Now let $x : \Sigma \to \mathbb{S}^3$ be a surface in the 3-sphere. The normal n is given by

$$n(u, v) \in T_{x(u,v)}\mathbb{S}^3 \quad \text{and} \quad \langle n, x_u\rangle_4 = 0 = \langle n, x_v\rangle_4$$

at each point $(u, v) \in \Sigma$, so that

$$x, \operatorname{span}\{x_u, x_v\}, n \text{ are all perpendicular.}$$

The first fundamental form I and second fundamental form II for surfaces in the 3-sphere are then calculated the same way as in the Euclidean case, (4.1) and (4.2), respectively.

Exercise 4.2. Calculate the first and second fundamental form of the following surfaces in the 3-sphere:

(1) equatorial sphere, given by

$$x(u,v) = (\cos u \cos v, \cos u \sin v, \sin u, 0)^t,$$

and

(2) Ciifford torus, given by $x(u,v) = \frac{1}{\sqrt{2}}(\cos u, \sin u, \cos v, \sin v)^t$.

4.1.3 Surfaces in the hyperbolic space

For a surface $x : \Sigma \to \mathbb{H}^3$, the normal n is given similarly to that in the 3-sphere,

$$n(u,v) \in T_{x(u,v)}\mathbb{S}^3 \quad \text{and} \quad \langle n, x_u\rangle_{3,1} = 0 = \langle n, x_v\rangle_{3,1},$$

so that

$$x, \text{span}\,\{x_u, x_v\}, n \text{ are all perpendicular}$$

with respect to the inner product $\langle\cdot,\cdot\rangle_{3,1}$. Using the normal n, the first fundamental form I and second fundamental form II for surfaces in the 3-sphere are again calculated the same way as in the Euclidean case, (4.1) and (4.2), respectively.

Exercise 4.3. Calculate the first and second fundamental form of the following surfaces in the hyperbolic space:

(1) equatorial sphere, given by

$$x(u,v) = (\cosh u, \sinh u \cos v, \sinh u \sin v, 0)^t,$$

and

(2) sphere, given by $x(u,v) = (a\cosh u, a\sinh u \cos u, a \sinh u \sin v, b)^t$ for $b^2 - a^2 = -1$.

4.2 Isothermic surfaces in spaceforms

Given a surface without umbilics (i.e. a surface with distinct principal curvatures on Σ) in some spaceform of constant sectional curvature, one can always find *curvature line coordinates* $(u,v) \in \Sigma$, i.e.

$$g_{12} = 0 \quad \text{and} \quad b_{12} = 0,$$

or

$$x_u \perp x_v \quad \text{and} \quad x_{uv} \in \text{span}\{x_u, x_v\}$$

where the perpendicularity depends on the ambient space. On the other hand, one can also always find *conformal coordinates* $(u, v) \in \Sigma$, that is,

$$g_{11} = g_{22} \quad \text{and} \quad g_{12} = 0.$$

Definition 4.4 ([6])**.** A surface is *isothermic* if there exist conformal curvature line coordinates, or *isothermic coordinates*.

Exercise 4.5. Check that all of the surfaces in Exercises 4.1, 4.2, 4.3 are isothermic. (Note: some surfaces may require a coordinate stretching.)

We now characterize the isothermicity of a surface via the cross-ratios defined in Section 3.6. To do this, let x be a surface in some spaceform with constant sectional curvature, parametrized by curvature line coordinates $(u, v) \in \Sigma$, and $X : \Sigma \to M_\kappa$ be its lift. For some $\epsilon > 0$, write $X(u, v), X(u + \epsilon, v), X(u + \epsilon, v + \epsilon), X(u, v + \epsilon)$ as X_1, X_2, X_3, X_4, respectively. Then from (3.6),

$$\mathrm{cr}_\epsilon := \mathrm{cr}(X_1, X_2, X_3, X_4) = \frac{\epsilon^{-4}}{\epsilon^{-4}} \frac{s_{12}s_{34} + s_{14}s_{23} - s_{13}s_{24} \pm \sqrt{\mathcal{E}}}{2s_{14}s_{23}}.$$

Note that for any $X_1, X_2, X_3 \in \mathcal{L}$, we have

$$\langle X_1, X_2 \rangle = -\frac{1}{2}\langle X_2 - X_1, X_2 - X_1 \rangle$$

and that

$$\begin{aligned}
\langle X_1, X_3 \rangle &= -\frac{1}{2}\langle X_3 - X_1, X_3 - X_1 \rangle \\
&= -\frac{1}{2}\langle X_3 - X_2 + X_2 - X_1, X_3 - X_2 + X_2 - X_1 \rangle \\
&= -\frac{1}{2}\big(\langle X_3 - X_2, X_3 - X_2 \rangle + 2\langle X_3 - X_2, X_2 - X_1 \rangle \\
&\qquad\qquad + \langle X_2 - X_1, X_2 - X_1 \rangle\big).
\end{aligned}$$

Using these expressions, we can calculate that

$$\lim_{\epsilon \to 0} \mathcal{E} = 0,$$

and that

$$\lim_{\epsilon \to 0} \mathrm{cr}_\epsilon = \frac{\langle X_u, X_u \rangle^2 + \langle X_v, X_v \rangle^2 - (\langle X_u, X_u \rangle + 2\langle X_u, X_v \rangle + \langle X_v, X_v \rangle)^2}{2\langle X_v, X_v \rangle^2}.$$

Finally, using (3.4), we learn that

$$\lim_{\epsilon \to 0} \mathrm{cr}_\epsilon = \frac{g_{11}^2 + g_{22}^2 - (g_{11} + g_{22})^2}{2g_{22}^2} = \frac{-2g_{11}g_{22}}{2g_{22}^2} = -\frac{g_{11}}{g_{22}}.$$

Lemma 4.6. *Let x be a surface parametrized by curvature line coordinates (u, v), and let X be its lift into M_κ. Then,*

$$\lim_{\epsilon \to 0} \mathrm{cr}_\epsilon = -\frac{g_{11}}{g_{22}}.$$

Now we turn to the condition that characterizes the isothermicity of a surface parametrized by curvature lines.

Lemma 4.7. *Let x be a surface parametrized by curvature line coordinates (u, v). x is isothermic if and only if*

$$\frac{g_{11}}{g_{22}} = \frac{\alpha(u)}{\beta(v)} \tag{4.3}$$

for some strictly positive functions α and β.

Proof. If the surface is isothermic, then $g_{11} = g_{22}$, so one direction is trivially true. Now suppose that (4.3) holds. Define

$$\tilde{u}(u) := \int \sqrt{\alpha(u)}\,\mathrm{d}u \quad \text{and} \quad \tilde{v}(v) := \int \sqrt{\beta(v)}\,\mathrm{d}v$$

so that

$$\left(\frac{\mathrm{d}\tilde{u}}{\mathrm{d}u}\right)^2 = \alpha(u) \quad \text{and} \quad \left(\frac{\mathrm{d}\tilde{v}}{\mathrm{d}v}\right)^2 = \beta(v).$$

Since α and β are strictly positive, $\tilde{u}$ and $\tilde{v}$ are monotone increasing functions. Therefore, we use $\tilde{u}$ and $\tilde{v}$ as coordinate change functions and consider $x(\tilde{u}, \tilde{v})$. Labeling the coefficients of first and second fundamental form calculated with respect to coordinates $(\tilde{u}, \tilde{v})$ as $\tilde{g}_{ij}$ and $\tilde{b}_{ij}$, respectively, the chain rule then tells us that

$$\tilde{g}_{11} = g_{11}\left(\frac{\mathrm{d}u}{\mathrm{d}\tilde{u}}\right)^2 = \frac{g_{11}}{\alpha(u)} = \frac{g_{22}}{\beta(v)} = g_{22}\left(\frac{\mathrm{d}\tilde{v}}{\mathrm{d}v}\right)^2 = \tilde{g}_{22},$$

while

$$\tilde{g}_{12} = g_{12}\frac{\mathrm{d}u}{\mathrm{d}\tilde{u}}\frac{\mathrm{d}v}{\mathrm{d}\tilde{v}} = 0 = b_{12}\frac{\mathrm{d}u}{\mathrm{d}\tilde{u}}\frac{\mathrm{d}v}{\mathrm{d}\tilde{v}} = \tilde{b}_{12}.$$

Hence, $(\tilde{u}, \tilde{v})$ are isothermic coordinates for x. □

Combining the two lemmata, we arrive at the following important characterization of isothermic surfaces:

Theorem 4.8. *Let x be a surface parametrized by curvature line coordinates (u, v) and X be its lift into M_κ. Then x is isothermic if and only if*

$$\lim_{\epsilon \to 0} \mathrm{cr}_\epsilon = -\frac{\alpha(u)}{\beta(v)} \tag{4.4}$$

for some strictly positive functions α, β.

The cross-ratios characterization of isothermic surfaces lets us apply the properties of cross-ratios to the theory of isothermic surfaces: First, noting that Möbius transformations are diffeomorphisms which preserve the order of contact (see [39, Proposition 2.6], for example), we see that Möbius transformations preserve curvature lines. Since cross-ratios are also Möbius invariant, we see that isothermicity is also Möbius invariant.

Furthermore, the projective invariance of cross-ratios tells us that above characterization of isothermic surfaces is projectively invariant as well: $X(u, v)$ is isothermic if and only if $c(u, v)X(u, v)$ is isothermic.

Therefore, we see that isothermicity is a well-defined notion for surfaces in the conformal 3-sphere, letting us treat isothermic surfaces in any spaceforms with constant sectional curvature uniformly.

4.3 Discrete isothermic surfaces in spaceforms

In this section, we describe how discrete isothermic surfaces are defined in Möbius geometry. In the discretization process of a smooth geometric object (usually, a class of surfaces), one not only needs to define the discrete object, but also justify the definition by recovering a comprehensive theory of the geometric object in question in the language of discrete differential geometry. For example, the definition of discrete isothermic surfaces (which we describe below) has been shown to satisfy the following characteristics, like for the smooth counterpart, within the context of discrete differential geometry: discrete isothermic surfaces

- include many well-known subclasses such as discrete minimal surfaces or discrete cmc surfaces (with discrete mean curvature having its own justification) [2], [29],
- arises from the permutability of Darboux transformations for smooth isothermic surfaces [26],

- are characterized by the existence of Christoffel transformations [2, Theorem 6],
- allow for second order deformations in Möbius geometry via Calapso transformations [28, Definition 3.11], and
- admit Darboux transformations having discrete Ribaucour sphere congruences [29].

We introduce how one can recover the definition of discrete isothermic surfaces within the context of Möbius geometry, so that the notion is extended to surfaces in all spaceforms with constant sectional curvature.

For $(m,n) \in \mathbb{Z}^2$, and let $f : \mathbb{Z}^2 \to \mathbb{R}^3, \mathbb{S}^3$ or $\mathbb{H}^3$, and $F : \mathbb{Z}^2 \to M_\kappa$ be the lift of f into the lightcone. In the discrete case, we write $f_{m,n} = f(m,n)$, and we also sometimes abbreviate $f(m,n), f(m+1,n), f(m+1,n+1), f(m,n+1)$ as f_i, f_j, f_k, f_ℓ, respectively. Finally, we call $(ijk\ell)$ in the domain an *elementary quadrilateral*.

The uniform approach for studying smooth isothermic surfaces in conformal 3-sphere gives a hint to a uniform discretization of isothermic surfaces in spaceforms. The cross-ratios characterization in Theorem 4.8 gave us the projective invariance and Möbius invariance of isothermic surfaces for free: therefore, we use the cross-ratios condition (4.4) as the starting point of our discretization:

From (4.4), we replace $X(u,v)$ by $F(m,n)$, and drop the limit (since limits do not exist in the discrete case) to get

$$\operatorname{cr}(F_{m,n}, F_{m+\epsilon,n}, F_{m+\epsilon,n+\epsilon}, F_{m,n+\epsilon}) = -\frac{\alpha_m}{\beta_n}.$$

Finally, letting $\epsilon = 1$ since our domain is $\mathbb{Z}^2$, we get the definition of discrete isothermic surfaces in [2, Definition 1] and [5, Corollary 3.5]:

Definition 4.9. Let f be a discrete surface over $\mathbb{Z}^2$ into some spaceform with constant sectional curvature, and let $F : \mathbb{Z}^2 \to M_\kappa$ be its lift. Then f is isothermic if, on any elementary quadrilateral,

$$\operatorname{cr}(F_{m,n}, F_{m+1,n}, F_{m+1,n+1}, F_{m,n+1}) = -\frac{\alpha_m}{\beta_n}.$$

Note that in the statement for Lemma 4.6, if we assume isothermicity, or conformal curvature line condition, then $g_{11} = g_{22}$, so

$$\lim_{\epsilon \to 0} \operatorname{cr}_\epsilon = -1.$$

Discretizing this relation gives:

Definition 4.10. Let f be a discrete surface over $\mathbb{Z}^2$ into some spaceform with constant sectional curvature, and let $F : \mathbb{Z}^2 \to M_\kappa$ be its lift. Then f is isothermic if, on any elementary quadrilateral,

$$\mathrm{cr}(F_{m,n}, F_{m+1,n}, F_{m+1,n+1}, F_{m,n+1}) = -1.$$

Definition 4.9 of discrete isothermic surfaces is called the definition in the *broad sense*, while that in Definition 4.10 is called the definition in the *narrow sense*.

Remark 4.11. The difference arises from the fact that unlike smooth counterparts, discrete surfaces cannot be readily reparametrized. For example, one must use the broad sense definition to show that discrete isothermic surfaces admit Calapso transformations.

Exercise 4.12 (Discrete Clifford torus with non-constant cross-ratios)**.** We let m_{per}, n_{per} be some constants (representing the length of the periodicity in the m, n, directions, respectively, and consider

$$f(m,n) = \left(\cos\tfrac{2\pi n}{n_{per}}\left(\sqrt{2}+\cos\tfrac{2\pi m}{m_{per}}\right), \sin\tfrac{2\pi n}{n_{per}}\left(\sqrt{2}+\cos\tfrac{2\pi m}{m_{per}}\right), \sin\tfrac{2\pi m}{m_{per}}\right).$$

Show that f has cross-ratios

$$\mathrm{cr}(F_i, F_j, F_k, F_\ell) = \frac{-\sin^2\frac{\pi}{m_{per}}}{\sin^2\frac{\pi}{n_{per}}\left(\sqrt{2}+\cos\frac{2\pi m}{m_{per}}\right)\left(\sqrt{2}+\cos\frac{2\pi(m+1)}{m_{per}}\right)}.$$

Exercise 4.13 (Discrete Clifford torus with constant cross-ratios)**.** Consider

$$f(m,n) = \frac{1}{\sqrt{2}+\cos\frac{2\pi m}{m_{per}}}\left(\sin\tfrac{2\pi m}{m_{per}}, \cos\tfrac{2\pi n}{n_{per}}, \sin\tfrac{2\pi n}{n_{per}}\right).$$

Show that F has cross-ratios

$$\mathrm{cr}(F_i, F_j, F_k, F_\ell) = -1.$$

5 Recommended further selected readings

Here, we recommend some literature for those interested in further study of surface theory and discretizations in sphere geometries. The list here is by no

means exhaustive, as we only list the works that have had a direct influence in the creation of these notes.

For a more comprehensive introduction to Möbius geometry, using both the Minkowski model and the quaternionic model, we recommend the encyclopedic book [27] by Udo Hertrich-Jeromin. The book generalizes the discussion of Möbius geometry to the conformal n-sphere, and discusses both smooth and discrete isothermicity. Another remarkable feature of the book is the explanation of the historical context of isothermic surfaces and their transformations.

Isothermic surfaces constitute an integrable class of surfaces, as shown by [22], and hence their transformations can be explained via the dressing methods of [40]. The work by Francis Burstall [7] takes this point of view, and describes isothermic surfaces in the general conformal n-sphere using Clifford algebra. Furthermore, this work shows that the the simple factor dressings of Terng and Uhlenbeck [37, 38] in the context of isothermic surfaces amounts to Darboux transformations.

The unified description for the theory of conformal geometry and isothermic surfaces can be obtained if one utilizes the machinery of gauge theoretic and vector bundle approach. This is the viewpoint taken by Francis Burstall and David Calderbank in their work [9, 10].

One can even generalize the concept of isothermicity further, and the work of Francis Burstall, Neil Donaldson, Franz Pedit, and Ulrich Pinkall does exactly this in [12] by defining isothermicity in symmetric R-spaces, offering conformal geometry as an example. Furthermore, they relate the discrete theory to the smooth theory in the paper.

For a more elementary introduction, we recommend the excellent notes by Francis Burstall [8]. In these notes, the theory of integrable surfaces is presented via the existence of a 1-parameter family of flat connections, and describes the transformations in this context, providing K-surfaces (surfaces with negative constant Gaussian curvature) and isothermic surfaces as examples, including the formulation of the well-known Bäcklund transformations and Darboux transformations, respectively.

Another work highly suited for understanding the theory of conformal geometry in the Minkowski picture is the doctoral thesis [34] of Susana Santos. The thesis contains numerous explicit calculations that should help anyone interested in the Minkowski model of Möbius geometry.

Within the context of 1-parameter family of flat connections of isothermic surfaces arises the concept of polynomial conserved quantities: these serve as a powerful tool for identifying certain classes of surfaces, including minimal and constant mean curvature surfaces, from the class of isothermic surfaces. A paper by Francis Burstall and Susana Santos develops the theory of polynomial conserved quantities for isothermic surfaces and their behavior under transformations in [18].

Möbius geometry is not too distant from Lie sphere geometry: if Möbius geometry is concerned with transformations that map points to points, and spheres to spheres, Lie sphere geometry generalizes Möbius geometry in that it is concerned with transformations that map points and spheres to points and spheres. (In fact, Möbius geometry is a subgeometry of Lie sphere geometry.) One has the classical work [1] by Wilhelm Blaschke, and also Thomas Cecil's recent book [20] serves as a great introduction to Lie sphere geometry.

In Möbius geometry, isothermic surfaces are the deformable class of surfaces, as shown in [19]; in Lie sphere geometry, the class of Ω-surfaces (defined by Demoulin in [23–25]) plays the role of the deformable class of surfaces [1]. Ω-surfaces can be characterized as having a pair of isothermic sphere congruences; therefore, the rich theory of isothermic surfaces can be extended to surfaces that are not isothermic, but are Ω: for example, flat surfaces and linear Weingarten surfaces. For a clean description of Ω-surfaces utilizing the gauge theoretic tools and vector bundles, we recommend the doctoral thesis [32] by Mason Pember.

In fact, using the polynomial conserved quantities, one can identify certain classes of surfaces among Ω-surfaces as well. Francis Burstall, Udo Hertrich-Jeromin, and the second author characterizes flat surfaces in $\mathbb{H}^3$ in [15] and linear Weingarten surfaces in [16]. Then, Francis Burstall, Udo Hertrich-Jeromin, Mason Pember, and the second author further characterizes isothermic surfaces, Guichard surfaces, and L-isothermic surfaces as subclasses of Ω-surfaces via polynomial conserved quantites in [13].

Moving onto discrete surface theory, one must start from the broadly encompassing book [4] written by Alexander Bobenko and Yuri Suris. The book contains results of many different papers that formulated the theory of discrete differential geometry with integrability at its heart, including [3] on discrete K-surfaces, [2] on discrete isothermic surfaces and discrete minimal nets, [5] on the Möbius geometric characterization of discrete isothermic surfaces, [33, 35] on discrete mean

and Gaussian curvature via discrete Steiner's formula, to name a few.

Among the subclasses of discrete isothermic surfaces, various classes have been discretized: Building on the definition of discrete minimal surfaces of Bobenko and Pinkall in [2], Udo Hertrich-Jeromin recovers the Calapso transformations for discrete isothermic surfaces, and defines discrete constant mean curvature 1 surfaces in [28]. Then using the cmc-1 surfaces in $\mathbb{H}^3$, Tim Hoffmann, the second author, Takeshi Sasaki, and Masaaki Yoshida discretizes the flat surfaces and linear Weingarten surfaces of Bryant type in $\mathbb{H}^3$ in [31].

Using a bit of a different approach, discrete constant mean curvature surfaces in the Euclidean space are defined in [29] by Udo Hertrich-Jeromin, Tim Hoffman, and Ulrich Pinkall, using a characterization for smooth constant mean curvature surfaces found in [30].

The flat connections approach is again well-suited to studying the theory of discrete isothermic surfaces and their transformations. This approach is explored in [17] by Francis Burstall, Udo Hertrich-Jeromin, the second author, and Susana Santos, where they characterize discrete isothermic surfaces in the Minkowski model of Möbius geometry via the existence of a 1-parameter family of discrete flat connections, and define discrete polynomial conserved quantities to identify discrete constant mean curvature surfaces among discrete isothermic surfaces, making contact with the previous definition of discrete cmc surfaces.

With the concept of polynomial conserved quantities available in the discrete setting, Francis Burstall, Udo Hertrich-Jeromin, and the second author defines discrete linear Weingarten surfaces in the context of Lie sphere geometry in the work [14]. Discrete Ω-surfaces are lightly touched upon here, and a more comprehensive approach to discrete Ω-surfaces is done in [11].

Finally, for those who found the approach and explanation in these notes helpful in studying Möbius geometry, we recommend reading [21]. The work uses a similar approach to explaining isothermic surfaces and their transformations in Möbius geometry and Ω-surfaces and their transformations in Lie sphere geometry, with the aim of understanding the underlying integrable structure of discrete isothermic surfaces and sphere congruences.

Acknowledgements

These notes are based on the lectures given at "Introductory Workshop on Discrete Differential Geometry" held at Korea University on January 21-24, 2019. The authors would like to express their gratitude to the organizers of this conference, especially Professor Seong-Deog Yang for the hospitality shown during the visit and the encouragement of the publication of these notes. Furthermore, the authors would like to thank Dr. Mason Pember for indispensable comments on these notes and Dr. Masashi Yasumoto for fruitful discussions. The first author was partially supported by JSPS/FWF Bilateral Joint Project I3809-N32 "Geometric shape generation" and Grant-in-Aid for JSPS Fellows 19J10679; the second author was partially supported by two JSPS grants, Grant-in-Aid for Scientific Research (C) 15K04845 and (S) 17H06127 (P.I.: M.-H. Saito).

References

[1] W. Blaschke. *Vorlesungen über Differentialgeometrie und geometrische Grundlagen von Einsteins Relativitätstheorie III: Differentialgeometrie der Kreise und Kugeln.* Berlin: Springer, 1929.

[2] A. I. Bobenko and U. Pinkall. Discrete isothermic surfaces. *J. Reine Angew. Math.* **475**: 187–208, 1996. DOI: 10.1515/crll.1996.475.187.

[3] A. I. Bobenko and U. Pinkall. Discrete surfaces with constant negative Gaussian curvature and the Hirota equation. *J. Differential Geom.* **43**(3): 527–611, 1996.

[4] A. I. Bobenko and Y. B. Suris. *Discrete differential geometry.* Graduate Studies in Mathematics 98. Providence, RI: American Mathematical Society, 2008. xxiv+404.

[5] A. I. Bobenko and Y. B. Suris. Isothermic surfaces in sphere geometries as Moutard nets. *Proc. R. Soc. Lond. Ser. A Math. Phys. Eng. Sci.* **463**(2088): 3171–3193, 2007. DOI: 10.1098/rspa.2007.1902.

[6] E. Bour. Théorie de la déformation des surfaces. *J. Éc. Impériale Polytech.* **39**: 1–148, 1862.

[7] F. E. Burstall. Isothermic surfaces: conformal geometry, Clifford algebras and integrable systems. In: *Integrable systems, geometry, and topology*. C.-L. Terng (Ed.). Vol. 36. AMS/IP Stud. Adv. Math. Providence, RI: Amer. Math. Soc., 2006, 1–82.

[8] F. E. Burstall. Notes on transformations in integrable geometry. In: *Special metrics and group actions in geometry*. S. G. Chiossi, A. Fino, E. Musso, F. Podestà, and L. Vezzoni (Eds.). Vol. 23. Springer INdAM Ser. Cham: Springer, 2017, 59–80. DOI: 10.1007/978-3-319-67519-0_3.

[9] F. E. Burstall and D. M. J. Calderbank. Conformal submanifold geometry I-III, 2010. arXiv: 1006.5700 [math].

[10] F. E. Burstall and D. M. J. Calderbank. Conformal submanifold geometry IV-V. In progress.

[11] F. E. Burstall, J. Cho, U. Hertrich-Jeromin, M. Pember, and W. Rossman. Discrete Ω and Guichard surfaces. In progress.

[12] F. E. Burstall, N. M. Donaldson, F. Pedit, and U. Pinkall. Isothermic submanifolds of symmetric R-spaces. *J. Reine Angew. Math.* **660**: 191–243, 2011. DOI: 10.1515/crelle.2011.075.

[13] F. E. Burstall, U. Hertrich-Jeromin, M. Pember, and W. Rossman. Polynomial conserved quantities of Lie applicable surfaces. *Manuscripta Math.* **158**(3-4): 505–546, 2019. DOI: 10.1007/s00229-018-1033-0.

[14] F. E. Burstall, U. Hertrich-Jeromin, and W. Rossman. Discrete linear Weingarten surfaces. *Nagoya Math. J.* **231**: 55–88, 2018. DOI: 10.1017/nmj.2017.11.

[15] F. E. Burstall, U. Hertrich-Jeromin, and W. Rossman. Lie geometry of flat fronts in hyperbolic space. *C. R. Math. Acad. Sci. Paris* **348**(11-12): 661–664, 2010. DOI: 10.1016/j.crma.2010.04.018.

[16] F. E. Burstall, U. Hertrich-Jeromin, and W. Rossman. Lie geometry of linear Weingarten surfaces. *C. R. Math. Acad. Sci. Paris* **350**(7-8): 413–416, 2012. DOI: 10.1016/j.crma.2012.03.018.

[17] F. E. Burstall, U. Hertrich-Jeromin, W. Rossman, and S. D. Santos. Discrete surfaces of constant mean curvature. In: *Development in differential geometry of submanifolds*. S.-P. Kobayashi (Ed.). Vol. 1880. RIMS Kôkyûroku. Kyoto: Res. Inst. Math. Sci. (RIMS), 2014, 133–179. arXiv: 0804.2707.

[18] F. E. Burstall and S. D. Santos. Special isothermic surfaces of type d. *J. Lond. Math. Soc. (2)* **85**(2): 571–591, 2012. DOI: 10.1112/jlms/jdr050.

[19] E. Cartan. Les espaces à connexion conforme. *Ann. Soc. Pol. Math.* **2**: 171–221, 1923.

[20] T. E. Cecil. *Lie sphere geometry*. Second. Universitext. With applications to submanifolds. New York: Springer, 2008. xii+208.

[21] J. Cho, K. Naokawa, Y. Ogata, M. Pember, W. Rossman, and M. Yasumoto. Discretization of isothermic surfaces in Lie sphere geometry. In progress.

[22] J. Cieśliński, P. Goldstein, and A. Sym. Isothermic surfaces in $\mathbf{E}^3$ as soliton surfaces. *Phys. Lett. A* **205**(1): 37–43, 1995. DOI: 10.1016/0375-9601(95)00504-V.

[23] A. Demoulin. Sur les surfaces Ω. *C. R. Acad. Sci. Paris* **153**: 927–929, 1911.

[24] A. Demoulin. Sur les surfaces R et les surfaces Ω. *C. R. Acad. Sci. Paris* **153**: 705–707, 1911.

[25] A. Demoulin. Sur les surfaces R et les surfaces Ω. *C. R. Acad. Sci. Paris* **153**: 590–593, 1911.

[26] A. Demoulin. Sur les systèmes et les congruences K. *C. R. Acad. Sci. Paris* **150**: 156–159, 1910.

[27] U. Hertrich-Jeromin. *Introduction to Möbius differential geometry*. Vol. 300. London Mathematical Society Lecture Note Series. Cambridge: Cambridge University Press, 2003. xii+413.

[28] U. Hertrich-Jeromin. Transformations of discrete isothermic nets and discrete cmc-1 surfaces in hyperbolic space. *Manuscripta Math.* **102**(4): 465–486, 2000. DOI: 10.1007/s002290070037.

[29] U. Hertrich-Jeromin, T. Hoffmann, and U. Pinkall. A discrete version of the Darboux transform for isothermic surfaces. In: *Discrete integrable geometry and physics (Vienna, 1996)*. A. I. Bobenko and R. Seiler (Eds.). Vol. 16. Oxford Lecture Ser. Math. Appl. New York: Oxford Univ. Press, 1999, 59–81.

[30] U. Hertrich-Jeromin and F. Pedit. Remarks on the Darboux transform of isothermic surfaces. *Doc. Math.* **2**: 313–333, 1997.

[31] T. Hoffmann, W. Rossman, T. Sasaki, and M. Yoshida. Discrete flat surfaces and linear Weingarten surfaces in hyperbolic 3-space. *Trans. Amer. Math. Soc.* **364**(11): 5605–5644, 2012. DOI: 10.1090/S0002-9947-2012-05698-4.

[32] M. Pember. Special surface classes. Ph.D. Thesis. University of Bath, 2015.

[33] H. Pottmann, Y. Liu, J. Wallner, A. I. Bobenko, and W. Wang. Geometry of multi-layer freeform structures for architecture. *ACM Trans. on Graph. (TOG)* **26**(3): 65-1–65-11, 2007. DOI: 10.1145/1276377.1276458.

[34] S. D. Santos. Special isothermic surfaces. Ph.D. Thesis. University of Bath, 2008.

[35] W. K. Schief. On the unification of classical and novel integrable surfaces. II. Difference geometry. *R. Soc. Lond. Proc. Ser. A Math. Phys. Eng. Sci.* **459**(2030): 373–391, 2003. DOI: 10.1098/rspa.2002.1008.

[36] J. Stillwell. *The four pillars of geometry.* New York: Springer, 2005. 228 pp.

[37] C.-L. Terng and K. Uhlenbeck. Bäcklund transformations and loop group actions. *Comm. Pure Appl. Math.* **53**(1): 1–75, 2000. DOI: 10.1002/(SICI)1097-0312(200001)53:1<1::AID-CPA1>3.3.CO;2-L.

[38] K. Uhlenbeck. Harmonic maps into Lie groups: classical solutions of the chiral model. *J. Differential Geom.* **30**(1): 1–50, 1989. DOI: 10.4310/jdg/1214443286.

[39] M. Umehara and K. Yamada. *Differential geometry of curves and surfaces.* Singapore: World Sci. Publishing, 2017.

[40] V. E. Zakharov and A. B. Šabat. Integration of the nonlinear equations of mathematical physics by the method of the inverse scattering problem. II. *Funktsional. Anal. i Prilozhen.* **13**(3): 13–22, 1979. DOI: 10.1007/BF01077483.

Chapter 3

A short lecture on topological crystallography and a discrete surface theory

Hisashi Naito (内藤 久資)
Graduate School of Mathematics, Nagoya University, Nagoya 464-8602, Japan
naito@math.nagoya-u.ac.jp

Abstract

In this note, we discuss topological crystallography, which is a mathematical theory of crystal structures. The most symmetric structure among all placements of the graph is obtained by a variational principle in topological crystallography. We also discuss a theory of trivalent discrete surfaces in 3-dimensional Euclidean space, which are mathematical models of crystal/molecular structures.

1 Introduction

Geometric analysis is a field of analysis on geometric objects such as manifolds, surfaces, and metric spaces. Discrete geometric analysis is an analysis on *discrete* geometric objects, for example, graphs, and contains the spectral theory and the probability theory of graphs. Topological crystallography and a discrete surface

S.-D. Yang (ed.), *An introduction to discrete differential geometry.*
Anam Lecture Notes in Mathematics Volume 2

theory based on crystal/molecular structures are also parts of discrete geometric analysis.

Topological crystallography is a mathematical theory of crystal structures, which is founded by M. Kotani and T. Sunada [20–22, 39]. In physics, chemistry, and mathematics, crystal structures are described by space groups, which denote symmetry of placements of atoms. The usual description of crystals contains bonds between atoms in crystals. However, space groups do not consider such atomic bonds. Graphs are also natural notions to describe crystal structure, since vertices and edges of graphs correspond to atoms and atomic bonds in crystals, respectively. On the other hand, one of the important notions of physical phenomena is the principle of the least action, which corresponds to the variational principle in mathematics. That is to say, to describe physical phenomena, first we define an energy functional, which is called a Lagrangian in physics, and then we may find such phenomena as minimizers of the energy functional. There is no direct relationship between descriptions of crystal structures by using space groups and the principle of the least action.

Topological crystallography gives us a direct relationship between symmetry of crystal structures and the variational principle. Precisely, for a given graph structure which describes a crystal, we define the energy of realizations of the graph (placements of vertices of the graph in suitable dimensional Euclidean space), and obtain a "good" structure as a minimizer of the energy. Moreover, such structures give us most symmetric among all placements of the graph, which is proved by using the theory of random walk on graphs.

Molecular structures can be also described by using graph theory. The Hückel molecular orbital method, which is an important theory in physical chemistry, and the tight binding approximation for studying electronic states of crystals can be regarded as spectral theories of graphs from mathematical viewpoints. In this way, discrete geometric analysis can be applied to physics, chemistry, and related technologies.

In the first few sections, we discuss topological crystallography including graph theory and geometry. The most important bibliography of this part is T. Sunada's lecture note [38]. The author discusses an introduction to topological crystallography along with it.

On the other hand, we can regard some of crystal/molecular structures, for

example, fullerenes and carbon nanotubes (see Section 3.3), as surfaces, especially, as discrete surfaces. Recently, sp^2-carbon structures (including fullerenes and nanotubes) are paid attention to in sciences and technologies, since they have rich π-electrons and hence rich physical properties. In mathematical words, sp^2-carbon structures can be regarded as trivalent graphs in $\mathbb{R}^3$, and hence trivalent *discrete surfaces*. There are many discrete surface theories in mathematics, but they are discretization or discrete analogue of continuous/smooth objects. For example, discrete surfaces of triangulations are used in computer graphics, which is a discretization of smooth real objects. In other words, conventional discrete surface theories are "from continuous to discrete". In contrast, discrete surfaces, which describe crystal/molecular structures, are essentially discrete. Even for the case of trivalent discrete surfaces, it is not easy to define curvatures of them.

In the last few sections, we discuss a theory of trivalent discrete surfaces in $\mathbb{R}^3$, and also discuss subdivisions/convergences of them. Hence, our discrete surface theory is "from discrete to continuous".

2 Preliminaries

2.1 Graph theory

Here, we prepare a graph theory to describe topological crystals and discrete surfaces. Definitions and notations are followed by standard text books of graph theory, for example [3, 5].

Definition 2.1. An ordered pair $X = (V, E)$ is called a *graph*, if V is a countable set and $E = \{(u, v) : u, v \in V\}$. An element $v \in V$ is called a vertex of X, and an element $e \in E$ is called an edge of X. For each element $e = (u, v) \in E$, we may also write $u = o(e)$ and $v = t(e)$, which are called the *origin* and the *terminus* of e.

Definition 2.2. A graph $X = (V, E)$ is called *finite*, if the number of vertices $|V|$ and the number of edges $|E|$ are finite.

For a vertex $v \in V$, write $E_v = \{(v, u) \in E\}$, which is the set of edges with $o(e) = v$. The number of edges emanating with $v \in V$ is called the *degree* $\deg(v) = |E_v|$ of v. If $\deg(v)$ is finite for any $v \in V$, then the graph X is called *locally finite*. For any $e = (u, v) \in E$, $\overline{e} = (v, u) \in E$, then X is called *non-oriented*, otherwise X is called *oriented*.

In this note, we only consider non-oriented and locally finite graphs. Moreover, we admit graphs which contain a loop $(u, u) \in E$ and multiple edges.

Definition 2.3. For a graph $X = (V, E)$, successive edges

$$(u_1, u_2)(u_2, u_3) \cdots (u_{k-2}, u_{k-1})(u_{k-1}, u_k).$$

where $(u_i, u_j) \in E$, is called a *path* between u_1 and u_k, and if $u_1 = u_k$ and the path does not contains backtracking edges, it is called a *closed path*. A graph is *connected*, if there exists a path between arbitrary two vertices. A connected graph is called *tree*, if the graph contains no closed path.

Example 2.4. Both graphs in Fig. 2.1 are the same as each other, and are called K_4 graph. Each vertex of K_4 graph is connected with all of the other vertices. A graph with such a property is called a *complete graph*. The K_4 graph is the complete graph with 4 vertices.

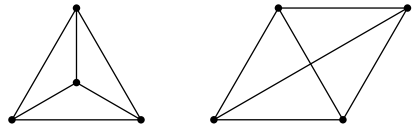

Figure 2.1: K_4 graph, each is different figure of the same graph.

Definition 2.5. Let $X = (V, E)$ be a finite graph with $V = \{v_i\}_{i=1}^n$. The *adjacency matrix* $A = A_X$ of X is an $n \times n$ matrix defined by

$$a_{ij} = \text{number of edges } (v_i, v_j).$$

If a graph X is non-oriented, then the adjacency matrix of X is symmetric.

Remark 2.6. Let A be an adjacency matrix of a graph X,

(1) (i, j)-element of A^k expresses number of paths from v_i to v_j by k-steps

(2) if A^{n-1} $(n = |V|)$ is not block diagonal, then X is connected

(3) if X is simple and non-oriented, then $(1/6)\,\mathrm{tr}(A^3)$ expresses the number of triangles contained in X

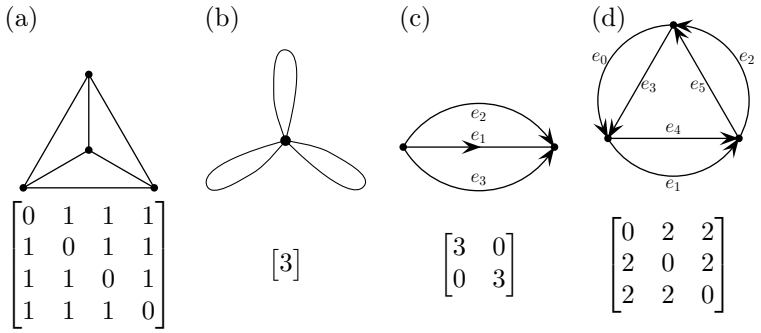

Figure 2.2: Examples of graphs and their adjacency matrices.

Definition 2.7. Let $X = (V, E)$ be a finite non-oriented graph. A tree $X_1 = (V, E_1)$ is called a *spanning tree* of X, if it satisfies $E_1 \subset E$ and for any $e \in E \setminus E_1$, $(V, E_1 \cup \{e\})$ contains a closed path (see Fig. 2.3).

Figure 2.3: Each graph is a spanning tree of K_4 graph.

Now, we also consider homology groups of graphs. A graph $X = (V, E)$ can be considered as a 1-dimensional CW complex as follows: the 0-dimensional chain group C_0 is the $\mathbb{Z}$-module consisted by V, and the 1-dimensional chain group C_1 is the $\mathbb{Z}$-module consisted by E. The boundary operator $\partial\colon C_1 \longrightarrow C_0$ is defined by

$$\partial(e) = t(e) - o(e),$$

where $o(e)$ and $t(e)$ are the origin and terminus of the edge e, namely, $o(e) = u$ and $t(e) = v$, if $e = (u, v)$. The homology group $H_0(X, \mathbb{Z})$ and $H_1(X, \mathbb{Z})$ is defined by

$$H_1(X, \mathbb{Z}) = \ker \partial \subset C_1(X), \quad H_0(X, \mathbb{Z}) = C_0(X)/\operatorname{image} \partial.$$

The following proposition explains particular properties for the first homology group on graphs.

Proposition 2.8 (Sunada [39]). *Let $X = (V, E)$ be a locally finite graph. Then, any non-trivial closed path e satisfies $[e] \neq [0] \in H_1(X, \mathbb{Z})$. Conversely, for each non-zero element $h \in H_1(X, \mathbb{Z})$, there exists a closed path e in X such that $h = [e]$.*

Proof. Let $e = e_1 \cdots e_k$ ($e_i \in E$) a path in X. Then, we may write $e = e_1 + \cdots + e_k \in C_1(X, \mathbb{Z})$, and $\partial(e) = t(e_1) - o(e_1) + t(e_2) - o(e_2) + \cdots + t(e_k) - o(e_k)$. Since $o(e_{i+1}) = t(e_i)$, we obtain $\partial(e) = t(e_1) - o(e_k)$. Assuming e is closed, that is $o(e_1) = t(e_k)$, we obtain $\partial(e) = 0$, and $[e] \neq [0] \in H_1(X, \mathbb{Z})$.

Conversely, we take an $h \in H_1(X, \mathbb{Z}) = \ker \partial \subset C_1(X, \mathbb{Z})$, and let $C_1(X) = \mathrm{span}\{e_i : i = 1, \ldots, n\}$, then there exists $\alpha_i \in \mathbb{Z}$ such that $h = \alpha_1 e_1 + \cdots + \alpha_n e_n$, and $\partial h = 0$. The equation $\partial h = \sum \alpha_i (t(e_i) - o(e_i))$ implies h is the sum of closed paths (see [38, p.41]). □

Proposition 2.8 implies that an elements of $H_1(X, \mathbb{Z})$ corresponds to a closed path of X. Hence we obtain a method for counting the rank of $H_1(X, \mathbb{Z})$.

Proposition 2.9. *Let $X = (V, E)$ be a finite non-oriented graph, and $X_1 = (V, E_1)$ be a spanning tree of X. Then, the first homology group $H_1(X, \mathbb{Z})$ of X satisfies* $\operatorname{rank} H_1(X, \mathbb{Z}) = |E| - |E_1|$.

Proof. Since X_1 is a tree, X_1 does not contain closed path. For each edge $e_0 = (u, v) \in E \setminus E_1$, we may find unique path $e = e_1 \cdots e_k$ in X_1 with $o(e_1) = v$, $t(e_k) = u$, and hence, $\widetilde{e_0} = e_0 e$ is a closed path in X. By Proposition 2.8, we obtain $[\widetilde{e_0}] \in H_1(X, \mathbb{Z})$. Therefore, for each $e_i \in E \setminus E_1$, there exists $[\widetilde{e_i}] \in H_1(X, \mathbb{Z})$ by a similar manner, and $\{[\widetilde{e_i}]\}$ are linearly independent. □

Example 2.10. The rank of the first homology group of graphs in Fig. 2.2 are (a) 3, (b) 3, (c) 2, and (d) 4, respectively.

Remark 2.11. An algorithm to find a spanning tree of a finite graph is well-known as Kruskal's algorithm, which finds a spanning tree within $O(|E| \log |E|)$ (see for example [1]).

2.2 Covering spaces

Definitions and notations are followed by standard text books of geometry and topology, for example [36].

Definition 2.12. Let X and X_0 be topological spaces. The space X is a *covering space* of X_0 if there exists a surjective continuous map $p\colon X \longrightarrow X_0$, which is called a *covering map*, such that for each $x \in X_0$, there exists an open neighbourhood U of x and open sets $\{V_i\} \subset X$ satisfying $p^{-1}(U) = \sqcup V_i$ with $p|_{V_i}\colon V_i \longrightarrow U$ homeomorphic.

Theorem 2.13.

(1) For any topological space X_0, there exists the unique simply connected covering space $\tilde{X}$, which is called the universal covering *of X_0.*

(2) If $p\colon X \longrightarrow X_0$ is a covering map, then there exists a transformation group T on X such that for any $\sigma \in T$, $p \circ \sigma = p$. The group T is called the covering transformation group*.*

(3) The covering transformation group of $p\colon \tilde{X} \longrightarrow X$ is the fundamental group $\pi_1(X)$ of X.

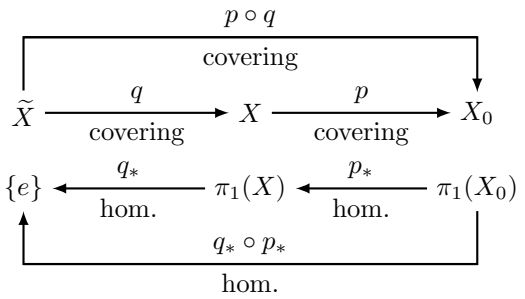

Example 2.14.

(1) The real line $\mathbb{R}$ is a covering space of S^1, since $p\colon \mathbb{R} \longrightarrow S^1$, $p(x) = x \pmod{2\pi}$. Since $\mathbb{R}$ is simply connected and the covering transformation group of p is $\mathbb{Z}$, we obtain $\pi_1(S^1) \cong \mathbb{Z}$.

(2) The 2-dimensional Euclidean space $\mathbb{R}^2$ is a covering space of $T^2 = \mathbb{R}^2/\mathbb{Z}^2$, since $p\colon \mathbb{R}^2 \longrightarrow T^2$, $p(x, y) = (x \pmod{2\pi}, y \pmod{2\pi})$. Since $\mathbb{R}^2$ is simply connected and the covering transformation group of p is $\mathbb{Z}^2$, we obtain $\pi_1(T^2) \cong \mathbb{Z}^2$.

Definition 2.15 (Sunada [39])**.** A covering $p\colon X \longrightarrow X_0$ with an abelian covering transformation group is called an *abelian covering*. For any topological

space X_0, there exists a *maximal abelian covering* space X, since $H_1(X_0, \mathbb{Z}) = \pi_1(X_0)/[\pi_1(X_0), \pi_1(X_0)]$ is a maximal abelian subgroup of $\pi_1(X_0)$

Example 2.16. The universal covering graph of the 3-bouquet graph X (Fig. 2.2 (b)) is a tree graph with the degree 3. The fundamental group $\pi_1(X)$ is the free group with 3 elements, and the first homology group $H_1(Z, \mathbb{Z})$ is $\mathbb{Z}^3$. For any normal subgroup $S \subset H_1(X, \mathbb{Z})$, there exists a graph X_S such that X_S is a covering graph of X with its covering transformation group S.

3 Topological crystals and their standard realization

The classical description of crystallography is based on group theory, and they describe symmetries of crystals. For example, in the classical crystallography, the diamond crystal is classified as the space group $Fd\overline{3}m$ (see Section A.1), and the group does not contain information of chemical bonds of atoms in the crystal.

The theory of topological crystals is developed by Kotani–Sunada [19–22]. The theory describes symmetries of crystals including chemical bonds of atoms, and it is based on variational problems.

3.1 Topological crystals and their realizations

In this section, we assume that graphs are connected non-oriented locally finite, which may include self-loops and multiple edges.

Definition 3.1 (Sunada [39])**.** A connected non-oriented locally finite graph $X = (V, E)$, which may include self-loops and multiple edges, is called a *topological crystal* (or a *crystal lattice*), if and only if there exists an abelian group G which acts freely on X. The topological crystal is *d-dimensional* if the rank of the abelian group G is d.

By this definition, for a topological crystal $X = (V, E)$, there exists a finite graph $X_0 = (V_0, E_0)$ satisfying $X/G = X_0$, for an abelian subgroup $G \subset H_1(X_0, \mathbb{Z})$, and X is a covering graph of X_0 whose covering transformation group is G. On the contrary, for a given connected non-oriented finite graph $X_0 = (V_0, E_0)$ and an abelian subgroup $G \subset H_1(X_0, \mathbb{Z})$, there exists a topological crystal X with $X/G = X_0$, by taking a suitable covering graph.

Definition 3.2 (Sunada [39])**.** A topological crystal X is called *maximal abelian* if and only if $G = H_1(X_0, \mathbb{Z})$.

Example 3.3. A square lattice X (Fig. 3.1 (a)) is a topological crystal whose base graph X_0 is the graph in Fig. 3.3 (a) (the 2-bouquet graph). Since the covering transformation group G is $G = H_1(X_0, \mathbb{Z})$ and $\operatorname{rank} G = \operatorname{rank} H_1(X_0, \mathbb{Z}) = 2$, the topological crystal X is 2-dimensional and maximal abelian.

Example 3.4. A triangular lattice X (Fig. 3.1 (b)) is a topological crystal whose base graph X_0 is the graph in Fig. 2.2 (b). Since the covering transformation group G satisfies $\operatorname{rank} G = 2$ but $H_1(X_0, \mathbb{Z}) = 3$, the topological crystal X is 2-dimensional and not maximal abelian.

Example 3.5. A hexagonal lattice X (Fig. 3.1 (c)) is a topological crystal whose base graph X_0 is the graph in Fig. 2.2 (c). Since the covering transformation group G is $G = H_1(X_0, \mathbb{Z})$ and $\operatorname{rank} G = \operatorname{rank} H_1(X_0, \mathbb{Z}) = 2$, the topological crystal X is 2-dimensional and maximal abelian.

Example 3.6. A kagome lattice X (Fig. 3.1 (d)) is a topological crystal whose base graph X_0 is the graph in Fig. 2.2 (d). Since the covering transformation group G satisfies $\operatorname{rank} G = 2$ but $H_1(X_0, \mathbb{Z}) = 4$, the topological crystal X is 2-dimensional and not maximal abelian.

Example 3.7. A diamond lattice X (Fig. 3.19) is a topological crystal whose base graph X_0 is the graph in Fig. 2.2 (b) (the 3-bouquet graph). Since the covering transformation group G is $G = H_1(X_0, \mathbb{Z})$ and $\operatorname{rank} G = \operatorname{rank} H_1(X_0, \mathbb{Z}) = 3$, the topological crystal X is 3-dimensional and maximal abelian.

Definition 3.8 (Sunada [39])**.** Given d-dimensional topological crystal $X = (V, E)$, a piecewise linear map $\Phi\colon X \longrightarrow \mathbb{R}^d$ is called a *realization* of X. More precisely, first we define $\Phi\colon V \longrightarrow \mathbb{R}^d$, and define $\Phi(e)$ by linear interpolation between $\Phi(o(e))$ and $\Phi(t(e))$.

Definition 3.9 (Sunada [39])**.** A realization Φ of a d-dimensional topological crystal X is called a *periodic realization*, if there exists an injective homomorphism $\rho\colon G \longrightarrow \mathbb{R}^d$ satisfying

$$\Phi(gv) = \Phi(v) + \rho(g), \quad (v \in V,\ g \in G).$$

Example 3.10. Three realizations in Fig. 3.2 are periodic realizations of a hexagonal lattice. These are different periodic realizations of the same graph. The

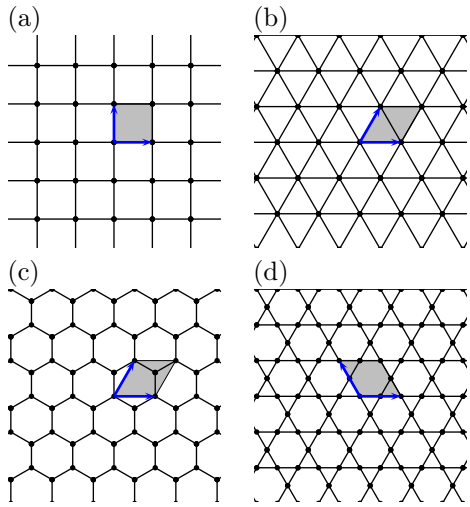

Figure 3.1: Standard realizations of representative 2-dimensional topological crystals. (a) A square lattice, (b) a triangular lattice, (c) a hexagonal lattice, and (d) a kagome lattice. Blue vectors are basis of parallel translations.

realization (b) is the most symmetric, and the main problem of this section is to explain the reason why nature selects (b) by mathematics.

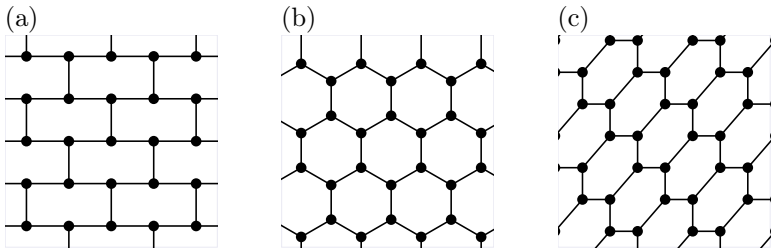

Figure 3.2: Different realizations of the hexagonal lattice. These three lattices have the same topological structure.

Definition 3.11 (Sunada [39])**.** Let X be a d-dimensional topological crystal with the base graph $X_0 = (V_0, E_0)$, G be an abelian group acting on X, and Φ or (Φ, ρ) be a periodic realization of X, where $\rho\colon G \longrightarrow GL(d, \mathbb{R})$. The *energy* and

the *normalized energy* of Φ are defined by

$$E(\Phi) = \sum_{e \in E_0} |\Phi(t(e)) - \Phi(o(e))|^2, \tag{3.1}$$

and

$$E(\Phi, \rho) = \mathrm{Vol}(\Gamma)^{2/d} \sum_{e \in E_0} |\Phi(t(e)) - \Phi(o(e))|^2, \quad \Gamma = \rho(G), \tag{3.2}$$

respectively.

The energy of Φ is a discrete analogue of the Dirichlet energy for smooth maps, since $\Phi(t(e)) - \Phi(o(e))$ is a discretization of differential of smooth maps.

Definition 3.12 (Sunada [39])**.** For a topological crystal X with fixed lattice $\Gamma = \rho(G)$, a critical point Φ of the energy E is called a *harmonic realization* of X.

In the followings, we abbreviate $\boldsymbol{v} = \Phi(v)$ and $\boldsymbol{e} = \Phi(e)$ for $v \in V$ and $e \in E$, as long as there are no misunderstandings.

Proposition 3.13 (Sunada [39])**.** *For a topological crystal X, a realization Φ is harmonic if and only if*

$$\sum_{(u,v) \in (E_0)_v} (\boldsymbol{u} - \boldsymbol{v}) = \boldsymbol{0}, \quad \textit{for all } v \in V_0. \tag{3.3}$$

That is to say, the sum of vectors creating edges emanating from each v is zero, in other words, each vertex of V satisfies the "balancing condition".

Proof. First, we note that we have $E(\Phi) = E(\Phi, \rho)$ by fixing Γ with $\mathrm{Vol}(\Gamma) = 1$. Let $\Phi_t \colon X \longrightarrow \mathbb{R}^d$ be a variation of Φ with $\Phi_0 = \Phi$. Differentiating $E(\Phi_t)$ by t and using the "integration by parts", we may calculate as

$$\begin{aligned} \frac{d}{dt} E(\Phi_t) &= \sum_{v \in V_0} \sum_{u \in V_v} \big\langle \boldsymbol{v}(t) - \boldsymbol{u}(t), \boldsymbol{v}'(t) - \boldsymbol{u}'(t) \big\rangle \\ &= 2 \sum_{v \in V_0} \sum_{u \in V_v} \big\langle \boldsymbol{v}(t) - \boldsymbol{u}(t), \boldsymbol{u}'(t) \big\rangle, \end{aligned}$$

where $\boldsymbol{v}(t) = \Phi_t(v)$ and $\boldsymbol{v}'(t) = \frac{d}{dt}\Phi_t(v)$. Therefore, we obtain

$$\frac{d}{dt}E(\Phi_t)\Big|_{t=0} = 2\sum_{v\in V_0}\sum_{u\in V_v}\langle \boldsymbol{v}-\boldsymbol{u}, \boldsymbol{x}_u\rangle, \quad \boldsymbol{x}_u = \Phi_t'(u)\big|_{t=0},$$

and get the result. □

Remark 3.14.

(1) In the Definition 3.12, if we do not assume that the lattice Γ is fixed, then critical points admit $\Phi = 0$.

(2) The equation (3.3) is equivalent to a linear equation

$$\begin{aligned} -\deg(v)\boldsymbol{v} + \sum_{u\in(V_0)_v}\boldsymbol{u} = 0, \quad \text{for all } v \in V_0, \\ \Delta_X\Phi = 0, \end{aligned} \tag{3.4}$$

where $\Delta_X = A_X - \mathrm{diag}(\deg(v))$ and is called the *Laplacian* of X.

For a smooth map $u\colon \Omega \longrightarrow \mathbb{R}$ with $u|_{\partial\Omega} = 0$, where Ω is a domain in $\mathbb{R}^N$, the Dirichlet energy E of u is defined by $E(u) = \frac{1}{2}\int_\Omega |\nabla u|^2\, dV$, and its Euler-Lagrange equation is $\Delta u = 0$ (the Laplace equation). This is a reason why the critical points of E for topological crystals are called harmonic.

Example 3.15. Realizations (b) and (c) of Fig. 3.2 are harmonic, since each vertex $v \in V_0$ satisfies the balance condition (3.4), but the realization (a) of Fig. 3.2 is not harmonic. Hence, the harmonic condition (3.3) or (3.4) are not suffice to select (b) among three realizations in Fig. 3.2.

Proposition 3.16 (Sunada [39])**.** *Harmonic realizations of X are unique up to affine transformations.*

Proof. First, note that the equation (3.3) is invariant under affine transformations. Let $\{e_i\}_{i=1}^d$ be a $\mathbb{Z}$-basis of the abelian group G, which acts on X. Assume $\Phi_1(X)$ and $\Phi_2(X)$ are harmonic realizations of X with respect to lattice $\Gamma_1 = \rho_1(L)$ and $\Gamma_2 = \rho_2(L)$, respectively. Then, there exists an $A \in GL(d,\mathbb{R})$ such that $\rho_1(g) = A\rho_2(g)$ for $g \in G$. Hence, we obtain that there exists $\boldsymbol{b} \in \mathbb{R}^d$ such that $\Phi_1 = A\Phi_2 + \boldsymbol{b}$. □

Definition 3.17 (Sunada [39])**.** For a topological crystal X, *standard* realizations of X are critical points among all realization Φ and Γ with $\mathrm{Vol}(\Gamma) = 1$.

A Standard realization are also called an *equilibrium placement* defined by Delgado-Friedrichs–O'Keeffe [6].

Theorem 3.18 (Kotani–Sunada [22], Sunada [39])**.** *For any topological crystals X, there exists the unique standard realization up to Euclidean motions.*

Kotani–Sunada proved Theorem 3.18 by using a theory of harmonic maps. Eells–Sampson [9] proved the existence theorem of harmonic maps from compact Riemannian manifolds into non-positively curved Riemannian manifolds. The energy (3.1) is the Dirichlet energy of maps from 1-dimensional CW complex into a Euclidean space. Hence, by Eells–Sampson's theorem, there exists a standard realization (an energy minimizing harmonic map) in each homotopy class. Sunada also gave another proof of Theorem 3.18 in his lecture note [39]. On the other hand, the existence of standard realizations can be also proved by showing the strong convexity of the energy (3.1).

Theorem 3.19 (Sunada [37–39])**.** *For a d-dimensional topological crystal X, a realization Φ is standard if and only if*

$$\sum_{e \in E_0} \boldsymbol{e} = \boldsymbol{0}, \tag{3.5}$$

$$\sum_{e \in E_0} \langle \boldsymbol{x}, \boldsymbol{e} \rangle \boldsymbol{e} = c\boldsymbol{x} \quad \textit{for all } \boldsymbol{x} \in \mathbb{R}^d \textit{ and for some } c > 0. \tag{3.6}$$

Proof. First, we define $T\colon \mathbb{R}^d \longrightarrow \mathbb{R}^d$ by $T\boldsymbol{x} = \sum_{e \in E_0} \langle \boldsymbol{x}, \boldsymbol{e} \rangle \boldsymbol{e}$. Since

$$\langle T\boldsymbol{x}, \boldsymbol{y} \rangle = \sum_{e \in E_0} \langle \boldsymbol{x}, \boldsymbol{e} \rangle \langle \boldsymbol{y}, \boldsymbol{e} \rangle = \langle \boldsymbol{x}, T\boldsymbol{y} \rangle, \tag{3.7}$$

we obtain that T is symmetric. We would prove that Φ is a standard realization if and only if there exists a positive constant $c > 0$ such that $T = cI$.

On the other hand, for any symmetric matrix T of size d with positive eigenvalues, there exists an orthogonal matrix P such that $P^T T P = \operatorname{diag}(\lambda_1, \dots, \lambda_d)$, where $\lambda_j > 0$ are eigenvalues of T. The inequality of arithmetic and geometric means implies

$$\operatorname{tr} T = \operatorname{tr} P^T T P \geq d(\det P^T T P)^{1/d} = d(\det T)^{1/d},$$

and the equality holds if and only if $T = \lambda I_d$.

Here, we write $E_0 = \{e_\alpha\}_{\alpha=1}^{|E_0|}$, and $\boldsymbol{e}_i = (e_{\alpha 1}, \dots, e_{\alpha d}) \in \mathbb{R}^d$. Since the equation (3.6) is equivalent to

$$\langle T\boldsymbol{x}, \boldsymbol{y}\rangle = \sum_{e\in E_0} \langle \boldsymbol{e}, \boldsymbol{x}\rangle\langle \boldsymbol{e}, \boldsymbol{y}\rangle = c\langle \boldsymbol{x}, \boldsymbol{y}\rangle, \tag{3.8}$$

taking an orthogonal basis $\{\boldsymbol{x}_j\}_{j=1}^d$ of $\mathbb{R}^d$, and set $\boldsymbol{x} = \boldsymbol{x}_j$, and $\boldsymbol{y} = \boldsymbol{x}_k$, we obtain

$$\sum_{\alpha=1}^{|E_0|} e_{\alpha j} e_{\alpha k} = c\delta_{jk}, \tag{3.9}$$

and

$$\mathrm{Vol}(\Gamma)^{2/d} E(\Phi, \rho) = \sum_{e\in E_0} |\boldsymbol{e}|^2 = \sum_{\alpha=1}^{|E_0|}\sum_{j=1}^{d} e_{\alpha j}^2 = cd. \tag{3.10}$$

Now, we assume that (Φ_1, ρ_1) is a standard realization of X and (Φ_2, ρ_2) is a harmonic realization of X. By Proposition 3.16, there exists an $A = (a_{ij}) \in GL(d, \mathbb{R})$ and $\boldsymbol{b} \in \mathbb{R}^d$ such that $\Phi_2 = A\Phi_1 + \boldsymbol{b}$ and $\rho_1 = A\rho_2$. Then, we obtain

$$\mathrm{Vol}(\Gamma_1) = |\det A|\,\mathrm{Vol}(\Gamma_2), \quad f_{\alpha i} = \sum_{j=1}^{d} a_{ij} e_{\alpha j},$$

and

$$\begin{aligned}
\mathrm{Vol}(\Gamma_2)^{2/d} E(\Phi_2, \rho_2) &= \sum_{i=1}^{d}\sum_{\alpha=1}^{|E_0|} f_{\alpha i}^2 = \sum_{i=1}^{d}\sum_{j,k=1}^{d}\sum_{\alpha=1}^{|E_0|} a_{ij}a_{ik}e_{\alpha j}e_{\alpha_k} \\
&= \sum_{i=1}^{d}\sum_{j,k=1}^{d}\sum_{\alpha=1}^{|E_0|} a_{ij}a_{ik}\delta_{jk} = c\sum_{i=1}^{d}\sum_{j=1}^{d} a_{ij}a_{ij} = c\,\mathrm{tr}\,A^TA \\
&\geq cd(\det A^TA)^{1/d} = cd(\det A)^{2/d} = cd(\mathrm{Vol}(\Gamma_2)/\mathrm{Vol}(\Gamma_1))^{2/d} \\
&= cd\,\mathrm{Vol}(\Gamma_2)E(\Phi_1, \rho_1).
\end{aligned}$$

This implies that $E(\Phi_2, \rho_2) \geq E(\Phi_1, \rho_1)$ if and only if the equation (3.6) holds. □

Theorem 3.20 (Sunada [37–39])**.** *Assume that Φ is a standard realization of a d-dimensional topological crystal. Then, each element $\sigma \in \mathrm{Aut}(X)$ extends as an element of $\mathrm{Aut}(\Phi(X)) \subset O(d) \ltimes \mathbb{R}^d$ (Euclidean motion group of $\mathbb{R}^d$).*

Theorem 3.20 means that standard realizations, which are obtained by a variational principle, have maximum symmetry among all the realizations of a topological crystal.

Recently, Kajigaya–Tanaka [14] study the existence of discrete harmonic maps into Riemann surface of genus greater than one.

Example 3.21. The realization (b) of Fig. 3.2 is a standard realization of a hexagonal lattices, whereas, the realization (c) of Fig. 3.2 is not a standard.

Example 3.22. Let $\triangle ABC$ be a triangle on a plane and O be the barycenter of the triangle, and consider a graph $G = (V, E)$ consisting $V = \{O, A, B, C\}$ and $E = \{(O, A), (O, B), (O, C)\}$. By a property of the barycenter of triangles, we obtain $\overrightarrow{OA} + \overrightarrow{OB} + \overrightarrow{OC} = \mathbf{0}$. That is to say, the balancing condition (3.3) holds for $O \in V$; however, the condition (3.6) only holds for the case that $\triangle ABC$ is a regular triangle.

Definition 3.23 (Sunada [37–39])**.** A topological crystal X of degree n is called *strongly isotropic*, if there exists $g \in \mathrm{Aut}(X)$ such that $g(u) = v$ and $g(e_i) = f_{\sigma(i)}$, for any $u, v \in V$, and for any permutation $\sigma \in \mathfrak{S}_n$, where $E_u = \{e_i\}_{i=1}^n$ and $E_v = \{f_j\}_{j=1}^n$.

Theorem 3.24 (Sunada [37])**.** *2-dimensional strongly isotropic topological crystals are hexagonal lattices only. 3-dimensional strongly isotropic topological crystals are diamond lattices and K_4 lattices (and their mirror image) only.*

Remark 3.25. A square lattice does not have the strongly isotropic property. Let X be a square lattice. Consider a vertex $v \in V$, $g = \mathrm{id} \in \mathrm{Aut}(X)$, and let e_1, e_2, e_3, $e_4 \in E_v$ be edges to north, west, south, and east. If X has the strongly isotropic property, then any $\sigma \in \mathfrak{S}_4$, $g(e_i) = e_{\sigma(i)}$ for $i = 1, 2, 3, 4$. However, we exchange edges by the permutation $\sigma(1, 2, 3, 4) = (2, 1, 3, 4)$, then, the graph structure could not preserved. Hence, a square lattice is not strongly isotropic.

Graphenes and diamonds have nice physical properties (see Section 3.3), and they are carbon structure of standard realizations of hexagonal and diamond lattices, which are strongly isotropic. Hence, we may expect that K_4-carbons are also nice physical properties.

Remark 3.26. Kotani–Sunada considered topological crystals from probabilistic motivations [18, 19, 21, 37]. A *random walk* on a graph $X = (V, E)$ is a stochastic process associated with $p\colon E \longrightarrow [0, 1]$ satisfying $\sum_{e \in E_x} p(e) = 1$. In the case of

$p(e) = 1/(|E_x|)$, the random walk is called *simple random walk*. The function p is considered as *transition probability* from $o(e)$ to $t(e)$. Define $p_X(n, x, y) = \sum p(e_1) \cdots p(e_n)$, where summation over all paths with $e = e_1 \cdots e_n$, $o(e_1) = x$, $t(e_n) = y \in V$, is called n-step probability from x to y.

Let X be a d-dimensional topological crystal, Kotani–Sunada studied when the simple random walk on X "converges" to a Brownian motion on $\mathbb{R}^d$ as the mesh of X becomes finer, and proved that if a realization of X is standard, then there exists constants C depending only on X such that

$$\frac{1}{\deg(y)} p_X(n, x, y) \sim \frac{C}{(4\pi n)^{d/2}} \left(1 + c_1(x, y) n^{-1} + O(n^{-2})\right) \text{ as } n \to \infty,$$
$$c_1(x, y) = -\frac{C}{4} |\boldsymbol{x} - \boldsymbol{y}|^2 + g(x) + g(y) + c, \text{ for certain } g \text{ and } c,$$

which means that $p_X(n, x, y)$ "converges" to the heat kernel $p_{\mathbb{R}^d}(t, \boldsymbol{x}, \boldsymbol{y})$ as $n \uparrow \infty$.

3.2 Explicit constructions of standard realizations

In this section, we demonstrate how to construct a standard realization from given base graph explicitly.

Let $X_0 = (V_0, E_0)$ be a finite graph with $d = \operatorname{rank} H_1(X_0, \mathbb{Z})$. We define a natural inner product on d-dimensional vector space $C_1(X_0, \mathbb{R})$ by

$$\langle e_1, e_2 \rangle = \begin{cases} 1 & \text{if } e_1 = e_2, \\ -1 & \text{if } e_1 = \overline{e_2}, \\ 0 & \text{otherwise,} \end{cases}$$

for e_1, $e_2 \in E_0$. By using the inner product, we may identify $C_1(X_0, \mathbb{R})$ to $\mathbb{R}^{|E_0|}$, hence we may also identify $H_1(X_0, \mathbb{R})$ to $\mathbb{R}^d$.

Let $X = (V, E)$ be the maximum abelian covering of X_0, and $\pi \colon X \longrightarrow X_0$ be the covering map. Fix a vertex $v_0 \in V_0$, and define $\Phi \colon X \longrightarrow H_1(X_0, \mathbb{R})$ by

$$\Phi(v) = P(\pi(e_1)) + \cdots + P(\pi(e_n)), \tag{3.11}$$

where $e = e_1 \cdots e_n$ is a path in X connecting $v_0 = o(e_1)$ and $v = t(e_n)$, and $P \colon C_1(X_0, \mathbb{R}) \longrightarrow H_1(X_0, \mathbb{R})$ is the orthogonal projection.

Proposition 3.27 (Sunada [39]). *The map* $\Phi\colon X \longrightarrow H_1(X_0,\mathbb{R})$ *defined by* (3.11) *is a harmonic realization of* X*, namely,*

$$\sum_{e\in(E_0)_v} P(e) = 0 \in H_1(X_0,\mathbb{R}). \tag{3.12}$$

Proof. First, we prove that

$$\sum_{e\in(E_0)_v} \langle e, c\rangle = 0 \tag{3.13}$$

for an arbitrary closed path $c = e_1\cdots e_n$ in X_0. If c does not contain an edge whose origin or terminus is v, then the equation (3.13) obviously holds. Let e_j and e_{j+1} be edges in c satisfying $t(e_j) = o(e_{j+1}) = v$, then $\langle e, e_j + e_{j+1}\rangle = 1 - 1 = 0$. Hence, we obtain (3.13).

The equality (3.13) implies that

$$\sum_{e\in(E_0)_v} e \in H_1(X_0,\mathbb{R})^{\perp},$$

since $H_1(X_0,\mathbb{R})$ is generated by closed paths in X_0. Therefore, we obtain

$$0 = P\left(\sum_{e\in(E_0)_v} e\right) = \sum_{e\in(E_0)_v} P(e),$$

and hence we get (3.12). □

Proposition 3.28 (Sunada [39]). *The map* $\Phi\colon X \longrightarrow H_1(X_0,\mathbb{R})$ *defined by* (3.11) *is a standard realization of* X*, namely, there exists a constant* $c > 0$ *such that*

$$\sum_{e\in E_0} \Big(\langle P(e), x\rangle\Big)^2 = c|x|^2, \quad x \in H_1(X_0,\mathbb{R}). \tag{3.14}$$

Proof. Since the set of oriented edges $E_0^o := \{e_i\}_{i=1}^n$ is an orthonormal basis of $C_1(X_0,\mathbb{R})$, we obtain

$$\sum_{e\in E_0^o} \Big(\langle P(e), x\rangle\Big)^2 = \sum_{e\in E_0^o} \big(\langle e, x\rangle\big)^2 = |x|^2,$$

and

$$\sum_{e\in E_0}\Big(\big\langle P(e),x\big\rangle\Big)^2=\sum_{e\in E_0^o}\Big(\big\langle P(e),x\big\rangle\Big)^2+\sum_{\overline{e}\in E_0^o}\Big(\big\langle P(e),x\big\rangle\Big)^2$$
$$=2\sum_{e\in E_0^o}\Big(\big\langle P(e),x\big\rangle\Big)^2,$$

hence we get (3.14) □

By the above arguments, the realization Φ of X_0 is into $H_1(X_0,\mathbb{R})/H_1(X_0,\mathbb{Z})$ with the period lattice Γ. The torus $H_1(X_0,\mathbb{R})/H_1(X_0,\mathbb{Z})$ is called an *Albanese torus*. Therefore, to calculate explicit coordinates of standard realizations, we should compute correspondences between the Albanese torus and $\mathbb{R}^d/\mathbb{Z}^d$.

3.2.1 Explicit algorithm in cases of maximum abelian coverings

Now, we explain explicit algorithm to obtain a standard realization of a d-dimensional topological crystal X, which is a maximum abelian covering of $X_0=(V_0,E_0)$. This method is followed by Sunada [39] and Naito [28]. In the followings, set $b=\operatorname{rank}H_1(X_0,\mathbb{Z})$.

Step 1 First, compute a spanning tree $X_1=(V_0,E_1)$ of X_0 by Kruskal's algorithm, and set $E_0\setminus E_1=\{e_i\}_{i=1}^b$ and $E_1=\{e_i\}_{i=b+1}^{|E|}$. Then, we may select a $\mathbb{Z}$-basis $\{\alpha_i\}_{i=1}^b$ of $H_1(X_0,\mathbb{Z})$ as follows. For each edge $e_i\in E_0\setminus E_1$, we may find a path p_i in E_1 such that $o(p_i)=t(e_i)$ and $t(p_i)=o(e_i)$. The path $p_ie_i\in E_0$ is a closed path in E_0, and hence by Propositions 2.8 and 2.9, we may set $\alpha_i=[p_ie_i]$.

Step 2 Since $\{\alpha_i\}_{i=1}^b$ is a $\mathbb{Z}$-basis of $H_1(X_0,\mathbb{Z})$, for each edge $e\in E_0$ there exists $a_i(e)\in\mathbb{R}$ such that

$$P(e)=\sum_{i=1}^b a_i(e)\alpha_i\in H_1(X_0,\mathbb{R}). \tag{3.15}$$

Since $e\in C_1(X_0,\mathbb{R})$ and P is the orthogonal projection from $C_1(X_0,\mathbb{R})$ onto $H_1(X_0,\mathbb{R})$. $P(e)$ satisfies

$$\big\langle P(e)-e,\alpha_j\big\rangle=0,\ \text{for any } j. \tag{3.16}$$

Substituting (3.15) into (3.16), we obtain

$$\sum_{i=1}^{b} a_i(e)\langle \alpha_i, \alpha_j \rangle = \langle e, \alpha_j \rangle. \tag{3.17}$$

Set $A = (\langle \alpha_i, \alpha_j \rangle) \in GL(b, \mathbb{R})$, and $\boldsymbol{a}(e) = (a_i(e))^T$, $\boldsymbol{b}(e) = (\langle e, \alpha_i \rangle)^T \in \mathbb{R}^b$, then (3.17) is written as

$$\boldsymbol{a}(e) = A^{-1}\boldsymbol{b}(e). \tag{3.18}$$

We get $\boldsymbol{a}(e)$ for each $e \in E_0$, then we obtain the realization

$$P(e) = \boldsymbol{e} = \sum_{i=1}^{b} a_i(e)\alpha_i, \text{ in } H_1(X_0, \mathbb{R}). \tag{3.19}$$

On the other hand, we easily calculate $\boldsymbol{b}(e)$ and A, since e and α_i are given by linear combinations of $\{e_i\}_{i=1}^{b}$ and $\{e_i\}_{i=b=1}^{|E|}$. Therefore, by (3.18), we obtain $\boldsymbol{a}(e)$. We remark that the matrix A is the Gram matrix of the basis $\{\alpha_i\}_{i=1}^{b}$. Taking an orthonormal basis $\{\boldsymbol{x}_i\}_{i=1}^{b}$ of $H_1(X_0, \mathbb{R})$ and write

$$\alpha_i = \sum_{j=1}^{b} \beta_{ij}\boldsymbol{x}_j, \tag{3.20}$$

then we obtain the expression of the realization in the Cartesian coordinates of $H_1(X_0, \mathbb{R}) \equiv \mathbb{R}^b$ as

$$\boldsymbol{e} = \sum_{i=1}^{b} a_i(e)\alpha_i = \sum_{i=1}^{b} \left(\sum_{j=1}^{b} a_i(e)\beta_{ij} \right) \boldsymbol{x}_j \text{ for } e \in E_0. \tag{3.21}$$

To obtain the relation (3.20), we may use the Cholesky decomposition. The Cholesky decomposition, which is a special case of LU decomposition, gives us the decomposition $A = X^T X$ for any positive definite symmetric matrix A by an upper triangular matrix X (see for example [35]).

Step 3 Fix a vertex $v_0 \in V_0$, and set $\boldsymbol{v_0} = \boldsymbol{0}$ (origin of $\mathbb{R}^b$). For each vertex $v_j \in V_0$, we find the shortest path $e = e_{j1} \cdots e_{jk} \in E_1$ with $o(e_{j1}) = v_0$ and $t(e_{jk}) = v_j$, which is a shortest path in the spanning tree finding in Step 1 connecting v_0 and v_j. By using (3.19), we obtain

$$\boldsymbol{v}_j = \sum_{i=1}^{k} \boldsymbol{e}_{ji} = \sum_{i=1}^{k} \sum_{k=1}^{b} a_k(e_{ji})\alpha_k. \tag{3.22}$$

In the above, we realize edges in the spanning tree. Hence, to complete calculation, we compute realizations of edges which are not contained in the spanning tree. For each $e_\ell \in E_0 \setminus E_1$, we define $\boldsymbol{w}_\ell \in \mathbb{R}^b$ by

$$\boldsymbol{w}_\ell = \boldsymbol{v}(e_\ell) + \boldsymbol{e}_\ell, \tag{3.23}$$

where $v(e_\ell) = o(e_\ell)$.

Vertices $\{\boldsymbol{v}_j\}_{j=1}^{|V|} \sqcup \{\boldsymbol{w}_\ell\}_{\ell=1}^{b} \subset \mathbb{R}^b$ (or edges $\{\boldsymbol{e}_i\}_{i=1}^{|E_0|}$) with the period lattice $\{\alpha_i\}_{i=1}^{b}$ give us a standard realization of X with period lattice Γ. The set of realizations of edges $\{\boldsymbol{e}_j\}_{j=1}^{|E|}$ is called the *building block*. In other words, Information of adjacency of the graph and the building block give us a standard realization.

Remark 3.29. Dijkstra's algorithm gives us shortest paths from a vertex to any other vertices within $O(|E| + |V| \log |V|)$ (see for example [1]).

Example 3.30 (**Square lattices in** $\mathbb{R}^2$, Fig. 3.1 (a), Sunada [39, Section 8.3]). The base graph $X_0 = (V_0, E_0)$ of square lattices in $\mathbb{R}^2$ is the 2-bouquet graph (Fig. 3.3 (a)), and $\operatorname{rank} H_1(X_0, \mathbb{R}) = 2$. Write $V_0 = \{v_0\}$ and $E_0 = \{e_1, e_2\}$, as in Fig. 3.3 (a), then a spanning tree of X_0 is $X_1 = (V_0, \{\emptyset\})$, namely, $E_1 = \{\emptyset\}$. Hence, we may take $\alpha_1 = e_1$ and $\alpha_2 = e_2$ as a $\mathbb{Z}$-basis of $H_1(X_0, \mathbb{Z})$, and obtain

$$A = \begin{bmatrix} \langle \alpha_1, \alpha_1 \rangle & \langle \alpha_1, \alpha_2 \rangle \\ \langle \alpha_2, \alpha_1 \rangle & \langle \alpha_2, \alpha_2 \rangle \end{bmatrix} = \begin{bmatrix} 1 & 0 \\ 0 & 1 \end{bmatrix}, \quad A^{-1} = A,$$

$$\begin{bmatrix} \boldsymbol{b}(e_1) & \boldsymbol{b}(e_2) \end{bmatrix} = \begin{bmatrix} \langle e_1, \alpha_1 \rangle & \langle e_2, \alpha_1 \rangle \\ \langle e_1, \alpha_2 \rangle & \langle e_2, \alpha_2 \rangle \end{bmatrix} = \begin{bmatrix} 1 & 0 \\ 0 & 1 \end{bmatrix},$$

$$\begin{bmatrix} \boldsymbol{a}(e_1) & \boldsymbol{a}(e_2) \end{bmatrix} = A \begin{bmatrix} \boldsymbol{b}(e_1) & \boldsymbol{b}(e_2) \end{bmatrix} = \begin{bmatrix} 1 & 0 \\ 0 & 1 \end{bmatrix}.$$

On the other hand, the shortest paths from $\boldsymbol{v}_0$ to other vertices are

$$\operatorname{spath}(\boldsymbol{v}_0, \boldsymbol{w}_i) = (\boldsymbol{v}_0 \boldsymbol{w}_i), \quad i = 1, 2.$$

Since $\{\alpha_i\}_{i=1}^{2}$ is orthonormal, hence, we obtain

$$\boldsymbol{v}_0 = \begin{bmatrix} 0 \\ 0 \end{bmatrix}, \quad \boldsymbol{w}_1 = \boldsymbol{v}_0 + a(e_1) = \begin{bmatrix} 1 \\ 0 \end{bmatrix}, \quad \boldsymbol{w}_2 = \boldsymbol{v}_0 + a(e_2) = \begin{bmatrix} 0 \\ 1 \end{bmatrix},$$

and the period lattice is

$$\begin{bmatrix} \boldsymbol{x}_1 & \boldsymbol{x}_2 \end{bmatrix} = \begin{bmatrix} 1 & 0 \\ 0 & 1 \end{bmatrix}.$$

The above datas allows us to write figure in Fig. 3.1 (a).

Example 3.31 (**Hyper-cubic lattice in** $\mathbb{R}^n$, Sunada [39, Section 8.3]). A generalization of Example 3.30 is hyper-cubic lattices in $\mathbb{R}^n$. In case of $n = 3$, it is called cubic lattices. The base graph $X_0 = (V_0, E_0)$ of hyper-cubic lattices is the n-bouquet graph (Fig. 3.3 (b)), namely $V_0 = \{v\}$, $E_0 = \{e_i\}_{i=1}^n$, as in Fig. 3.3 (b). Since a spanning tree of X_0 is $X_1 = (V_0, \{\emptyset\})$, we may take an orthonormal $\mathbb{Z}$-basis of $H_1(X_0, \mathbb{Z})$ by $\{\alpha_i\}_{i=1}^n$, where $\alpha_i = e_i$. By similar calculations, we obtain

$$A = A^{-1} = \left[a(e_i)\right] = \left[b(e_i)\right] = E_n \quad \text{(the identity matrix of size } n\text{)}.$$

Hence, we obtain

$$\boldsymbol{v}_0 = \boldsymbol{0}, \quad \boldsymbol{w}_i = \boldsymbol{x}_i \quad \text{(standard } i\text{-th unit vector of } \mathbb{R}^n\text{)} \quad i = 1, \ldots, n,$$

and the period lattice is $\left[\boldsymbol{x}_i\right] = E_n$. A standard realization of hyper-cubic lattices is an orthonormal lattice in $\mathbb{R}^n$.

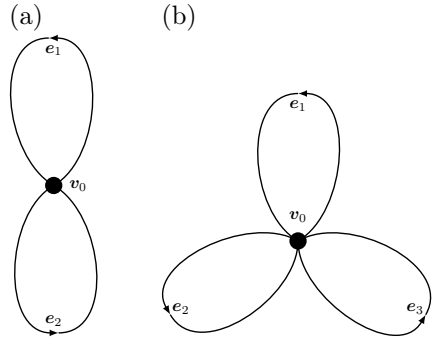

Figure 3.3: (a) The 2-bouquet graph, which is the base graph of square lattices, (b) the 3-bouquet graph, which is the base graph of cubic lattices.

Example 3.32 (**Hexagonal lattices**, Fig. 3.1 (c), Sunada [39, Section 8.3]). The base graph $X_0 = (V_0, E_0)$ of hexagonal lattices in $\mathbb{R}^2$ is the graph with two vertices and three edges connecting both vertices (Fig. 3.4 (a)), and $\operatorname{rank} H_1(X_0, \mathbb{R}) = 2$. Write $V_0 = \{v_0, v_1\}$ and $E_0 = \{e_1, e_2, e_3\}$ as in Fig. 3.4, then a spanning tree of X_0 is $X_1 = (V_0, \{e_3\})$. Hence, we may take $\alpha_1 = e_1 - e_3$ and $\alpha_2 = e_2 - e_3$ as a

$\mathbb{Z}$-basis of $H_1(X_0, \mathbb{Z})$, and obtain

$$A = \begin{bmatrix} 2 & 1 \\ 1 & 2 \end{bmatrix}, \quad A^{-1} = \frac{1}{3}\begin{bmatrix} 2 & -1 \\ -1 & 2 \end{bmatrix}$$
$$\begin{bmatrix} \boldsymbol{b}(e_1) & \boldsymbol{b}(e_2) & \boldsymbol{b}(e_3) \end{bmatrix} = \begin{bmatrix} 1 & 0 & -1 \\ 0 & 1 & -1 \end{bmatrix},$$
$$\begin{bmatrix} \boldsymbol{a}(e_1) & \boldsymbol{a}(e_2) & \boldsymbol{a}(e_3) \end{bmatrix} = \frac{1}{3}\begin{bmatrix} 2 & -1 & -1 \\ -1 & 2 & -1 \end{bmatrix}.$$

The shortest paths from $\boldsymbol{v}_0$ to other vertices are

$$\mathrm{spath}(\boldsymbol{v}_0, \boldsymbol{w}_i) = (\boldsymbol{v}_0 \boldsymbol{w}_i) \quad i = 1, 2.$$

Since $\{\alpha_i\}_{i=1}^2$ is not orthonormal, we choice the basis as

$$\begin{bmatrix} \alpha_1 \\ \alpha_2 \end{bmatrix} = \begin{bmatrix} \sqrt{2} & 0 \\ 1/\sqrt{2} & \sqrt{3/2} \end{bmatrix} =: X,$$

then we obtain

$$\boldsymbol{v}_0 = \boldsymbol{0},$$
$$\boldsymbol{w}_1 = \frac{2}{3}\alpha_1 - \frac{1}{3}\alpha_2 = \begin{bmatrix} 1/\sqrt{2} \\ -1/\sqrt{6} \end{bmatrix},$$
$$\boldsymbol{w}_2 = -\frac{1}{3}\alpha_1 + \frac{2}{3}\alpha_2 = \begin{bmatrix} 0 \\ \sqrt{2/3} \end{bmatrix},$$
$$\boldsymbol{w}_3 = -\frac{1}{3}\alpha_1 - \frac{1}{3}\alpha_2 = \begin{bmatrix} -1/\sqrt{2} \\ -1/\sqrt{6} \end{bmatrix},$$

and the period lattice is

$$\begin{bmatrix} \boldsymbol{x}_1 & \boldsymbol{x}_2 \end{bmatrix} = X.$$

Note that $\langle \boldsymbol{w}_i, \boldsymbol{w}_j \rangle = (-1/2)|\boldsymbol{w}_i|\,|\boldsymbol{w}_j|$ $(i \neq j)$ are satisfied. The above datas allow us to write figure in Fig. 3.1 (c).

Example 3.33 (**Diamond lattices**, Sunada [39, Section 8.3]). The base graph $X_0 = (V_0, E_0)$ of a diamond lattices in $\mathbb{R}^3$ is the graph with two vertices and four edges connecting both vertices, and $\mathrm{rank}\, H_1(X_0, \mathbb{R}) = 3$ (see Fig. 3.18). Write $V_0 = \{v_0, v_1\}$ and $E_0 = \{e_1, e_2, e_3, e_4\}$, where $e_i = (v_0, v_1)$, then a spanning tree

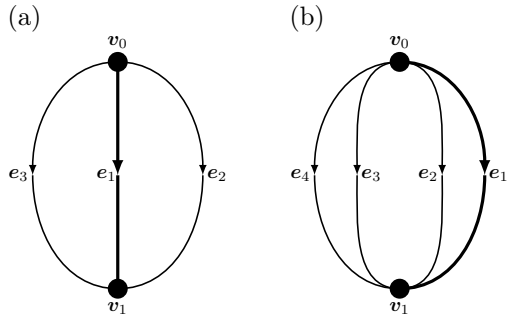

Figure 3.4: (a) The base graph of hexagonal lattices, (b) the base graph of diamond lattices. Thick edges consist a spanning tree of them.

of X_0 is $X_1 = (V_0, \{e_4\})$. Hence, we may take $\alpha_i = e_i - e_4$ $(i = 1, 2, 3)$ as a $\mathbb{Z}$-basis of $H_1(X_0, \mathbb{Z})$, and obtain

$$A = \begin{bmatrix} 2 & 1 & 1 \\ 1 & 2 & 1 \\ 1 & 1 & 2 \end{bmatrix}, \quad A^{-1} = \frac{1}{4}\begin{bmatrix} 3 & -1 & -1 \\ -1 & 3 & -1 \\ -1 & -1 & 3 \end{bmatrix}$$

$$\begin{bmatrix} \boldsymbol{b}(e_1) & \boldsymbol{b}(e_2) & \boldsymbol{b}(e_3) & \boldsymbol{b}(e_4) \end{bmatrix} = \begin{bmatrix} 1 & 0 & 0 & -1 \\ 0 & 1 & 0 & -1 \\ 0 & 0 & 1 & -1 \end{bmatrix},$$

$$\begin{bmatrix} \boldsymbol{a}(e_1) & \boldsymbol{a}(e_2) & \boldsymbol{a}(e_3) & \boldsymbol{a}(e_4) \end{bmatrix} = \frac{1}{4}\begin{bmatrix} 3 & -1 & -1 & -1 \\ -1 & 3 & -1 & -1 \\ -1 & -1 & 3 & -1 \end{bmatrix},$$

$$\begin{bmatrix} \alpha_1 \\ \alpha_2 \\ \alpha_3 \end{bmatrix} = \begin{bmatrix} \sqrt{2} & 0 & 0 \\ 1/\sqrt{2} & \sqrt{3/2} & 0 \\ 1/\sqrt{2} & 1/\sqrt{6} & 2/\sqrt{3} \end{bmatrix} =: X.$$

The shortest paths from $\boldsymbol{v}_0$ to other vertices are

$$\mathrm{spath}(\boldsymbol{v}_0, \boldsymbol{w}_i) = (\boldsymbol{v}_0 \boldsymbol{w}_i) \quad i = 1, 2, 3.$$

Hence, we obtain

$$\begin{aligned}
\boldsymbol{v}_0 &= \mathbf{0}, \\
\boldsymbol{w}_1 &= \frac{3}{4}\alpha_1 - \frac{1}{4}\alpha_2 - \frac{1}{4}\alpha_3 = \begin{bmatrix} 1/\sqrt{2} \\ -1/\sqrt{6} \\ -1/(2\sqrt{3}) \end{bmatrix}, \\
\boldsymbol{w}_2 &= -\frac{1}{4}\alpha_1 + \frac{3}{4}\alpha_2 - \frac{1}{4}\alpha_3 = \begin{bmatrix} 0 \\ \sqrt{2/3} \\ -1/(2\sqrt{3}) \end{bmatrix}, \\
\boldsymbol{w}_3 &= -\frac{1}{4}\alpha_1 - \frac{1}{4}\alpha_2 + \frac{3}{4}\alpha_3 = \begin{bmatrix} 0 \\ 0 \\ 2/\sqrt{3} \end{bmatrix}, \\
\boldsymbol{w}_4 &= -\frac{1}{4}\alpha_1 - \frac{1}{4}\alpha_2 - \frac{1}{4}\alpha_3 = \begin{bmatrix} -1/\sqrt{2} \\ -1/\sqrt{6} \\ -1/(2\sqrt{3}) \end{bmatrix}.
\end{aligned}$$

The period lattice is

$$\begin{bmatrix} \boldsymbol{x}_1 & \boldsymbol{x}_2 & \boldsymbol{x}_3 \end{bmatrix} = X.$$

Note that $\langle \boldsymbol{w}_i, \boldsymbol{w}_j \rangle = (-1/3)|\boldsymbol{w}_i|\,|\boldsymbol{w}_j|$ $(i \neq j)$ are satisfied.

Example 3.34 (**Gyroid lattices (K_4 lattices)**, Sunada [39, Section 8.3]). The base graph $X_0 = (V_0, E_0)$ of a gyroid lattices in $\mathbb{R}^3$ is the K_4 graph, which is the complete graph of four vertices, and $\operatorname{rank} H_1(X_0, \mathbb{R}) = 3$. Write $V_0 = \{v_i\}_{i=1}^4$ and $E_0 = \{e_i\}_{i=1}^4$ as in Fig. 3.5 (a), and take a spanning tree X_1 of X_0 as in Fig. 3.5 (b). Hence, we may take

$$\alpha_1 = e_1 + e_4 - e_2, \quad \alpha_2 = e_2 + e_5 - e_3, \quad \alpha_3 = e_3 + e_6 - e_1$$

as a $\mathbb{Z}$-basis of $H_1(X_0, \mathbb{Z})$, and obtain

$$A = \begin{bmatrix} 3 & -1 & -1 \\ -1 & 3 & -1 \\ -1 & -1 & 3 \end{bmatrix}, \quad A^{-1} = \frac{1}{4}\begin{bmatrix} 2 & 1 & 1 \\ 1 & 2 & 1 \\ 1 & 1 & 2 \end{bmatrix}$$

$$\boldsymbol{b} = \begin{bmatrix} 1 & -1 & 0 & 1 & 0 & 0 \\ 0 & 1 & -1 & 0 & 1 & 0 \\ -1 & 0 & 1 & 0 & 0 & 1 \end{bmatrix}, \quad \boldsymbol{a} = \frac{1}{4}\begin{bmatrix} 1 & -1 & 0 & 2 & 1 & 1 \\ 0 & 1 & -1 & 1 & 2 & 1 \\ -1 & 0 & 1 & 1 & 1 & 2 \end{bmatrix},$$

$$\begin{bmatrix} \alpha_1 \\ \alpha_2 \\ \alpha_3 \end{bmatrix} = \begin{bmatrix} \sqrt{3} & 0 & 0 \\ -1/\sqrt{3} & 2\sqrt{2/3} & 0 \\ -1/\sqrt{3} & -\sqrt{2/3} & \sqrt{2} \end{bmatrix} =: X,$$

Let $\{w_i\}_{i=1}^3$ be as in Fig. 3.5 (b), then the shortest paths from $\boldsymbol{v}_0$ to other vertices are

$$\mathrm{spath}(\boldsymbol{v}_0, \boldsymbol{v}_i) = (\boldsymbol{v}_0\boldsymbol{v}_i), \quad \mathrm{spath}(\boldsymbol{v}_0, \boldsymbol{w}_i) = (\boldsymbol{v}_0\boldsymbol{v}_i)(\boldsymbol{v}_i\boldsymbol{w}_i), \quad i = 1,\, 2,\, 3.$$

Hence, we obtain

$\boldsymbol{v}_0 = \boldsymbol{0}$,

$$\boldsymbol{v}_1 = \tfrac{1}{4}\alpha_1 - \tfrac{1}{4}\alpha_3 = \begin{bmatrix} 1/\sqrt{3} \\ 1/(2\sqrt{6}) \\ -1/(2\sqrt{2}) \end{bmatrix}, \quad \boldsymbol{w}_1 = \boldsymbol{v}_1 + \tfrac{1}{2}\alpha_1 + \tfrac{1}{4}\alpha_2 + \tfrac{1}{4}\alpha_3 = \begin{bmatrix} 2/\sqrt{3} \\ 1/\sqrt{6} \\ 0 \end{bmatrix}$$

$$\boldsymbol{v}_2 = \tfrac{1}{4}\alpha_2 - \tfrac{1}{4}\alpha_1 = \begin{bmatrix} -1/\sqrt{3} \\ 1/\sqrt{6} \\ 0 \end{bmatrix}, \quad \boldsymbol{w}_2 = \boldsymbol{v}_2 + \tfrac{1}{4}\alpha_1 + \tfrac{1}{2}\alpha_2 + \tfrac{1}{4}\alpha_3 = \begin{bmatrix} -1/\sqrt{3} \\ 5/(2\sqrt{6}) \\ 1/(2\sqrt{2}) \end{bmatrix}$$

$$\boldsymbol{v}_3 = \tfrac{1}{4}\alpha_3 - \tfrac{1}{4}\alpha_2 = \begin{bmatrix} 0 \\ -\sqrt{3}/(2\sqrt{2}) \\ 1/(2\sqrt{2}) \end{bmatrix}, \quad \boldsymbol{w}_3 = \boldsymbol{v}_3 + \tfrac{1}{4}\alpha_1 + \tfrac{1}{4}\alpha_2 + \tfrac{1}{2}\alpha_3 = \begin{bmatrix} 0 \\ -\sqrt{3}/(2\sqrt{2}) \\ 3/(2\sqrt{2}) \end{bmatrix}.$$

A gyroid lattice is called a K_4 lattice since its base graph is K_4. It is also called a Laves' graph of girth ten, a $(10, 3)$-*a* network, and a diamond twin. The minimum length of closed path (without backtracking paths) is called the *girth* of the graph. The girth of a gyroid lattice is 10 (see Fig. 3.8), and hence, it is called $(10, 3)$-*a* network.

Remark 3.35. We can also take coordinates which all vertices have rational numbers. Taking

$$\begin{bmatrix} \alpha_1 \\ \alpha_2 \\ \alpha_3 \end{bmatrix} = \begin{bmatrix} -1 & 1 & -1 \\ -1 & -1 & 1 \\ 1 & -1 & -1 \end{bmatrix},$$

then

$$\boldsymbol{v}_1 = \frac{1}{2}\begin{bmatrix} 0 \\ -1 \\ 1 \end{bmatrix}, \qquad \boldsymbol{v}_2 = \frac{1}{2}\begin{bmatrix} 1 \\ 0 \\ -1 \end{bmatrix}, \qquad \boldsymbol{v}_3 = \begin{bmatrix} -1 \\ 1 \\ 0 \end{bmatrix},$$
$$\boldsymbol{w}_1 = \frac{1}{2}\begin{bmatrix} -1 \\ -2 \\ 1 \end{bmatrix}, \qquad \boldsymbol{w}_2 = \begin{bmatrix} 1 \\ -1 \\ -2 \end{bmatrix}, \qquad \boldsymbol{w}_3 = \begin{bmatrix} -2 \\ 1 \\ -1 \end{bmatrix}.$$

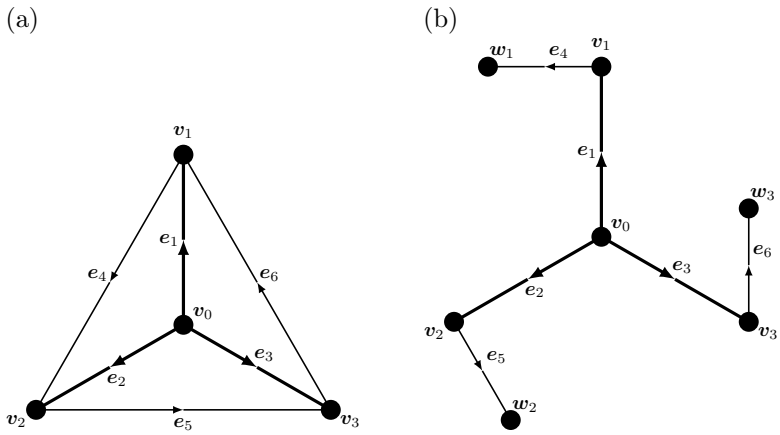

Figure 3.5: (a) The base graph of gyroid (K_4) lattices, thick edges consist a spanning tree of them. (b) building block (in the abstract graph) of gyroid lattices.

Remark 3.36. Let $\Phi(X)$ be a standard realization of diamond or cubic lattices, and $C \in O(3)\backslash SO(3)$. Then, $C(\Phi(X))$ and $\Phi(X)$ are mutually congruent, namely, $\Phi(X)$ and its mirror image are mutually congruent in $\mathbb{R}^3$. This property is called *chiral symmetry*. On the other hand, a standard realization of K_4 lattices is not chiral symmetric. Taking a $C \in O(3) \setminus SO(3)$, $X' = XC$ and constructing the realization as in Example 3.34, then we obtain a chiral image of $\Phi(X)$.

3.2.2 Explicit algorithm for generic cases

In general, a standard realization of d-dimensional topological crystal X is not maximal abelian covering of a base graph X_0. In this section, we assume that

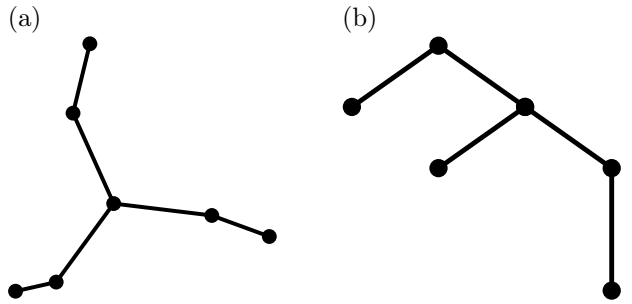

Figure 3.6: (a) A building block of a gyroid lattice (K_4 lattice) viewed from a perpendicular direction of the plane consisted by $\boldsymbol{v}_1$, $\boldsymbol{v}_2$, and $\boldsymbol{v}_3$, (b) one viewed from a parallel direction of it.

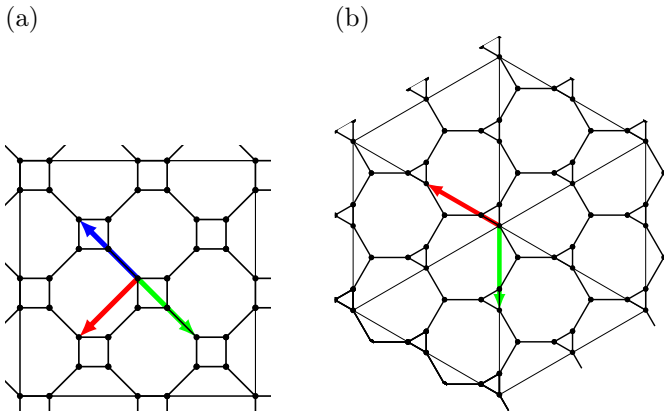

Figure 3.7: A gyroid (K_4) lattice from (a) $(0,0,1)$-direction and (b) $(1,1,1)$-direction by using coordinates in Remark 3.35. The blue, red, and green vectors are $\boldsymbol{\alpha}_1$, $\boldsymbol{\alpha}_2$, and $\boldsymbol{\alpha}_3$, respectively. In (b), $\boldsymbol{\alpha}_1$ is the vector perpendicular to the paper from the back to the front.

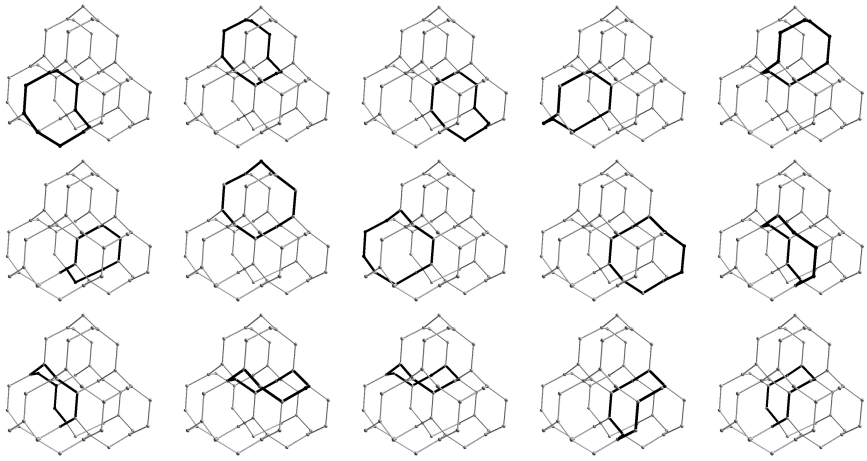

Figure 3.8: Fifteen 10-members rings pass through a vertex in a gyroid lattice. Each ring is mutually congruent.

$d < b = \operatorname{rank} H_1(X_0, \mathbb{Z})$, and explain explicit algorithm to obtain a standard realization of X. This method is followed by Sunada [39].

Since $d < b$, the standard realization is constructed in a d-dimensional subspace V of $H_1(X_0, \mathbb{R})$, whose orthogonal subspace H is called the *vanishing subspace*, namely, $H_1(X_0, \mathbb{R}) = V \oplus H$, and $V = H^{\perp}$ with $\dim H = b - d$.

Step 1 By using the method of Step 1 in Section 3.2.1, find a $\mathbb{Z}$-basis $\{\alpha_i\}_{i=1}^{b}$ of $H_1(X_0, \mathbb{Z})$, such that $\{\alpha_i\}_{i=d+1}^{b}$ is a basis of the vanishing subspace H, using a linear transformation if necessary.

Step 2 Compute A, $\boldsymbol{b}(e)$, and $\boldsymbol{a}(e)$ as in Step 2 of Section 3.2.1, then we obtain a standard realization of a topological crystal $\widetilde{X}$, which is a maximal abelian covering of the base graph X_0. This realization $\Phi^{\max}$ is in $H_1(X_0, \mathbb{R}) \cong \mathbb{R}^b$.

Step 3 Let $p\colon H_1(X_0, \mathbb{R}) \longrightarrow H$ be the orthogonal projection, then $\{\beta_i\}_{i=1}^{d}$ is a $\mathbb{Z}$-basis of the period lattice, where $\beta_i = p(\alpha_i)$. We should obtain $B = (\langle \beta_i, \beta_j \rangle) \in GL(d, \mathbb{R})$ to calculate standard realizations of X. Since $\gamma_i - \alpha_i = p(\alpha_i) - \alpha_i \in H$,

we may write

$$p(\alpha_i) = \alpha_i + \sum_{j=b+1}^{d} d_{ij}\alpha_j$$

and $\langle p(\alpha_i), \alpha_k \rangle = 0$ for $k = b+1, \dots, d$, and hence we obtain

$$\langle \alpha_i, \alpha_k \rangle = -\sum_{j=b+1}^{d} d_{ij} \langle \alpha_j, \alpha_k \rangle, \quad k = b+1, \dots, d, \quad i = 1, \dots, b. \tag{3.24}$$

Write $A = \begin{bmatrix} A_{11} & A_{12} \\ A_{21} & A_{22} \end{bmatrix}$, where A_{11} is $d \times d$ matrix, A_{22} is $(b-d) \times (b-d)$ matrix, $A_{12}^T = A_{21}$, and $D = (d_{ij})$, then (3.24) implies

$$A_{12} = -DA_{22}. \tag{3.25}$$

Therefore, we obtain

$$\begin{aligned} \langle \beta_i, \beta_j \rangle &= \langle p(\alpha_i), p(\alpha_j) \rangle = \left\langle p^T p(\alpha_i), \alpha_j \right\rangle = \langle p(\alpha_i), \alpha_j \rangle \\ &= \left\langle \alpha_i + \sum_{k=b+1}^{d} d_{ik}\alpha_k, \alpha_j \right\rangle = \langle \alpha_i, \alpha_j \rangle + \sum_{k=b+1}^{d} d_{ik} \langle \alpha_k, \alpha_j \rangle, \end{aligned} \tag{3.26}$$

and thus, by (3.26), we obtain

$$B = A_{11} + DA_{21} = A_{11} - A_{12}A_{22}^{-1}A_{21}. \tag{3.27}$$

Since realizations of an edge $e \in E_0$ of the maximal abelian covering of X_0 is written as $\boldsymbol{e}^{\max} = \sum_{i=1}^{b} a(e)\alpha_i$, combining $P\colon C_1(X_0, \mathbb{R}) \longrightarrow H_1(X_0, \mathbb{R})$ and $p\colon H_1(X_0, \mathbb{R}) \longrightarrow H$, we obtain

$$p(P(e)) = p(\boldsymbol{e}^{\max}) = \boldsymbol{e} = \sum_{i=1}^{d} a(e)\beta_i. \tag{3.28}$$

Example 3.37 (**Triangular lattice**, Fig. 3.1 (b), Sunada [39, Section 8.3]). A triangular lattice is the projection of a cubic lattice in $\mathbb{R}^3$ onto a suitable 2-dimensional plane. Hence, $d = 2$ and $b = \operatorname{rank} H_1(X_0, \mathbb{R}) = 3$, and the base graph $X_0 = (V_0, E_0)$ of triangular lattices is the one of cubic lattices, i. e., X_0 is the 3-bouquet graph (3.3). Using notation in Example 3.31, take $\alpha_1 = e_1$, $\alpha_2 = e_2$,

$\alpha_3 = e_1 + e_2 + e_3$, and $H = \mathrm{span}\{\alpha_1, \alpha_2\}$, then we obtain

$$A = \begin{bmatrix} 1 & 0 & 1 \\ 0 & 1 & 1 \\ 1 & 1 & 3 \end{bmatrix}, \quad \boldsymbol{b}(e) = \begin{bmatrix} 1 & 0 & 0 \\ 0 & 1 & 0 \\ 1 & 1 & 1 \end{bmatrix}, \quad \boldsymbol{a}(e) = \begin{bmatrix} 1 & 0 & -1 \\ 0 & 1 & -1 \\ 0 & 0 & 1 \end{bmatrix}, \tag{3.29}$$

and

$$\boldsymbol{e}_1^{\max} = \alpha_1, \quad \boldsymbol{e}_2^{\max} = \alpha_2, \quad \boldsymbol{e}_3^{\max} = -\alpha_1 - \alpha_2 + \alpha_3. \tag{3.30}$$

By (3.28) and (3.30), we obtain

$$\boldsymbol{e}_1 = \beta_1, \quad \boldsymbol{e}_2 = \beta_2, \quad \boldsymbol{e}_3 = -\beta_1 - \beta_2, \tag{3.31}$$

and by (3.27) and (3.29), we also obtain

$$B = \left[\left\langle \beta_i, \beta_j \right\rangle\right] = \begin{bmatrix} 1 & 0 \\ 0 & 1 \end{bmatrix} - \frac{1}{3}\begin{bmatrix} 1 \\ 1 \end{bmatrix}\begin{bmatrix} 1 & 1 \end{bmatrix} = \begin{bmatrix} 1 & 0 \\ 0 & 1 \end{bmatrix} - \frac{1}{3}\begin{bmatrix} 1 & 1 \\ 1 & 1 \end{bmatrix} = \frac{1}{3}\begin{bmatrix} 2 & -1 \\ -1 & 2 \end{bmatrix}.$$

On the other hand, the shortest paths from $\boldsymbol{v}_0$ to other vertices are

$$\mathrm{spath}(\boldsymbol{v}_0, \boldsymbol{v}_i) = (\boldsymbol{v}_0 \boldsymbol{v}_i) = \boldsymbol{e}_i \quad i = 1,\, 2,\, 3.$$

By using the Cholesky decomposition, we may write

$$\begin{bmatrix} \beta_1 \\ \beta_2 \end{bmatrix} = \begin{bmatrix} \sqrt{2/3} & -1/\sqrt{6} \\ 0 & 1/\sqrt{2} \end{bmatrix},$$

and hence by (3.31), we obtain

$$\boldsymbol{e}_1 = \begin{bmatrix} \sqrt{2/3} \\ 0 \end{bmatrix}, \quad \boldsymbol{e}_2 = \begin{bmatrix} -1/\sqrt{6} \\ 1/\sqrt{2} \end{bmatrix}. \quad \boldsymbol{e}_3 = \begin{bmatrix} -1/\sqrt{6} \\ -1/\sqrt{2} \end{bmatrix},$$

and

$$\boldsymbol{v}_0 = \begin{bmatrix} 0 \\ 0 \end{bmatrix}, \quad \boldsymbol{v}_1 = \boldsymbol{v}_0 + \boldsymbol{e}_1 = \begin{bmatrix} \sqrt{2/3} \\ 0 \end{bmatrix},$$
$$\boldsymbol{v}_2 = \boldsymbol{v}_0 + \boldsymbol{e}_2 = \begin{bmatrix} -1/\sqrt{6} \\ 1/\sqrt{2} \end{bmatrix}. \quad \boldsymbol{v}_3 = \boldsymbol{v}_0 + \boldsymbol{e}_3 = \begin{bmatrix} -1/\sqrt{6} \\ -1/\sqrt{2} \end{bmatrix}.$$

The above datas allow us to write figure in Fig. 3.1 (b) (see also Fig. 3.9).

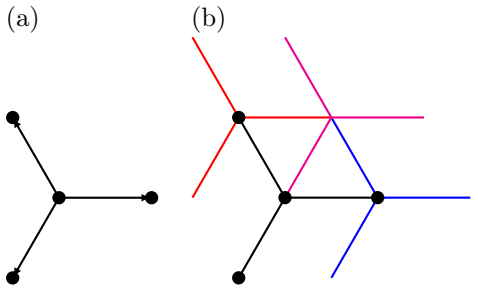

Figure 3.9: Building block of the triangular lattice, and its translations by $B = \{\boldsymbol{\beta}_1, \boldsymbol{\beta}_2\}$. (a) building block $\{\boldsymbol{b}\}$ of the triangular lattice, (b) the blue, red, and magenta blocks are the block translated by $\boldsymbol{\beta}_1$, $\boldsymbol{\beta}_2$, and $\boldsymbol{\beta}_1 + \boldsymbol{\beta}_2$.

Example 3.38 (**Kagome lattice**, Fig. 3.1 (d), Sunada [39, Section 8.3]). A kagome lattice is a standard realization in $\mathbb{R}^2$ whose base graph X_0 shown in Fig. 3.11 (a). The graph X_0 satisfies $b = \operatorname{rank} H_1(X_0, \mathbb{R}) = 4$, and we may select

$$\alpha_1 = e_1 - e_4, \quad \alpha_2 = e_2 - e_5, \quad \alpha_3 = e_1 + e_2 + e_3, \quad \alpha_4 = e_4 + e_5 + e_6,$$

and $H = \operatorname{span}\{e_1 + e_2 + e_3, e_4 + e_5 + e_6\}$. Then, we obtain

(3.32)

$$A = \begin{bmatrix} 2 & 0 & 1 & -1 \\ 0 & 2 & 1 & -1 \\ 1 & 1 & 3 & 0 \\ -1 & -1 & 0 & 3 \end{bmatrix},$$

$$\boldsymbol{b}(e) = \begin{bmatrix} 1 & 0 & 0 & -1 & 0 & 0 \\ 0 & 1 & 0 & 0 & -1 & 0 \\ 1 & 1 & 1 & 0 & 0 & 0 \\ 0 & 0 & 0 & 1 & 1 & 1 \end{bmatrix}, \quad \boldsymbol{a}(e) = \frac{1}{6} \begin{bmatrix} 3 & 0 & -3 & -3 & 0 & 3 \\ 0 & 3 & -3 & 0 & -3 & 3 \\ 1 & 1 & 4 & 1 & 1 & -2 \\ 1 & 1 & -2 & 1 & 1 & 4 \end{bmatrix},$$

(3.33)

$$\begin{aligned} \boldsymbol{e}_1^{\max} &= (1/6)(3\alpha_1 + \alpha_3 + \alpha_4), \\ \boldsymbol{e}_2^{\max} &= (1/6)(3\alpha_2 + \alpha_3 + \alpha_4), \\ \boldsymbol{e}_3^{\max} &= (1/6)(-3\alpha_1 - 3\alpha_2 + 4\alpha_3 - 2\alpha_4), \\ \boldsymbol{e}_4^{\max} &= (1/6)(-3\alpha_1 + \alpha_3 + \alpha_4), \\ \boldsymbol{e}_5^{\max} &= (1/6)(-3\alpha_2 + \alpha_3 + \alpha_4), \\ \boldsymbol{e}_6^{\max} &= (1/6)(3\alpha_1 + 3\alpha_2 - 2\alpha_3 + 4\alpha_4), \end{aligned}$$

By (3.28) and (3.33), we obtain

$$\begin{aligned} &\boldsymbol{e}_1 = (1/2)\beta_1, \quad \boldsymbol{e}_2 = (1/2)\beta_2, \quad \boldsymbol{e}_3 = -(1/2)(\beta_1+\beta_2), \\ &\boldsymbol{e}_4 = -(1/2)\beta_1, \quad \boldsymbol{e}_5 = -(1/2)\beta_2, \quad \boldsymbol{e}_6 = (1/2)(\beta_1+\beta_2), \end{aligned} \tag{3.34}$$

and by (3.27) and (3.34), we also obtain

$$B = \left[\langle \beta_i, \beta_j \rangle\right] = \begin{bmatrix} 2 & 0 \\ 0 & 2 \end{bmatrix} - \begin{bmatrix} 1 & -1 \\ 1 & -1 \end{bmatrix} \begin{bmatrix} 1/3 & 0 \\ 0 & 1/3 \end{bmatrix} \begin{bmatrix} 1 & 1 \\ -1 & -1 \end{bmatrix} = \frac{2}{3} \begin{bmatrix} 2 & -1 \\ -1 & 2 \end{bmatrix}$$

On the other hand, the shortest paths from $\boldsymbol{v}_0$ to other vertices are

$$\mathrm{spath}(\boldsymbol{v}_0, \boldsymbol{v}_i) = (\boldsymbol{v}_0\boldsymbol{v}_i) = \boldsymbol{e}_i \quad \mathrm{spath}(\boldsymbol{v}_0, \boldsymbol{w}_i) = (\boldsymbol{v}_0\boldsymbol{w}_i) = \boldsymbol{e}_{i+3} \quad i = 1, 2, 3.$$

By using the Cholesky decomposition, we may write

$$\begin{bmatrix} \beta_1 \\ \beta_2 \end{bmatrix} = \begin{bmatrix} 2/\sqrt{3} & -1/\sqrt{3} \\ 0 & 1 \end{bmatrix},$$

and hence by (3.34), we obtain

$$\boldsymbol{e}_1 = -\boldsymbol{e}_4 = \begin{bmatrix} 1/\sqrt{3} \\ 0 \end{bmatrix}, \quad \boldsymbol{e}_2 = -\boldsymbol{e}_5 = \begin{bmatrix} -1/(2\sqrt{3}) \\ 1/2 \end{bmatrix}. \quad \boldsymbol{e}_3 = -\boldsymbol{e}_6 = \begin{bmatrix} 1/(2\sqrt{3}) \\ 1/2 \end{bmatrix},$$

and

$$\boldsymbol{v}_0 = \begin{bmatrix} 0 \\ 0 \end{bmatrix}, \quad \boldsymbol{v}_1 = \boldsymbol{v}_0 + \boldsymbol{e}_1 = \begin{bmatrix} 1/\sqrt{3} \\ 0 \end{bmatrix}, \qquad \boldsymbol{v}_2 = \boldsymbol{v}_0 + \boldsymbol{e}_2 = \begin{bmatrix} -1/(2\sqrt{3}) \\ 1/2 \end{bmatrix},$$
$$\boldsymbol{w}_1 = \boldsymbol{v}_0 + \boldsymbol{e}_4 = \begin{bmatrix} -1/\sqrt{3} \\ 0 \end{bmatrix}, \qquad \boldsymbol{w}_2 = \boldsymbol{v}_0 + \boldsymbol{e}_5 = \begin{bmatrix} 1/(2\sqrt{3}) \\ -1/2 \end{bmatrix}.$$

The above datas allow us to write figure in Fig. 3.1 (d) (see also Fig. 3.10). Since $\triangle \boldsymbol{v}_0\boldsymbol{v}_1\boldsymbol{v}_2$ and $\triangle \boldsymbol{v}_0\boldsymbol{w}_1\boldsymbol{w}_2$ consist regular triangles, a standard realization of kagome lattices is consisted by regular triangles sharing vertices each other.

Next, we consider higher dimensional analogues of kagome lattices. As mentioned in Example 3.38, a standard realization of a kagome lattice consists by regular triangles sharing vertices each other. One of the 3-dimensional analogues of kagome lattices is a hyper-kagome lattice of type II, whose standard realization consists quadrilaterals sharing vertices each other. Since a triangles in $\mathbb{R}^2$ is a 1-simplex, the other is a hyper-kagome lattice of type I, whose standard realization consists 1-skeleton of 2-simplex sharing vertices each other.

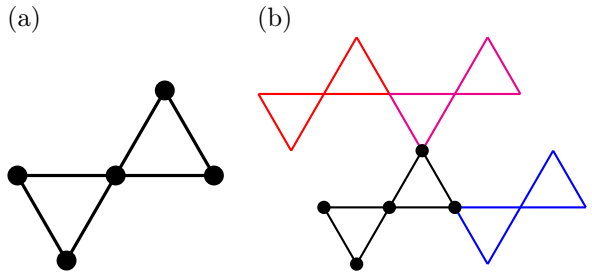

Figure 3.10: Building block of the kagome lattice, and its translations by $B = \{\boldsymbol{\beta}_1, \boldsymbol{\beta}_2\}$. (a) building block $\{\boldsymbol{b}\}$ of the kagome lattice, (b) the blue, red, and magenta blocks are blocks translated by $\boldsymbol{\beta}_1$, $\boldsymbol{\beta}_2$, and $\boldsymbol{\beta}_1 + \boldsymbol{\beta}_2$.

Example 3.39 (**3D kagome lattice of type I**, Sunada [39, Section 8.3]). One of the 3-dimensional analogues of kagome lattices is defined as follows. Let X_0 be a graph in Fig. 3.11 (b), and and $\widetilde{X}$ be its maximal abelian covering. Since $b = \operatorname{rank} H_1(X_0, \mathbb{R}) = 9$, $\widetilde{X}$ is 9-dimensional a topological crystal. Take a $\mathbb{Z}$-basis of $H_1(X_0, \mathbb{R})$ as

$$\begin{aligned}
&\alpha_1 = e_1 - e_4, && \alpha_2 = e_2 - e_5, && \alpha_3 = e_3 - e_6,\\
&\alpha_4 = e_7 - e_2 + e_1, && \alpha_5 = e_8 - e_3 + e_2, && \alpha_6 = e_9 - e_1 + e_3,\\
&\alpha_7 = e_{10} + e_5 - e_4, && \alpha_8 = e_{11} + e_6 - e_5, && \alpha_9 = e_{12} + e_4 - e_6,
\end{aligned}$$

and

$$H = \operatorname{span}\{\alpha_4, \alpha_5, \alpha_6, \alpha_7, \alpha_8, \alpha_9\}.$$

The number of vertices in a building block in $H_1(X_0, \mathbb{R})$ is 7, and the shortest paths from v_0 are

$$\begin{aligned}
&\operatorname{spath}(\boldsymbol{v}_0, \boldsymbol{v}_1) = \boldsymbol{e}_1, && \operatorname{spath}(\boldsymbol{v}_0, \boldsymbol{v}_2) = \boldsymbol{e}_2, && \operatorname{spath}(\boldsymbol{v}_0, \boldsymbol{v}_3) = \boldsymbol{e}_3,\\
&\operatorname{spath}(\boldsymbol{v}_0, \boldsymbol{w}_1) = -\boldsymbol{e}_4, && \operatorname{spath}(\boldsymbol{v}_0, \boldsymbol{w}_2) = -\boldsymbol{e}_5, && \operatorname{spath}(\boldsymbol{v}_0, \boldsymbol{w}_3) = -\boldsymbol{e}_6.
\end{aligned}$$

A building block are

$$\boldsymbol{e}_1 = \begin{bmatrix} 1/2 \\ 0 \\ 0 \end{bmatrix}, \quad \boldsymbol{e}_2 = \begin{bmatrix} 1/4 \\ \sqrt{3}/4 \\ 0 \end{bmatrix}, \quad \boldsymbol{e}_3 = \begin{bmatrix} 1/4 \\ 1/(4\sqrt{3}) \\ 1/\sqrt{6} \end{bmatrix},$$
$$\boldsymbol{e}_4 = \begin{bmatrix} -1/2 \\ 0 \\ 0 \end{bmatrix}, \quad \boldsymbol{e}_5 = \begin{bmatrix} -1/4 \\ -\sqrt{3}/4 \\ 0 \end{bmatrix}, \quad \boldsymbol{e}_6 = \begin{bmatrix} -1/4 \\ -1/(4\sqrt{3}) \\ -1/\sqrt{6} \end{bmatrix},$$
$$\boldsymbol{e}_7 = \begin{bmatrix} -1/4 \\ \sqrt{3}/4 \\ 0 \end{bmatrix}, \quad \boldsymbol{e}_8 = \begin{bmatrix} 0 \\ -1/(2\sqrt{3}) \\ 1/\sqrt{6} \end{bmatrix}, \quad \boldsymbol{e}_9 = \begin{bmatrix} 1/4 \\ -1/(4\sqrt{3}) \\ -1/\sqrt{6} \end{bmatrix},$$
$$\boldsymbol{e}_{10} = \begin{bmatrix} -1/4 \\ \sqrt{3}/4 \\ 0 \end{bmatrix}, \quad \boldsymbol{e}_{11} = \begin{bmatrix} 0 \\ -1/(2\sqrt{3}) \\ 1/\sqrt{6} \end{bmatrix}, \quad \boldsymbol{e}_{12} = \begin{bmatrix} 1/4 \\ -1/(4\sqrt{3} \\ -1/\sqrt{6} \end{bmatrix},$$

and

$$\begin{bmatrix} \beta_1 \\ \beta_2 \\ \beta_3 \end{bmatrix} = \begin{bmatrix} 1 & 0 & 0 \\ 1/2 & \sqrt{3}/2 & 0 \\ 1/2 & 1/(2\sqrt{3}) & \sqrt{2/3} \end{bmatrix},$$

then we obtain 3D kagome lattice of type I (Fig. 3.12). This lattice is sometimes called as *Pyrochlore lattice* or simply *hyper-kagome lattice*.

Example 3.40 (**3D kagome lattice of type II**, Sunada [39, Section 8.3]). The other 3-dimensional analogue of kagome lattices is defined as follows. Let X_0 be a graph in Fig. 3.11 (c), and and $\widetilde{X}$ be its maximal abelian covering. Since $b = \operatorname{rank} H_1(X_0, \mathbb{R}) = 5$, $\widetilde{X}$ is 5-dimensional a topological crystal. Take a $\mathbb{Z}$-basis of $H_1(X_0, \mathbb{R})$ as

$$\alpha_1 = e_1 - e_4, \quad \alpha_2 = e_2 - e_5, \quad \alpha_3 = e_3 - e_6,$$
$$\alpha_4 = e_1 + e_2 + e_3 + e_4, \quad \alpha_5 = e_5 + e_6 + e_7 + e_8,$$

and

$$H = \operatorname{span}\{e_1 + e_2 + e_3 + e_4, e_5 + e_6 + e_7 + e_8\}.$$

The number of vertices in a building block in $H_1(X_0, \mathbb{R})$ is 7, and the shortest paths from v_0 are

$$\operatorname{spath}(\boldsymbol{v}_0, \boldsymbol{v}_1) = \boldsymbol{e}_1, \quad \operatorname{spath}(\boldsymbol{v}_0, \boldsymbol{v}_2) = \boldsymbol{e}_1 + \boldsymbol{e}_2, \quad \operatorname{spath}(\boldsymbol{v}_0, \boldsymbol{v}_3) = \boldsymbol{e}_1 + \boldsymbol{e}_2 + \boldsymbol{e}_3,$$
$$\operatorname{spath}(\boldsymbol{v}_0, \boldsymbol{w}_1) = \boldsymbol{e}_5, \quad \operatorname{spath}(\boldsymbol{v}_0, \boldsymbol{w}_2) = \boldsymbol{e}_5 + \boldsymbol{e}_6, \quad \operatorname{spath}(\boldsymbol{v}_0, \boldsymbol{w}_3) = \boldsymbol{e}_5 + \boldsymbol{e}_6 + \boldsymbol{e}_7.$$

A building block are

$$\boldsymbol{e}_1 = \begin{bmatrix} (1/2)\sqrt{3/2} \\ 0 \\ 0 \end{bmatrix}, \quad \boldsymbol{e}_2 = \begin{bmatrix} -1/(2\sqrt{6}) \\ 1/\sqrt{3} \\ 0 \end{bmatrix}, \quad \boldsymbol{e}_3 = \begin{bmatrix} -1/(2\sqrt{6}) \\ -1/(2\sqrt{3}) \\ 1/2 \end{bmatrix},$$
$$\boldsymbol{e}_4 = \begin{bmatrix} -1/(2\sqrt{6}) \\ -1/(2\sqrt{3} \\ -1/2 \end{bmatrix}, \quad \boldsymbol{e}_5 = \begin{bmatrix} -(1/2)\sqrt{3/2} \\ 0 \\ 0 \end{bmatrix}, \quad \boldsymbol{e}_6 = \begin{bmatrix} 1/(2\sqrt{6}) \\ -1/\sqrt{3} \\ 0 \end{bmatrix},$$
$$\boldsymbol{e}_7 = \begin{bmatrix} 1/(2\sqrt{6}) \\ 1/(2\sqrt{3}) \\ -1/2 \end{bmatrix}, \quad \boldsymbol{e}_8 = \begin{bmatrix} 1/(2\sqrt{6}) \\ 1/(2\sqrt{3}) \\ 1/2 \end{bmatrix},$$

and

$$\begin{bmatrix} \beta_1 \\ \beta_2 \\ \beta_3 \end{bmatrix} = \begin{bmatrix} \sqrt{3/2} & -1/\sqrt{6} & -1/\sqrt{6} \\ 0 & 2/\sqrt{3} & -1/\sqrt{3} \\ 0 & 0 & 1 \end{bmatrix},$$

then we obtain 3D kagome lattice of type II (Fig. 3.13).

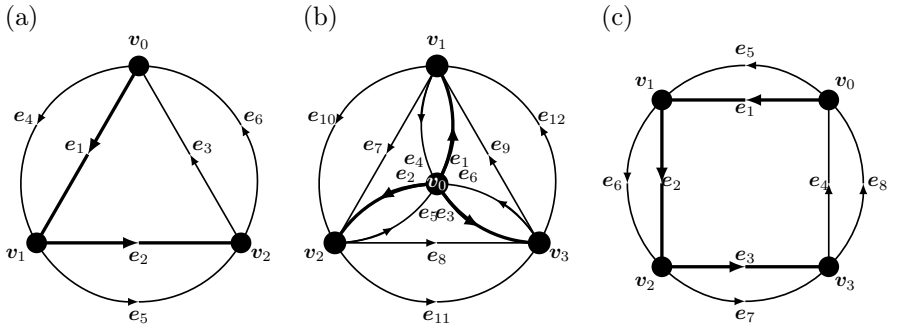

Figure 3.11: (a) The base graph of kagome lattices, (b) the base graph of 3D kagome lattices of type I, (c) the base graph of 3D kagome lattices of type II.

Example 3.41 (**Cairo pentagonal tiling**, Sunada [39, Section 8.3]). A periodic tessellations is also considered as a topological crystal. A Cairo pentagonal tiling (Fig. 3.14 (b)) is a tessellation by congruent pentagons, and it is topologically equivalent to the basketweave tiling (Fig. 3.14 (a)). It is also called MacMahon's net [30]. Here, we compute a standard realization of the cairo pentagonal tiling.

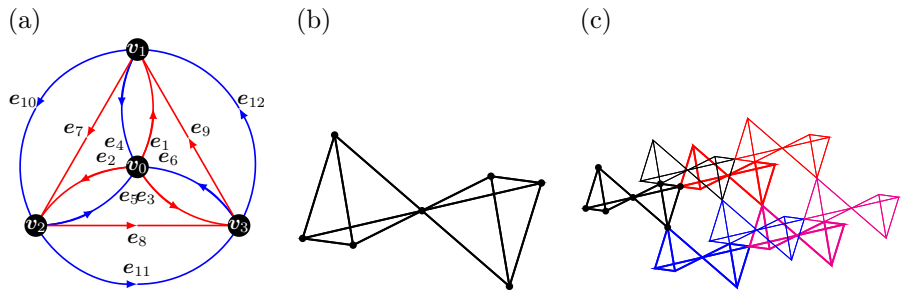

Figure 3.12: Building block of the 3D kagome lattice of type I, and its translations by $B = \{\boldsymbol{\beta}_1, \boldsymbol{\beta}_2, \boldsymbol{\beta}_3\}$. (a) Each graph consisted by blue edges with vertices and by red edges with vertices is a tetrahedral graph. (b) building block $\{\boldsymbol{b}\}$, (c) the blue, red, and magenta blocks are blocks translated by $\boldsymbol{\beta}_1$, $\boldsymbol{\beta}_2$, and $\boldsymbol{\beta}_1 + \boldsymbol{\beta}_2$. The thin layer are translated by $\boldsymbol{\beta}_3$ of above them.

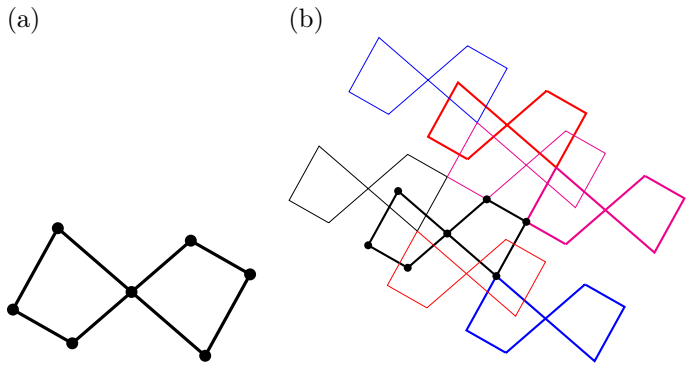

Figure 3.13: Building block of the 3D kagome lattice of type II, and its translations by $B = \{\boldsymbol{\beta}_1, \boldsymbol{\beta}_2, \boldsymbol{\beta}_3\}$. (a) building block $\{\boldsymbol{b}\}$, (b) the blue, red, and magenta blocks are blocks translated by $\boldsymbol{\beta}_1$, $\boldsymbol{\beta}_2$, and $\boldsymbol{\beta}_1 + \boldsymbol{\beta}_2$. The thin layer are translated by $\boldsymbol{\beta}_3$ of above them.

We number vertices and edges of the graph of a fundamental region of the basketweave tiling as Fig. 3.14 (a). Taking a basis $\{\boldsymbol{p}_1, \boldsymbol{p}_2\}$ of the period lattice, then we obtain the equation of harmonic realizations (the equation of the balancing condition) as

(3.35)
$$
\begin{aligned}
4\boldsymbol{v}_0 &= \boldsymbol{v}_2 + (\boldsymbol{v}_9 - \boldsymbol{p}_2) + (\boldsymbol{v}_4 - \boldsymbol{p}_1) + (\boldsymbol{v}_{11} - \boldsymbol{p}_1 - \boldsymbol{p}_2), & 4\boldsymbol{v}_1 &= \boldsymbol{v}_3 + \boldsymbol{v}_4 + (\boldsymbol{v}_9 - \boldsymbol{p}_2) + (\boldsymbol{v}_{10} - \boldsymbol{p}_2),\\
3\boldsymbol{v}_2 &= \boldsymbol{v}_0 + \boldsymbol{v}_3 + \boldsymbol{v}_6, & 3\boldsymbol{v}_3 &= \boldsymbol{v}_1 + \boldsymbol{v}_2 + \boldsymbol{v}_7,\\
3\boldsymbol{v}_4 &= \boldsymbol{v}_1 + \boldsymbol{v}_5 + (\boldsymbol{v}_0 + \boldsymbol{p}_1), & 3\boldsymbol{v}_5 &= \boldsymbol{v}_7 + \boldsymbol{v}_4 + (\boldsymbol{v}_6 + \boldsymbol{p}_1),\\
4\boldsymbol{v}_6 &= \boldsymbol{v}_2 + \boldsymbol{v}_8 + (\boldsymbol{v}_5 - \boldsymbol{p}_1) + (\boldsymbol{v}_{11} - \boldsymbol{p}_1), & 4\boldsymbol{v}_7 &= \boldsymbol{v}_3 + \boldsymbol{v}_5 + \boldsymbol{v}_8 + \boldsymbol{v}_{10},\\
3\boldsymbol{v}_8 &= \boldsymbol{v}_6 + \boldsymbol{v}_7 + \boldsymbol{v}_9, & 3\boldsymbol{v}_9 &= \boldsymbol{v}_8 + \boldsymbol{v}_0 + \boldsymbol{p}_2 + \boldsymbol{v}_1 + \boldsymbol{p}_2,\\
3\boldsymbol{v}_{10} &= \boldsymbol{v}_7 + \boldsymbol{v}_1 + \boldsymbol{p}_2 + \boldsymbol{v}_{11}, & 3\boldsymbol{v}_{11} &= \boldsymbol{v}_{10} + \boldsymbol{v}_6 + \boldsymbol{p}_1 + \boldsymbol{v}_0 + \boldsymbol{p}_1 + \boldsymbol{p}_2.
\end{aligned}
$$

For a given basis $\{\boldsymbol{p}_1, \boldsymbol{p}_2\}$, we obtain a solution of (3.35) (a harmonic realization of the cairo pentagonal tiling) as

(3.36)
$$
\begin{aligned}
&\boldsymbol{v}_0 = \boldsymbol{0}, && \boldsymbol{v}_1 = (1/2)\boldsymbol{p}_1, && \boldsymbol{v}_2 = (1/8)(\boldsymbol{p}_1 + 2\boldsymbol{p}_2),\\
&\boldsymbol{v}_3 = (1/8)(3\boldsymbol{p}_1 + 2\boldsymbol{p}_2), && \boldsymbol{v}_4 = (1/8)(6\boldsymbol{p}_1 + \boldsymbol{p}_2), && \boldsymbol{v}_5 = (1/8)(6\boldsymbol{p}_1 + 3\boldsymbol{p}_2),\\
&\boldsymbol{v}_6 = (1/2\boldsymbol{p}_2, && \boldsymbol{v}_7 = (1/8)(4\boldsymbol{p}_1 + 4\boldsymbol{p}_2), && \boldsymbol{v}_8 = (1/8)(2\boldsymbol{p}_1 + 5\boldsymbol{p}_2),\\
&\boldsymbol{v}_9 = (1/8)(2\boldsymbol{p}_1 + 7\boldsymbol{p}_2), && \boldsymbol{v}_{10} = (1/8)(5\boldsymbol{p}_1 + 6\boldsymbol{p}_2), && \boldsymbol{v}_{11} = (1/8)(7\boldsymbol{p}_1 + 6\boldsymbol{p}_2).
\end{aligned}
$$

A harmonic realization (3.36) is standard if and only if $\{\boldsymbol{e}_i\}_{i=1}^{20}$ satisfies (3.6). Taking $\boldsymbol{f}_1 = (1, 0)^T$ and $\boldsymbol{f}_2 = (0, 1)^T$, and solving

$$
\sum_{i=1}^{20} \langle \boldsymbol{e}_i, \boldsymbol{f}_j \rangle \boldsymbol{e}_i = c\boldsymbol{f}_j, \quad j = 1, 2, \tag{3.37}
$$

then we obtain

$$
|\boldsymbol{p}_1| = |\boldsymbol{p}_2|, \quad \langle \boldsymbol{p}_1, \boldsymbol{p}_2 \rangle = 0. \tag{3.38}
$$

Substituting (3.38) into (3.36), we obtain a standard realization of a Cairo pentagonal tiling (Fig. 3.14 (b) and Fig. 3.15 (c)).

Remark 3.42. The carbon structure with regular hexagonal shaped is called a graphene (see Section 3.3), and the carbon structure with a Cairo pentagonal shaped is called a penta-graphene [43].

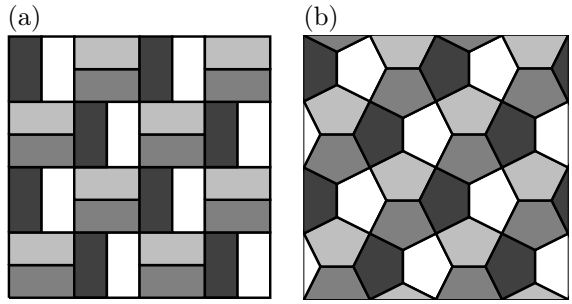

Figure 3.14: (a) A basketweave tiling, (b) a Cairo tiling. Both 1-skeletons of the tiling are topologically equivalent.

Remark 3.43. A Cairo pentagonal tiling is constructed by line segments joining four vertices of a square as in Fig. 3.16 (a) and (b). Define three kind of energies L, E and C by

$$L(t) = |\boldsymbol{a}-\boldsymbol{\alpha}| + |\boldsymbol{b}-\boldsymbol{\alpha}| + |\boldsymbol{c}-\boldsymbol{\beta}| + |\boldsymbol{d}-\boldsymbol{\beta}| + |\boldsymbol{\alpha}-\boldsymbol{\beta}| = 1 - 2t + 2\sqrt{1+4t^2},$$
$$E(t) = |\boldsymbol{a}-\boldsymbol{\alpha}|^2 + |\boldsymbol{b}-\boldsymbol{\alpha}|^2 + |\boldsymbol{c}-\boldsymbol{\beta}|^2 + |\boldsymbol{d}-\boldsymbol{\beta}|^2 + |\boldsymbol{\alpha}-\boldsymbol{\beta}|^2 = 8t^2 - 4t + 2,$$
$$C(t) = |\boldsymbol{a}-\boldsymbol{\alpha}|^{-1} + |\boldsymbol{b}-\boldsymbol{\alpha}|^{-1} + |\boldsymbol{c}-\boldsymbol{\beta}|^{-1} + |\boldsymbol{d}-\boldsymbol{\beta}|^{-1} + |\boldsymbol{\alpha}-\boldsymbol{\beta}|^{-1}.$$

For each $t \in (-1/2, 1/2)$, the configuration in Fig. 3.16 (b) yields a monohedral pentagon tiling. The energy L attains its minimum at $t = 1/(2\sqrt{3})$, and then the angle $\theta = \theta(t)$ in Fig. 3.16 (a) satisfies $\cos(\theta) = -1/2$, $(\theta = 2\pi/3)$. The minimum of L gives us the configuration of the minimum length of line segments, On the other hand, the energy E attains its minimum at $t = 1/4$, and then the angle θ satisfies $\cos(\theta) = -1/\sqrt{5}$. The minimum of E gives us a standard realization of the Cairo pentagonal tiling (see also Fig. 3.15 (c)). The energy C is based on the Coulomb repulsive force, and attains its local minimum at $t \sim 0.17264$, the angle θ satisfies $\cos(\theta) \sim -0.326374$.

Remark 3.44. This algorithm is easily programmable by using Kruskal's and Dijkstra's algorithms, and the Cholesky decomposition. To calculate the matrix A and vectors $a(e)$, $b(e)$, it is easy to set $e_i = (0, \ldots, 1, \ldots, 0) \in \mathbb{R}^{|E|}$.

Example 3.45. By using Mathematica, coordinates of vertices of standard realizations of topological crystals are easy to compute, if we obtain a $\mathbb{Z}$-basis of $H_1(X_0, \mathbb{Z})$ and a $\mathbb{Z}$-basis of vanishing subspace H (and a spanning tree of X_0).

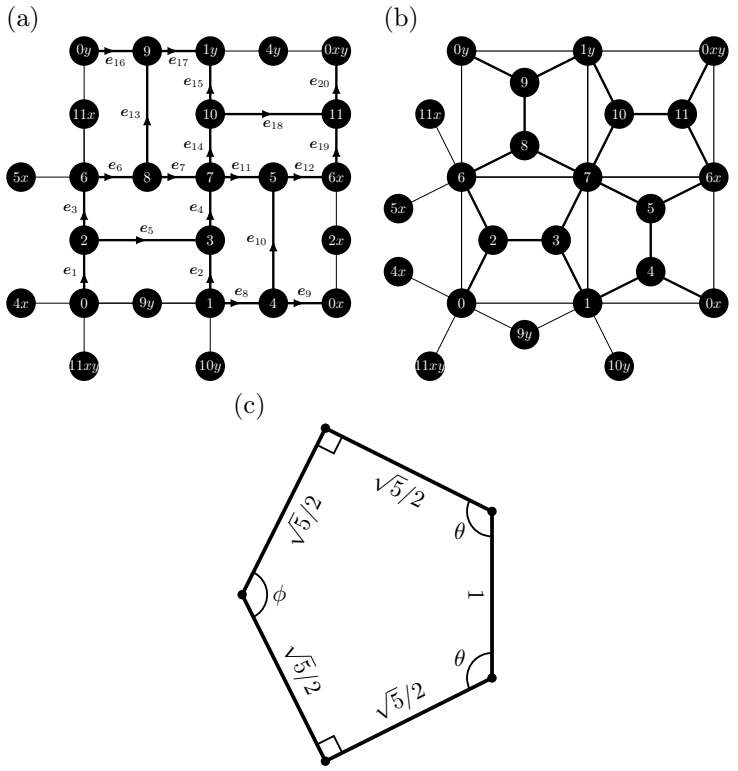

Figure 3.15: (a) Numbering of vertices and edges of a fundamental region of the basketweave tiling, (b) a fundamental region of a standard realization of the Cairo tiling, (c) the congruent-pentagon of the standard realization. The ratio of length of edges is $1 : (\sqrt{5}/2)$, and angles are $\cos(\theta) = -1/\sqrt{5}$ and $\cos(\phi) = -3/5$ ($\theta \sim 116.57°$ and $\phi \sim 126.87°$).

The following is a sample code of Mathematica to compute vertices of a kagome lattice (lines 1 and 3 are specific datas of a kagome lattice).

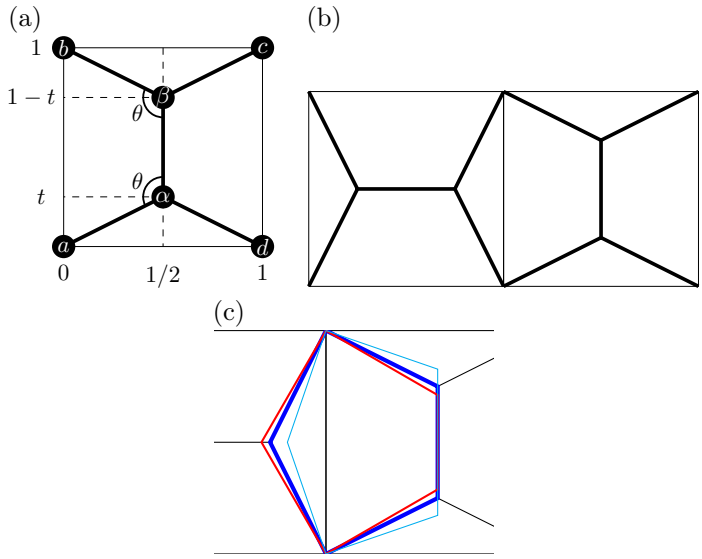

Figure 3.16: (a) Move α and β on the line $x = 1/2$, and calculate minimum of $L(t)$ and $E(t)$, (b) a building block of the pentagonal tiling, (c) the red, blue, and cyan pentagons are minimizers of L, E and C, respectively.

```
numberOfEdges=6;b=4;d=2;
e = IdentityMatrix[numberOfEdges];
alpha = {e[[1]]-e[[4]], e[[2]]-e[[5]], e[[1]]+e[[2]]+e[[3]],
e[[4]]+e[[5]]+e[[6]]};
matrixA = alpha.Transpose[alpha];
matrixb = Table[e[[j]].alpha[[i]], {i, 1, b}, {j, 1,
numberOfEdges}];
matrixa = Inverse[matrixA].matrixb;
matrixA11 = matrixA[[1;;d,1;;d]]; matrixA22 =
matrixA[[d+1;;b,d+1;;b]]; matrixA12 = matrixA[[1;;d,d+1;;b]];
matrixA21 = matrixA[[d+1;;b,1;;d]]; matrixB = matrixA11 -
matrixA12.Inverse[matrixA22].matrixA21;
matrixprojecta = matrixa[[1;;d]];
beta = CholeskyDecomposition[matrixB];
beta.matrixprojecta
```

The output of this code is

$$\begin{bmatrix} 1/\sqrt{3} & -1/(2\sqrt{3}) & -1/(2\sqrt{3}) & -1/\sqrt{3} & 1/(2\sqrt{3}) & 1/(2\sqrt{3}) \\ 0 & 1/2 & -1/2 & 0 & -1/2 & 1/2 \end{bmatrix},$$

which expresses coordinates of vertices of a kagome lattice. To obtain complete datas of standard realizations, we should obtain datas of building blocks by using datas of the shortest paths from an origin.

Remark 3.46. Crystallographers often call periodic realizations in $\mathbb{R}^2$ and $\mathbb{R}^3$ of graphs 2-*net* and 3-*net*, respectively. Names of 2-net of each lattice are

sq1	the regular square lattice,
hcb	the regular hexagonal lattice (honeycomb lattice)
hx1	the regular triangular lattice
kgm	the regular kagome lattice,
mcm	the 1-skeleton of Cairo pentagonal tiling,

and names of 3-net of each lattice are

pcu	the regular cubic lattice,
dia	the diamond lattice,
src	the gyroid lattice,
crs	the 3D kagome lattice of type I,
lvt	the 3D kagome lattice of type II.

Lists of 2-net and 3-net are available in EPINET [2].

3.3 Carbon structures and standard realizations

In this section, we consider carbon crystal structures via standard realizations.

Graphene is an allotrope of carbons, and is 2-dimensional crystal structure. Each carbon atom binds chemically other three carbon atoms by sp^2-orbitals (see Fig. 3.17). In mathematical view points, a graphene is a standard realization of a regular hexagonal lattice. A fundamental piece (Fig. 3.17) is a graph with four points, where each point locates at vertices of regular triangle and its barycenter. Translating the fundamental piece by $\boldsymbol{\alpha}_1$ and $\boldsymbol{\alpha}_2$ with $|\boldsymbol{\alpha}_i| = 1$ and $\langle \boldsymbol{\alpha}_1, \boldsymbol{\alpha}_2 \rangle = (1/2)|\boldsymbol{\alpha}_1|\,|\boldsymbol{\alpha}_2|$, we obtain a structure of graphenes.

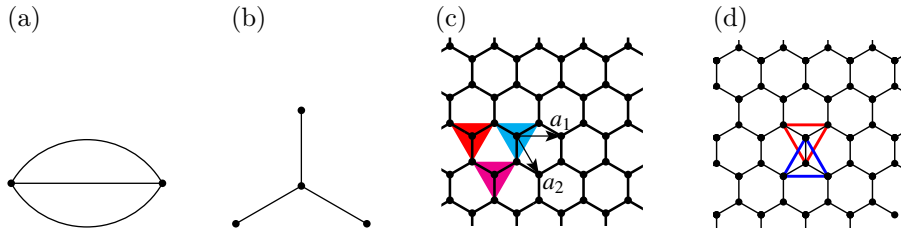

Figure 3.17: (a) The base graph of a regular hexagonal lattice, (b) a fundamental piece of a regular hexagonal lattice, (c) a graphene structure, which is constructed by (b) and its translations, (d) the barycenter of the blue regular triangle is a vertex of the red regular triangle. The blue triangle is consisted by $\boldsymbol{w}_1$, $\boldsymbol{w}_2$, and $\boldsymbol{w}_3$ (by using notations in Example 3.32), then the red is consisted by $\boldsymbol{v}_0$, $\boldsymbol{v}_0+\boldsymbol{\alpha}_1$, and $\boldsymbol{v}_0+\boldsymbol{\alpha}_1-\boldsymbol{\alpha}_2$. The barycenters of blue and red are $\boldsymbol{v}_0$ and $\boldsymbol{w}_1$, respectively.

Diamond is also an allotrope of carbons, and is 3-dimensional crystal structure. Each carbon atom binds chemically other four carbon atoms by sp^3-orbitals (see Fig. 3.18). In mathematical view points, a diamond is a standard realization of a graph, which can be called regular tetrahedral graph. A fundamental piece (Fig. 3.18) is a graph with five points, each points located at vertices of regular tetrahedron and its barycenter. Translating the fundamental piece by $\boldsymbol{\alpha}_1$, $\boldsymbol{\alpha}_2$, and $\boldsymbol{\alpha}_3$ with $|\boldsymbol{\alpha}_i|=1$ and $\langle \boldsymbol{\alpha}_i, \boldsymbol{\alpha}_j \rangle = (1/3)|\boldsymbol{\alpha}_i|\,|\boldsymbol{\alpha}_j|$ if $i \neq j$, we obtain a structure of diamonds.

By a textbook of physical chemistry, the space group of diamond structure is $Fd\bar{3}m$, which expresses face-centric structure with a glide reflection, three improper rotations, and certain reflections. Diamond structures are constructed shown in Fig. 3.19; however it is difficult to realize for mathematicians. On the other hand, the construction diamond structures by standard realizations is easy for mathematicians.

K_4 structures are obtained by standard realizations of the K_4 graph. The K_4 graph is the complete graph with four vertices (each vertex connects to all other vertices). Each carbon atom of K_4 structures binds chemically other three atoms by sp^2-orbitals (see Fig. 3.20). A fundamental piece is a graph with seven points. Translation vectors $\{\boldsymbol{\alpha}_i\}_{i=1}^3$ satisfy $|\boldsymbol{\alpha}_i| = 1$ and $\langle \boldsymbol{\alpha}_i, \boldsymbol{\alpha}_j \rangle = -(1/3)|\boldsymbol{\alpha}_i|\,|\boldsymbol{\alpha}_j|$ $(i \neq j)$. Moreover, K_4 structures have chirality, that is, A K_4 structure and its mirror image are not same.

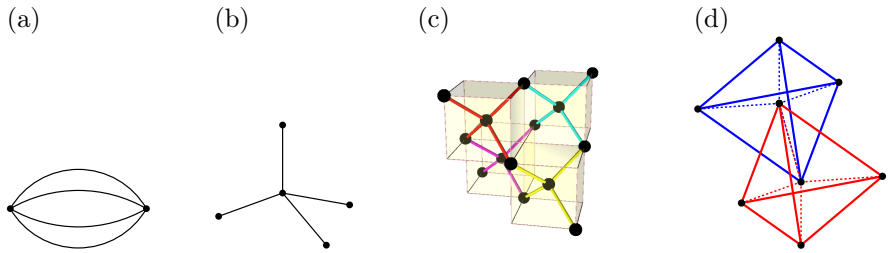

Figure 3.18: (a) The base graph of a diamond structure, (b) a fundamental piece of a diamond structure, whose vertices are located at vertices of a regular tetrahedron and its barycenter, (c) a diamond structure. A diamond structure is constructed by (b) and its translations. (d) the barycenter of the blue regular tetrahedron is a vertex of the red regular tetrahedron. The blue tetrahedron is consisted by $\boldsymbol{v}_1$, $\boldsymbol{v}_2$, $\boldsymbol{v}_3$, and $\boldsymbol{v}_4$ (by using notations in Example 3.33), then the red is consisted by $\boldsymbol{v}_0$, $\boldsymbol{w}_1 - \boldsymbol{w}_2 = \boldsymbol{v}_0 + \boldsymbol{\alpha}_1 - \boldsymbol{\alpha}_2$, $\boldsymbol{w}_1 - \boldsymbol{w}_3 = \boldsymbol{v}_0 + \boldsymbol{\alpha}_1 - \boldsymbol{\alpha}_3$, and $\boldsymbol{v}_0 + \boldsymbol{w}_1 - \boldsymbol{w}_4 = \boldsymbol{v}_0 + \boldsymbol{\alpha}_1$. The barycenters of blue and red are $\boldsymbol{v}_0$ and $\boldsymbol{w}_1$, respectively.

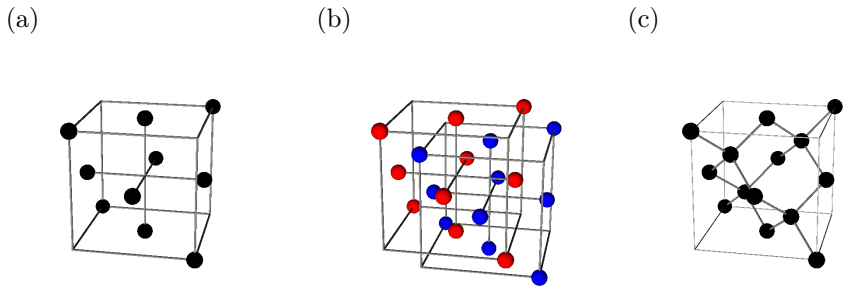

Figure 3.19: How to construct a diamond structure: (a) prepare a face-centric structure, (b) duplicate it and translate to a diagonal direction, and then (c) we obtain a diamond structure.

Physical property of the K_4 carbon is computed in the work [13] by Itoh–Kotani–Naito–Sunada–Kawazoe–Adschiri, it is physically meta-stable and metallic; however it has not composed yet. Recently, Mizuno–Shuku–Matsushita–Tsuchiizu–Hara–Wada–Shimizu–Awaga compose a K_4 structure other than carbons [27]. Their structure is a molecular-K_4, a radical molecule NDI-$\triangle(-)$ consists a K_4 crystal.

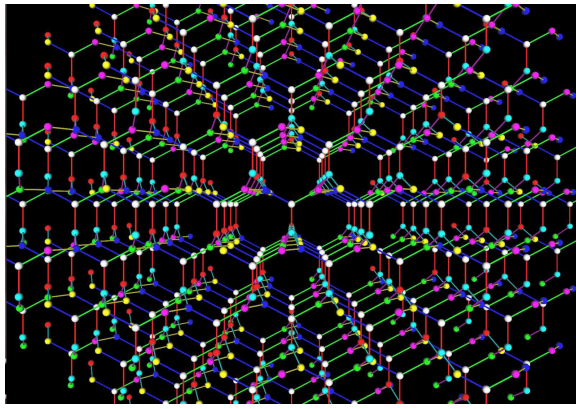

Figure 3.20: A K_4 structure, this is the image of the cover page of Notices Amer. Math. Soc., **55**, drawn by the author.

4 Negatively curved carbon structures

4.1 Carbon structures as discrete surfaces

In 1990's, several new sp^2-carbon structures, fullerenes (including C_{60}), graphene, and carbon nanotubes were found (See Fig. 4.1). These structures look like surfaces in $\mathbb{R}^3$. For example, a graphene, C_{60}, and a nanotube are similar to a plane, a sphere, and a cylinder, respectively. Each continuous surface in the above has non-negatively curved, i. e., the Gauss curvature of a sphere is positive, and theses of a cylinder and plane are zero. Hence, it is a natural question if an sp^2-carbon structure which looks like a negatively curved surface exists or not.

In the followings, we consider sp^2-carbon structures as "trivalent discrete surface" (realizations of 3-regular graphs in $\mathbb{R}^3$). Moreover, we assume that graphs are oriented surface graphs, that is, each graphs is realized on a oriented

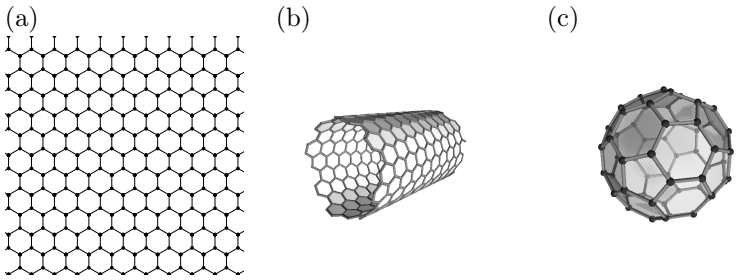

Figure 4.1: (a) Graphene, (b) (single wall) carbon nanotube, (c) C_{60} (an example of fullerenes).

surface without self-intersections. By the property of surface graphs, we can define the notion of "faces" (simple closed path) for trivalent discrete surfaces.

Definition 4.1. For an oriented surface graph $X = (V, E)$, the *Euler number* $\chi(X)$ of X is defined by

$$\chi(X) = |F| - |E| + |V|, \tag{4.1}$$

where $|F|$ is the number of faces of X.

Note that the Euler number $\chi(X)$ of an oriented graph X is same as the Euler number of the underlying surface.

Proposition 4.2. *Assume an oriented surface graph $X = (V, E)$ is trivalent (3-regular) graph, then we obtain $F = \sum N_k$, $E = (1/2)\sum kN_k$, $V = (1/3)\sum kN_k$, where N_k is the number of k-gon in X. Hence, we also obtain*

$$\chi(X) = \sum (1 - k/6)N_k. \tag{4.2}$$

Proof. Since X is an oriented surface graph, each edges shared by two faces, and hence, we obtain $|E| = (1/2)\sum kN_k$. Since X is trivalent, each vertex shared by three faces, and hence, we obtain $|V| = (1/3)\sum kN_k$. Substituting them into (4.1), we obtain (4.2). □

Remark 4.3. By Proposition 4.2, the number of hexagons does not affect to the Euler number. If X is positively curved ($\chi(X) > 0$), then at least one n-gon ($n \leq 5$) should be contained in X. If X is negatively curved ($\chi(X) < 0$), then at least one n-gon ($n \geq 7$) should be contained in X.

	N_5	N_6	N_7	N_8	$\lvert V\rvert$	$\lvert E\rvert$	$\lvert F\rvert$	χ
C_{60}	12	20	0	0	60	90	32	2
SWNT $\boldsymbol{c} = (6, 6)$	0	12	0	0	24	36	12	0
Mackay–Terrones'	0	90	0	12	192	288	102	-4

Table 4.1: Number of polygons of C_{60}, a single-wall nanotube (of fundamental region of it), where $\boldsymbol{c}$ is the chiral index of SWNT (see Section A.3), and Mackay–Terrones' structure (see Fig. 4.2 (b)).

By Proposition 4.2, if there exists an sp^2-carbon structure with $\chi(X) < 0$ (negatively curved), then at least one n-gon ($n \geq 7$) exists in X. In 1991, Mackay–Terrones [25] calculated an sp^2-carbon structure which is looked like a minimal surface (Schwarz P surface, $\chi(X) = -4$), which contains 12 of octagons (see also Lenosky–Gonze–Teter–Elser [24]).

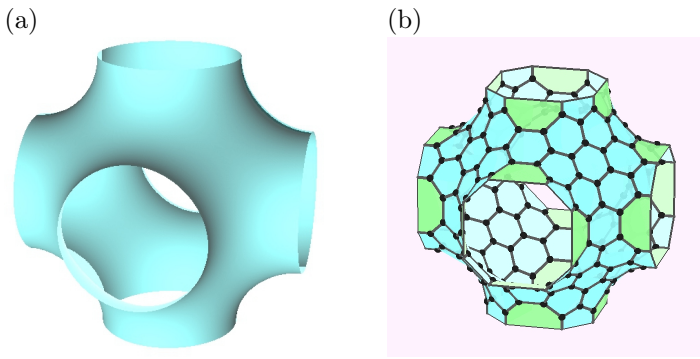

Figure 4.2: (a) Schwarz P surface, which is a triply periodic minimal surface (the Gauss curvature $K < 0$, the Euler number $\chi = -4$, and the genus $g = -3$), whose period lattice $\{\boldsymbol{e}_i\}_{i=1}^3$ satisfies $\langle \boldsymbol{e}_i, \boldsymbol{e}_j \rangle = \delta_{ij}$. (b) Mackay–Terrones' structure, the period lattice is the same as (a). Note that green faces in (b) are octagons (see also Table 4.1).

4.2 Construction of negatively curved carbon structures via standard realizations

Tagami–Liang–Naito–Kawazoe–Kotani [40] constructed negatively curved carbon crystals, which are different from the Mackay–Terrones' structure, by using stan-

dard realizations of topological crystals.

The fundamental region of Mackay–Terrones' structure has octahedral symmetry, which is same symmetry of truncated octahedrons. Truncated octahedrons consist eight hexagons, which have D_6-symmetry (see 4.3). Our method is, 1) we

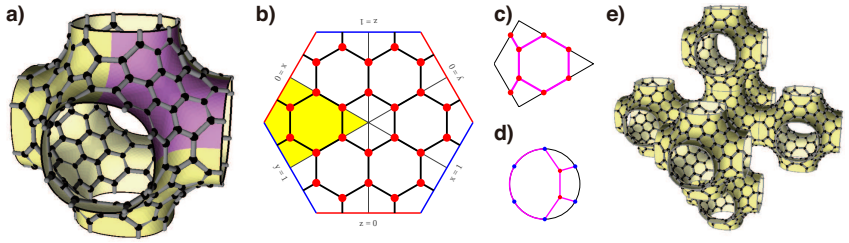

Figure 4.3: Symmetry of the Mackay–Terrones' structure. (c) is a fundamental region of D_6-action on a hexagon, which is diffeomorphic to (d). See also Fig. A.5 (Tagami–Liang–Naito–Kawazoe–Kotani [40]).

classify and construct a graph in a fundamental region of D_6-action on a hexagon, which is a trivalent graph when we extend to hexagon by D_6-action (Fig. 4.3 (c)), 2) we extends the graph obtained in 1 to the trivalent graph on a hexagon (Fig. 4.3 (b)), 3) we extends the graph obtained in 2 to the graph on a truncated octahedron (Fig. 4.3 (a)), and 4) we calculate a standard realization of the graph obtained in 3. The structure obtained in 4 is a candidate of sp^2-carbon structure with $K < 0$ ($\chi = -4$). In fact, we prove the following result.

Theorem 4.4 (Tagami–Liang–Naito–Kawazoe–Kotani [40])**.** *The equation to obtain standard realization is linear:* $\Delta \boldsymbol{x} = \boldsymbol{b}$*, where* $b_i = \pm \boldsymbol{e}_\alpha$*, if a vertex* v_i *is adjacent to a vertex in neighbouring cell. The linear equation is solvable if and only if* $\sum b_i = 0$*. The period lattice* $\{\boldsymbol{e}_i\}$ *which gives a standard realization is cubic, i. e.,* $\boldsymbol{e} = (\boldsymbol{e}_1, \boldsymbol{e}_2, \boldsymbol{e}_3)$ *is a period lattice of a standard realization, then* $\boldsymbol{e}^T \boldsymbol{e} = \boldsymbol{E}$*. If* Φ *is a standard realization, then* $\mathrm{Aut}(X) \subset \mathrm{Aut}(\Phi(X))$*, and hence* X *has the same symmetries with Mackay–Terrones' structure.*

In our method, we do not solve the equation (3.6). Instead, we only solve the harmonic equation (3.3) using cubic periodicity. Hence, we should prove that the realization is standard. To prove it, we use the Lagrange multiplier, and the result of the Lagrange multiplier is $\boldsymbol{e}^T \boldsymbol{e} = \boldsymbol{E}$. This shows that the harmonic realizations with the cubic lattice is standard.

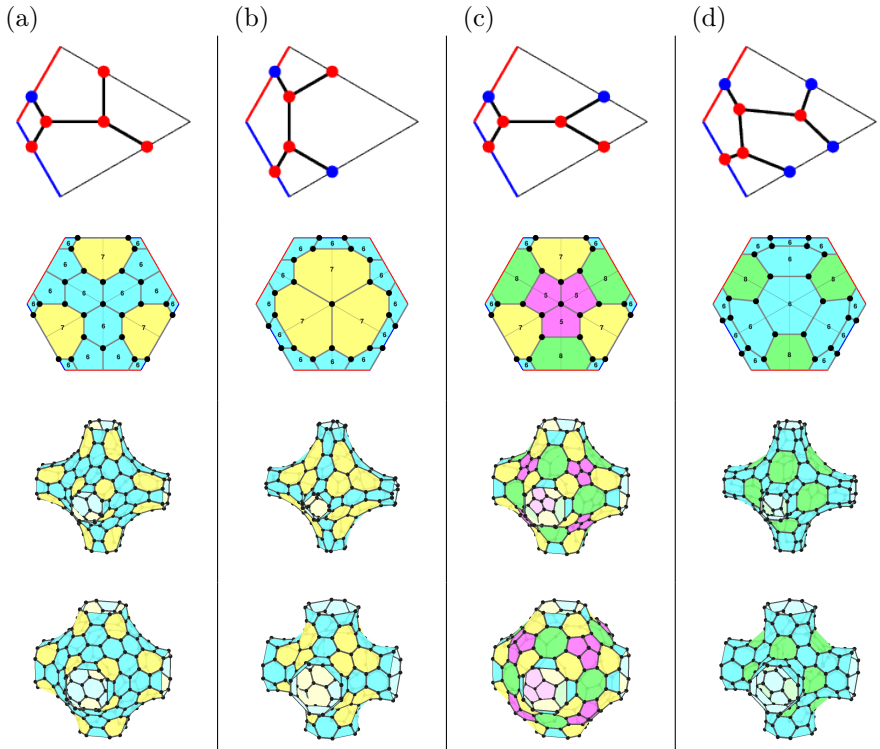

Figure 4.4: Mackay-like structures, which are physically stable. Physical stabilities are calculated by density functional theory (DFT). For the notion of "metal"/"semi-conductor", see Section A.2. (Tagami–Liang–Naito–Kawazoe–Kotani [40]).

Remark 4.5. No negatively curved sp^2-carbon structure has been synthesised so far. However, a piece of negatively curved carbon structure is chemically synthesised by Kawasumi–Zhang–Segawa–Scott–Itami [15].

5 A discrete surface theory

In the previous section, we explain "negatively" curved carbon structure; however, the definition of negativity is that the Euler number is negative. This is a similar situation with that "a surface with genus ≥ 2 cannot be non-negatively curved". Since the Gauss curvature of smooth surfaces is a function defined on each point of the surface, the negativity in the previous section is not a precise property for discrete surfaces.

On the other hand, there are many definitions of the Gauss curvature for discrete surfaces. One of the examples is a triangulation of a smooth surface, which is a discretization of a smooth surface. For triangulation of smooth surfaces, the Gauss curvature is defined by "angle defects", that is $K(p) = 2\pi - \sum \theta_i$, where θ_i is inner angle at p of each triangle gathering at p.

Applying the definition of the Gauss curvature by angle defects to the Mackay–Terrones' structure (a standard realization), we obtain $K \equiv 0$, since a standard realization of a trivalent topological crystal satisfies the "balance condition" (3.3), that is, each point and three neighbouring points are co-planer. Although each triangle of triangulations of smooth surfaces is planer, however, each face of the discrete surface is not planer.

Hence, we should construct a new definitions of the Gauss curvature and the mean curvature for trivalent discrete surfaces.

5.1 Curvatures of trivalent discrete surfaces

Definition 5.1 (Kotani–Naito–Omori [16])**.** Let $X = (V, E)$ be a trivalent graph, and $\Phi\colon X \longrightarrow \mathbb{R}^3$ be a realization of X. The realization Φ is called a *trivalent discrete surface* if and only if for each $x \in V$, at least two vectors of $\{\Phi(e) : e \in E_x\}$ are linearly independent.

We remark that this definition of trivalent discrete surfaces is not limited to topological crystals, and thus we can treat C_{60} and single-wall nanotubes (SWNTs) for example. But, the definition also contains K_4 structure as trivalent discrete surfaces, although, it does not look like a discrete surface.

Before giving a definition of curvatures for trivalent discrete surfaces, we recall properties of curvature for smooth surfaces in $\mathbb{R}^2$.

Definition 5.2 (Curvatures for smooth surfaces). Let $p\colon \Omega \subset \mathbb{R}^2 \longrightarrow \mathbb{R}^3$ be a smooth surface, and $n(x)$ be a unit normal vector at $x \in \Omega$. We define the first and the second fundamental forms by $\mathrm{I} = \langle dp, dp\rangle$, and $\mathrm{II} = -\langle dn, dp\rangle$, respectively. By using them, the Gauss curvature and the mean curvature are defined by $K(x) = \det(\mathrm{I}^{-1}\,\mathrm{II})$ and $H(x) = \frac{1}{2}\operatorname{tr}(\mathrm{I}^{-1}\,\mathrm{II})$, respectively.

Proposition 5.3. *For a smooth surface $p\colon \Omega \longrightarrow \mathbb{R}^3$ with a unit normal vector field n, the Gauss curvature K satisfies $\nabla_1 n(x) \times \nabla_2 n(x) = K(x)(\nabla_1 p(x) \times \nabla_2 p(x))$, and the mean curvature H satisfies $\frac{d}{dt}A(x,t)\Big|_{t=0} = -H(x)A(x)$, where $A(x)$ is the area element of p and $A(x,t)$ is the one of $p + tn$.*

To define curvatures for trivalent discrete surfaces which are an analogue of Definition 5.2, it may be suffice to define the covariant derivative and the unit normal vector at each vertex of trivalent discrete surfaces, and we should prove that curvatures for trivalent discrete surfaces satisfy similar properties of Proposition 5.3.

Definition 5.4 (Kotani–Naito–Omori [16])**.** Let $\Phi(X)$ be a trivalent discrete surface, $\boldsymbol{x} \in \Phi(X)$, and $\boldsymbol{x}_1$, $\boldsymbol{x}_2$, $\boldsymbol{x}_3$ its adjacency vertices. We define the unit normal vector at $\boldsymbol{x}$ as the normal vector of the plane through $\boldsymbol{e}_1$, $\boldsymbol{e}_2$, $\boldsymbol{e}_3$ (see Fig. 5.1), that is,

$$n(\boldsymbol{x}) = \frac{(\boldsymbol{e}_2 - \boldsymbol{e}_1) \times (\boldsymbol{e}_3 - \boldsymbol{e}_1)}{|(\boldsymbol{e}_2 - \boldsymbol{e}_1) \times (\boldsymbol{e}_3 - \boldsymbol{e}_1)|} = \frac{\boldsymbol{e}_1 \times \boldsymbol{e}_2 + \boldsymbol{e}_2 \times \boldsymbol{e}_3 + \boldsymbol{e}_3 \times \boldsymbol{e}_1}{|\boldsymbol{e}_1 \times \boldsymbol{e}_2 + \boldsymbol{e}_2 \times \boldsymbol{e}_3 + \boldsymbol{e}_3 \times \boldsymbol{e}_1|},$$

and the covariant derivative as

$$\nabla_{\boldsymbol{e}}\boldsymbol{x} = \mathrm{Proj}(\boldsymbol{e}) = \boldsymbol{e} - \big\langle \boldsymbol{e}, n(\boldsymbol{x})\big\rangle n(\boldsymbol{x}), \quad e \in E_x,$$

where $\boldsymbol{e}_i = \boldsymbol{x}_i - \boldsymbol{x}$.

Definition 5.5 (Kotani–Naito–Omori [16])**.** Let X be a trivalent discrete surface and $\boldsymbol{x}$ be a vertex of X. We define the first and the second fundamental forms by

$$\mathrm{I}(\boldsymbol{x}) = \begin{pmatrix} \langle \boldsymbol{e}_2 - \boldsymbol{e}_1, \boldsymbol{e}_2 - \boldsymbol{e}_1\rangle & \langle \boldsymbol{e}_2 - \boldsymbol{e}_1, \boldsymbol{e}_3 - \boldsymbol{e}_1\rangle \\ \langle \boldsymbol{e}_3 - \boldsymbol{e}_1, \boldsymbol{e}_2 - \boldsymbol{e}_1\rangle & \langle \boldsymbol{e}_3 - \boldsymbol{e}_1, \boldsymbol{e}_3 - \boldsymbol{e}_1\rangle \end{pmatrix},$$

$$\mathrm{II}(\boldsymbol{x}) = -\begin{pmatrix} \langle \boldsymbol{e}_2 - \boldsymbol{e}_1, n_2 - n_1\rangle & \langle \boldsymbol{e}_2 - \boldsymbol{e}_1, n_3 - n_1\rangle \\ \langle \boldsymbol{e}_3 - \boldsymbol{e}_1, n_2 - n_1\rangle & \langle \boldsymbol{e}_e - \boldsymbol{e}_1, n_3 - n_1\rangle \end{pmatrix},$$

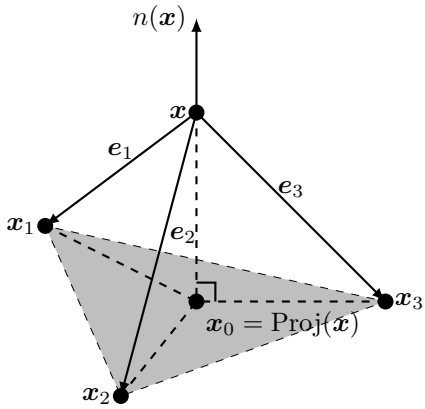

Figure 5.1: The unit normal vector for trivalent discrete surfaces. The area of the triangle filled in gray is the local area at $\boldsymbol{x}$.

and we define the Gauss curvature and the mean curvature at $\boldsymbol{x}$ by

$$K(\boldsymbol{x}) = \det(\mathrm{I}(\boldsymbol{x})^{-1}\,\mathrm{II}(\boldsymbol{x})),$$
$$H(\boldsymbol{x}) = \frac{1}{2}\operatorname{tr}(\mathrm{I}(\boldsymbol{x})^{-1}\,\mathrm{II}(\boldsymbol{x})).$$

Then, we obtain the following properties for curvatures of trivalent discrete surfaces.

Theorem 5.6 (Kotani–Naito–Omori [16])**.** *For a trivalent discrete surface Φ, the Gauss curvature K satisfies $\nabla_i n(\boldsymbol{x}) \times \nabla_j n(\boldsymbol{x}) = K(\boldsymbol{x})(\boldsymbol{e}_i \times \boldsymbol{e}_j)$, where $\nabla_i = \nabla_{e_i}$, and the mean curvature H satisfies $\frac{d}{dt}\Big|_{t=0} \mathcal{A}(\Phi+tn) = -2\sum_{x\in V} H(\boldsymbol{x})A(\boldsymbol{x})$, where $A(\boldsymbol{x}) = \boldsymbol{e}_1 \times \boldsymbol{e}_2 + \boldsymbol{e}_2 \times \boldsymbol{e}_3 + \boldsymbol{e}_3 \times \boldsymbol{e}_1$ is the local area at $\boldsymbol{x}$ and $\mathcal{A}(\Phi) = \sum_{x\in V} A(\boldsymbol{x})$ is the total area.*

Remark 5.7. Unfortunately, the second fundamental form II of trivalent discrete surfaces is *not* symmetric in general.

Theorem 5.8 (Kotani–Naito–Omori [16])**.** *Trivalent discrete surface Φ is called* ***minimal*** *if and only if $H(\boldsymbol{x}) = 0$, which is expressed by the system of linear equation*

$$\nabla_{\boldsymbol{e}_2-\boldsymbol{e}_3} n \times \nabla_{\boldsymbol{e}_1}\Phi + \nabla_{\boldsymbol{e}_3-\boldsymbol{e}_1} n \times \nabla_{\boldsymbol{e}_2}\Phi + \nabla_{\boldsymbol{e}_1-\boldsymbol{e}_2} n \times \nabla_{\boldsymbol{e}_3}\Phi = 0.$$

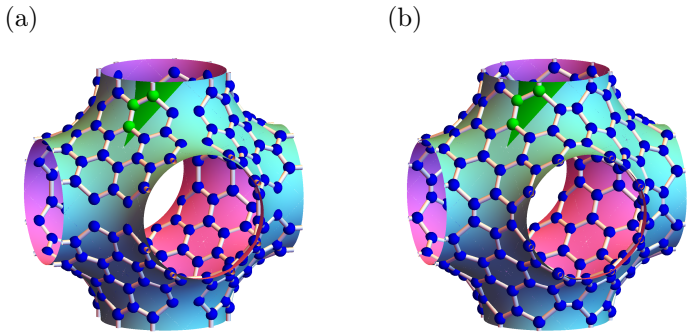

Figure 5.2: (a) Mackay–Terrones' structure (standard realization), (b) minimal realization of the same structure (Kotani–Naito–Omori [16]).

Proposition 5.9 (Kotani–Naito–Omori [16]). *If a trivalent discrete surface is a plane graph, then* $K \equiv 0$, $H \equiv 0$. *Here, a graph is called plane, if it is drawn in a plane without self-intersection. If a trivalent discrete surface satisfies* $\boldsymbol{x} = rn(\boldsymbol{x})$ *for any* $x \in V$, *then* $K \equiv 1/r^2$, $H \equiv -1/r$.

We call a surface satisfying the $\boldsymbol{x} = rn(\boldsymbol{x})$ *sphere shaped*. Regular polyhedra and semi-regular polyhedra (including C_{60}) are sphere shaped.

Proposition 5.10 (Kotani–Naito–Omori [16]). *Let* $\mathrm{CNT}(\lambda, \boldsymbol{c})$ *be a SWNT with the chiral index* $\boldsymbol{c} = (c_1, c_2)$ *and the scale factor* λ, *that is,*

$$(x, y) \mapsto (r(\lambda, \boldsymbol{c}) \cos(x/r(\lambda, \boldsymbol{c})), r(\lambda, \boldsymbol{c}) \sin(x/r(\lambda, \boldsymbol{c})), y).$$

Then the Gauss curvature and the mean curvature of $\mathrm{CNT}(\lambda, \boldsymbol{c})$ *are*

$$K(\lambda, \boldsymbol{c}) = \frac{4m_z(\boldsymbol{c})^2(m_x(\boldsymbol{c})^2 + m_y(\boldsymbol{c})^2)}{3r(\lambda, \boldsymbol{c})^2(m_x(\boldsymbol{c})^2 + m_y^2(\boldsymbol{c}) + (4/3)m_z(\boldsymbol{c})^2)^2},$$
$$H(\lambda, \boldsymbol{c}) = -\frac{m_x(\boldsymbol{c})}{2r(\lambda, \boldsymbol{c})} \cdot \frac{m_x(\boldsymbol{c})^2 + m_y(\boldsymbol{c})^2 + (8/3)m_z(\boldsymbol{c})^2}{(m_x(\boldsymbol{c})^2 + m_y(\boldsymbol{c})^2 + (4/3)m_z(\boldsymbol{c})^2)^{3/2}},$$

where $m_\alpha(\boldsymbol{c})$ *is a quantity defined from the chiral index. In particular,* $c_1 = c_2$, *then* $m_z(\boldsymbol{c}) = 0$, *and*

$$K(\lambda, \boldsymbol{c}) = 0, \quad H(\lambda, \boldsymbol{c}) = -\frac{1}{2r(\lambda, \boldsymbol{c})} \cos\frac{C_1}{2}.$$

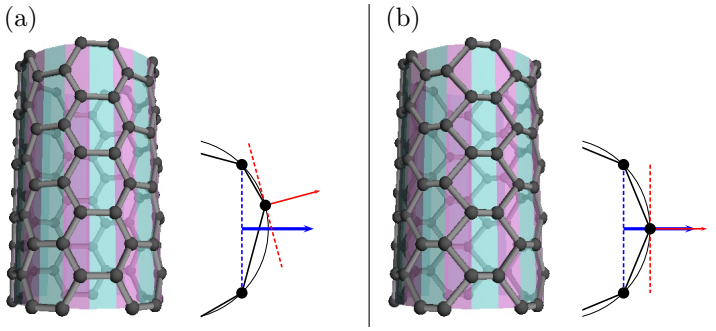

Figure 5.3: (a) CNT$(\lambda, \boldsymbol{c})$ satisfies $H \not\equiv 1/r$, whose normal vectors are not parallel to normal vectors of the underlying cylinder. (b) small change of CNT$(\lambda, \boldsymbol{c})$ satisfies $H \equiv 1/r$, whose normal vectors are parallel to normal vectors of the underlying cylinder (Kotani–Naito–Omori [16]).

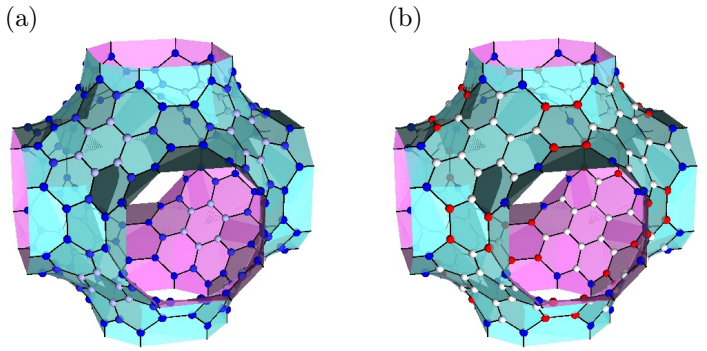

Figure 5.4: (a) The Gauss curvatures of Mackay–Terrones' structure, (b) the mean curvatures of Mackay–Terrones' structure. By our definition of curvatures, Mackay–Terrones' structure is *pointwise* negatively curved. Blue (red) vertices are negatively (positively) curved, and color densities expresses relative absolute values of curvatures (Kotani–Naito–Omori [16])

Remark 5.11. Curvatures of K_4 structure satisfy $K > 0$ and $H \equiv 0$. In the case of smooth surfaces, the mean curvature $H \equiv 0$ then the Gauss curvature $K \leq 0$, since the second fundamental form II is symmetric. On the other hand, in our discrete case, II is not symmetric, and thus $H \equiv 0$ does not imply $K \leq 0$,

5.2 Further problems

In [16], we discuss a convergence of sequence of "subdivision" of a trivalent discrete surface. In our context, there are no underlying continuous object, and trivalent discrete surfaces are essentially discrete object. For example, Mackay–Terrones' structure is constructed by Schwarz P surface as model, but there are no relations between the structure and the surface itself. We would find a "limit" of a sequence of trivalent discrete surfaces, and make a relationship a trivalent discrete surface and a continuous surface.

To discuss a convergence theory of trivalent discrete surfaces, we should consider how to subdivide a trivalent graph, and how to realize the subdivided graph. Goldberg–Coxeter subdivision for trivalent graphs defined by Dutour–Deza [7, 8] is the good definition to subdivide a trivalent graph (see also Goldberg [11] and Omori–Naito–Tate [31]). Kotani–Naito–Omori [16], Tao [41], and Kotani–Naito–Tao [17] discuss convergences of sequences of trivalent discrete surfaces.

On the other hand, eigenvalues of the Laplacian of graphs are one of the main objects in discrete geometric analysis (see for example [4, 12, 21]). Eigenvalues of the Laplacian of graphs are also interest from physical and chemical view points (see also Section A.2). Some properties of eigenvalues of Laplacians of Goldberg–Coxeter constructions of trivalent graphs are discussed in Omori–Naito–Tate [31].

A Appendix

A.1 Space groups in $\mathbb{R}^2$ and $\mathbb{R}^3$

Definition A.1. A discrete finite subgroup P of $O(d)$ is called a *point group* of $\mathbb{R}^d$, and a subgroup Γ of Euclidean motion group of $\mathbb{R}^d$ is called a *space group* of $\mathbb{R}^d$, if Γ is discrete subgroup and $\Gamma \cap T \cong \mathbb{Z}^d$, where T is the group of parallel transformations in $\mathbb{R}^d$.

A 2-dimensional point group P is extended to a space group, if and only if P is 3-, 4-, or 6-fold symmetry, that is to say, P is one of C_1, C_2, C_3, C_4, C_6, D_1,

D_2, D_3, D_4, and D_6. Here, C_n is the n-fold rotation group ($\cong \mathbb{Z}_n$ cyclic group), and D_n is the n-fold rotation and reflection group (dihedral group).

It is a very famous old result that the number of 2-dimensional space groups is 17. 2-dimensional space groups may contain parallel transformations, 2-, 3-, or 6-folds rotations with respect to a point, and glide reflections with respect to a line. Here, a glide reflection is the composition of a reflection and a parallel transformation.

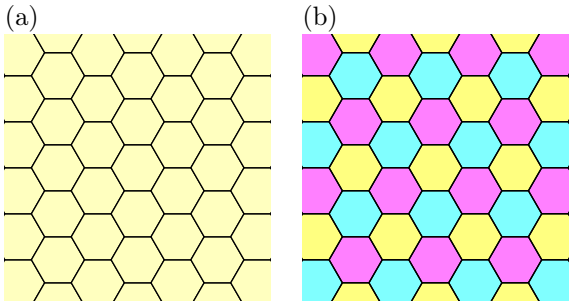

Figure A.1: Space groups of (a) and (b) are $P6m$ and $P3m1$. Since $P3m1$ is a subgroup of $P6m$, we can say that the figure (a) has higher symmetry than figure (b).

3-dimensional point groups are one of C_n, C_{nv}, C_{nh}, D_n, D_{nv}, D_{nh}, S_{2n}, T, T_d, T_h, O, O_h, I, and I_h. Here, C_{nv} (D_{nv}) and C_{nh} (D_{nh}) are $C_n(D_n)$ with additional mirror plane perpendicular (parallel) to the axis to rotation, respectively, and S_{2n} is $2n$-fold rotation and reflection axis. Group T, O, and I are well-known as polyhedral groups, T_d is T with improper rotations, T_h, O_h, and I_h are T, O, and I with reflections, respectively.

A 3-dimensional point group P extends a space group, if and only if P is 3-, 4-, or 6-fold symmetry, That is to say P is one of C_n, C_{nv}, C_{nh}, D_n, D_{nh}, and D_{nv}, ($n = 1, 2, 3, 4, 6$).

It is also a famous old result that number of 3-dimensional space groups is 230. 3-dimensional space groups may contain parallel transformations, 2-, 3-, or 6-folds rotations with respect to a point, reflections/glide reflections with respect to a line, and improper rotation. Here a improper rotation is product with rotation and reflection with respect to a line perpendicular to rotation axis.

The space group of diamond crystals is $Fd\overline{3}m$, where F, d, $\overline{3}$, and m mean that

"Face-centered cubic" structure, the group contains a glide reflection, the group contains 3 improper rotations, and the group contains a reflection, respectively.

A.2 Electronic properties of carbon structures

States of electrons of atoms, molecules, and solids follow the Schrödinger equation

$$-\Delta\psi + V\psi = E\psi, \quad \text{in } \mathbb{R}^3, \tag{A.1}$$

where V is a potential and E is the energy of an electron. In cases of crystal structures, the state ψ of electrons and the potential V are periodic, and hence taking the Fourier transformation of (A.1), we obtain

$$\widehat{H}\widehat{\psi}(\xi) = E(\xi)\widehat{\psi}(\xi), \tag{A.2}$$

where $H = -\Delta + V$. The dispersive relation $\xi \mapsto E(\xi)$ represents energies of electrons with the wave number ξ in a crystal.

As an example, we consider electronic states of graphenes. Considering π-electrons in graphenes, we obtain eigenvalues of $\widehat{H}$,

$$E(\xi) = \pm\sqrt{3 + 2\cos(\xi_1) + 2\cos(\xi_2) + 2\cos(\xi_1 - \xi_2)}. \tag{A.3}$$

As shown in Fig. A.2, the lower band (valence band) and the upper band (conductor band) attache at K and K' points with the Fermi energy (zero energy), and hence graphenes are conductor (metal). Moreover, at K and K' points, both bands have cone singularities. Such points are called *Dirac points*. On Dirac points, effective masses of electrons is zero, which are very important properties in solid state physics. Note that crystals whose conductor bands and valence bands intersects are called metals or conductors, and crystals whose conductor/valence bands does not intersects but its gap less than about 1 eV are called semi-conductors.

This calculation, which is called the *tight-binding approximation*, includes only interaction arise from nearest atoms with respect to each atom. Hence, the tight-binding approximations is based on graph theories, actions of an abelian group, and the Fourier transformations, mathematically.

To calculate of electronic states of C_{60}, we cannot apply the tight-binding approximation, since C_{60} is not a crystal structure, but a molecule structure. The

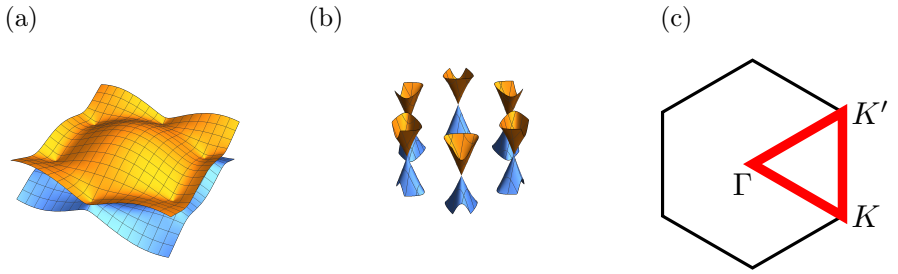

Figure A.2: (a) $E(\xi)$ of graphenes (band structure), (b) closed up $E(\xi)$ near K and K' points. (c) highly-symmetric points in the Fourier space.

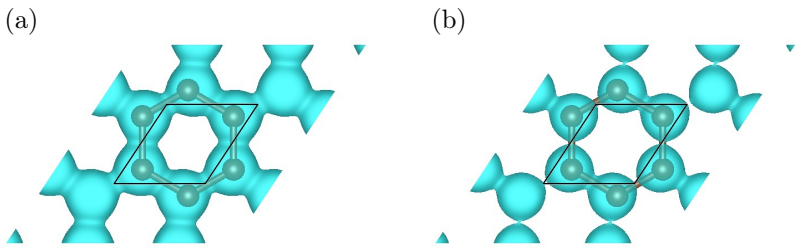

Figure A.3: Iso-surfaces of density of electrons in graphenes by using density functional theory (DFT). (a) probability 0.18, (b) probability 0.30.

Hückel method admits calculations of orbitals in hydrocarbon molecules, and is also based on graph theories. Let $X = (V, E)$ be the graph of a molecule structure, that is, V are set of carbon atoms, and E are set of covalent bonds between carbon atoms. Eigenvectors ψ of the adjacency matrix A of X are molecular orbitals of electrons, and their eigenvalues λ are energies of orbitals.

Example A.2. Consider benzene molecules (C_6H_6), which contains six carbon atoms, and whose graph is C_6 (the cyclic graph with six vertices), and number of electrons of π-orbitals (not using covalent bonds) is also six. Eigenvalues of adjacency matrix of C_6 are $\{2, 1, 1, -1, -1, -2\}$, and electrons in π-orbital occupy orbitals with energies $\{-1, -1, -2\}$ in the ground state, since each orbital can contain two electrons by Pauli's principle. We can write the wave function of the ground state as $\psi = \sum_{i=1}^{3} c_{ij}\chi_j$ by using eigenvectors $\{\chi_j\}_{j=1}^{6}$, and we obtain $\sum_{i=1}^{3} c_{ij}^2 = 1/2$. This means that π-electrons have equal distributions on each carbon atom.

By using similar calculations, we also obtain π-electrons have equal distributions on each carbon atom on C_{60} (see also Fig. A.4).

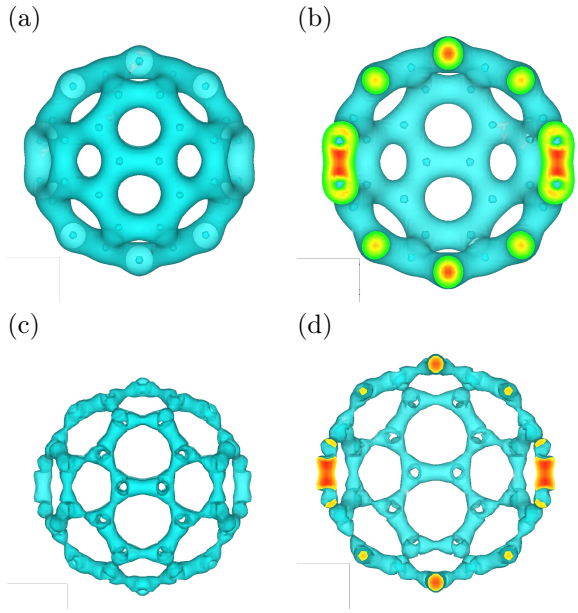

Figure A.4: Iso-surface of distributions of electrons of C_{60} by DFT. (a) probability 0.15, (b) its cut-model, (c) probability 0.25, (d) its cut-model.

A.3 Carbon nanotubes from geometric view points

Carbon nanotubes are carbon allotropes, whose carbon atoms chemically bind with other three atoms with sp^2-orbitals, and they are graphenes rolled up in cylinders. There are many types of carbon nanotubes. However, in this section, we only consider single wall nanotubes (SWNT). SWNTs have a parameter (*chiral index*) $\boldsymbol{c} = (c_1, c_2)$, which is defined as follows.

Choose a vertex of a regular hexagonal lattice (a graphene) as an origin $(0, 0)$, the select fundamental piece, whose vertices are $\{\boldsymbol{v}_i\}_{i=0}^3$ of a regular hexagonal

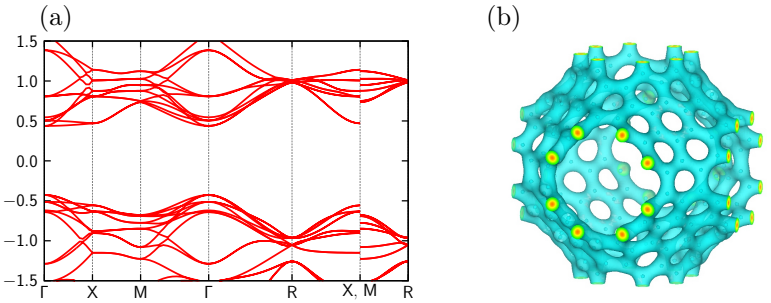

Figure A.5: DFT calculation result for Mackay-Terrones' structure. (a) electronic state, band gap is about 1 eV, and hence Mackay-Terrones' structure is semiconductor, (b) iso-surface of density of electrons ($p = 0.15$).

lattice (A.4), and translation vectors as (A.5):

$$\text{(A.4)} \quad \boldsymbol{v}_0 = (0,0), \quad \boldsymbol{v}_1 = (0,-1), \quad \boldsymbol{v}_2 = (1/2, \sqrt{3}/2), \quad \boldsymbol{v}_3 = (-1/2, \sqrt{3}/2),$$

$$\text{(A.5)} \quad \boldsymbol{a}_1 = (\sqrt{3}, 0), \quad \boldsymbol{a}_2 = (1/2, -\sqrt{3}/2).$$

Select (c_1, c_2) with $c_1 \in \mathbb{N}_{>0}$ and $c_2 \in \mathbb{N}_{\geq 0}$, and set $\boldsymbol{c} = c_1\boldsymbol{a}_1 + c_2\boldsymbol{a}_2$, we call $\boldsymbol{c}$ a *chiral vector* (or chiral index) of SWNT. On the other hand, $\boldsymbol{t} = (1/\gcd(c_1, c_2))((c_1+2c_2)\boldsymbol{a}_1 - (2c_1+c_2)\boldsymbol{a}_2)$, which is called a lattice vector, satisfies $\langle \boldsymbol{c}, \boldsymbol{t} \rangle = 0$.

A SWNT with the chiral index $\boldsymbol{c}$ is the structure identifying $\boldsymbol{0}$ and $\boldsymbol{c}$, along the line between $\boldsymbol{0}$ and $\boldsymbol{t}$. Note that the fundamental region of the SWNT with the chiral index $\boldsymbol{c}$ is the rectangle with vertices $\boldsymbol{0}$, $\boldsymbol{t}$, $\boldsymbol{t} + \boldsymbol{c}$, and $\boldsymbol{c}$. The diameter of a SWNT with chiral index $\boldsymbol{c} = (c_1, c_2)$ is $L = \sqrt{c_1^2 + c_1c_2 + c_2^2}$.

Recently, there are several research composing a SWNT with short length using organic chemistry (see for example [26]), and hence an index measuring the length of SWNTs is needed. Matsuno–Naito–Hitosugi–Sato–Kotani–Isobe propose such an index, which is called the *length index* of SWNT [26]:

$$\text{(A.6)} \qquad \frac{\sqrt{3}|c_1(a_1 - b_1) - c_2(a_2 - b_1)|}{2\sqrt{c_1^2 + c_1c_2 + c_2^2}},$$

with edge atoms coordinates (a_1, b_1) and (a_2, b_1). The index (A.6) measures how many benzene rings (hexagons) are in the length direction.

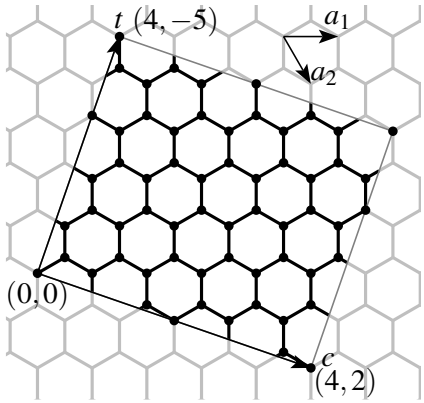

Figure A.6: Construction of a SWNT from a regular hexagonal lattice

SWNTs with $c_1 = c_2$ are called *zigzag type*, $c_2 = 0$ are called *armchair type*, and otherwise are called *chiral type*. These names come from shape of edges of SWNTs (see Fig. A.7).

(a) (b) (c)

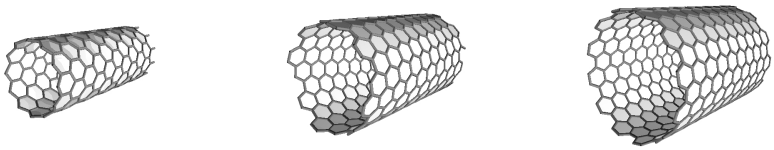

Figure A.7: (a) A zigzag type ($\boldsymbol{c} = (12, 0)$), (b) a chiral type ($\boldsymbol{c} = (12, 8)$), (c) an armchair type ($\boldsymbol{c} = (12, 12)$).

Electronic properties of SWNTs are also geometric. The following result is well-known, and is obtained by tight binding approximations. If $c_1 \equiv c_2 \pmod 3$, then SWNTs with $\boldsymbol{c} = (c_1, c_2)$ are metallic, if not, then such SWNTs are semiconductors.

Acknowledgement

This note is based on lectures in "Introductory Workshop on Discrete Differential Geometry" at Korea University on January 21–24, 2019. The author greatly thanks to organizers of the workshop, and hospitality of Korea University. The author thanks to Mr. Tomoya NAITO (Department of Physics, The University of Tokyo), who calculates Figures A.3, A.4, and A.5 by Density Functional Theory by using OpenMX [23, 32–34] and read my manuscript and give the author valuable comments. The author also thanks to Professor Motoko KOTANI (AIMR, Tohoku University) and Dr. Shintaro AKAMINE (Graduate School of Mathematics, Nagoya University), who read my manuscript and give the author valuable comments. This work is partially supported by KAKENHI 17H06466.

References

[1] A. V. Aho, J. E. Hopcroft, and J. D. Ullman. *The design and analysis of computer algorithms*. Reading, Mass.-London-Amsterdam: Addison-Wesley Publishing Co., 1975. x+470.

[2] Australian National University. *The EPINET Project*. URL: http://epinet.anu.edu.au.

[3] J. A. Bondy and U. S. R. Murty. *Graph theory*. Vol. 244. Graduate Texts in Mathematics. New York: Springer, 2008. xii+651. DOI: 10.1007/978-1-84628-970-5.

[4] D. Cvetković, P. Rowlinson, and S. Simić. *An introduction to the theory of graph spectra*. Vol. 75. London Mathematical Society Student Texts. Cambridge: Cambridge University Press, 2010. xii+364.

[5] G. Davidoff, P. Sarnak, and A. Valette. *Elementary number theory, group theory, and Ramanujan graphs*. Vol. 55. London Mathematical Society Student Texts. Cambridge: Cambridge University Press, 2003. x+144. DOI: 10.1017/CBO9780511615825.

[6] O. Delgado-Friedrichs and M. O'Keeffe. Identification of and symmetry computation for crystal nets. *Acta Cryst. A* **59**(4): 351–360, 2003. DOI: 10.1107/S0108767303012017.

[7] M. Deza and M. Dutour Sikirić. *Geometry of chemical graphs: polycycles and two-faced maps*. Vol. 119. Encyclopedia of Mathematics and its Applications. Cambridge: Cambridge University Press, 2008. x+306. DOI: 10.1017/CBO9780511721311.

[8] M. Dutour and M. Deza. Goldberg-Coxeter construction for 3- and 4-valent plane graphs. *Electron. J. Combin.* **11**(1): Research Paper 20, 49, 2004. DOI: 10.37236/1773.

[9] J. Eells Jr. and J. H. Sampson. Harmonic mappings of Riemannian manifolds. *Amer. J. Math.* **86**: 109–160, 1964. DOI: 10.2307/2373037.

[10] D. Fujita, Y. Ueda, S. Sato, N. Mizuno, T. Kumasaka, and M. Fujita. Self-assembly of tetravalent Goldberg polyhedra from 144 small components. *Nature* **540**(7634): 563–566, 2016. DOI: 10.1038/nature20771.

[11] M. Goldberg. A class of multi-symmetric polyhedra. *Tohoku Math. J.* **43**: 104–108, 1937.

[12] Y. Higuchi and T. Shirai. Some spectral and geometric properties for infinite graphs. In: *Discrete geometric analysis*. M. Kotani, T. Shirai, and T. Sunada (Eds.). Vol. 347. Contemp. Math. Providence, RI: Amer. Math. Soc., 2004, 29–56. DOI: 10.1090/conm/347/06265.

[13] M. Itoh, M. Kotani, H. Naito, T. Sunada, Y. Kawazoe, and T. Adschiri. New metallic carbon crystal. *Phys. Rev. Lett.* **102**(5): 055703, 2009. DOI: 10.1103/PhysRevLett.102.055703.

[14] T. Kajigaya and R. Tanaka. Uniformizing surfaces via discrete harmonic maps, 2019. arXiv: 1905.05427 [math].

[15] K. Kawasumi, Q. Zhang, Y. Segawa, L. T. Scott, and K. Itami. A grossly warped nanographene and the consequences of multiple odd-membered-ring defects. *Nature Chem* **5**(9): 739–744, 2013. DOI: 10.1038/nchem.1704.

[16] M. Kotani, H. Naito, and T. Omori. A discrete surface theory. *Comput. Aided Geom. Design* **58**: 24–54, 2017. DOI: 10.1016/j.cagd.2017.09.002.

[17] M. Kotani, H. Naito, and C. Tao. Construction of continuum from a discrete surface by its iterated subdivisions, 2018. arXiv: 1806.03531 [math].

[18] M. Kotani and T. Sunada. A central limit theorem for the simple random walk on a crystal lattice. In: *Proceedings of the Second ISAAC Congress, Vol. 1 (Fukuoka, 1999)*. H. G. W. Begehr, R. P. Gilbert, and J. Kajiwara (Eds.). Vol. 7. Int. Soc. Anal. Appl. Comput. Dordrecht: Kluwer Acad. Publ., 2000, 1–6. DOI: 10.1007/978-1-4613-0269-8_1.

[19] M. Kotani and T. Sunada. Albanese maps and off diagonal long time asymptotics for the heat kernel. *Comm. Math. Phys.* **209**(3): 633–670, 2000. DOI: 10.1007/s002200050033.

[20] M. Kotani and T. Sunada. Jacobian tori associated with a finite graph and its abelian covering graphs. *Adv. in Appl. Math.* **24**(2): 89–110, 2000. DOI: 10.1006/aama.1999.0672.

[21] M. Kotani and T. Sunada. Spectral geometry of crystal lattices. In: *Heat kernels and analysis on manifolds, graphs, and metric spaces (Paris, 2002)*. P. Auscher, T. Coulhon, and A. Grigor'yan (Eds.). Vol. 338. Contemp. Math. Providence, RI: Amer. Math. Soc., 2003, 271–305. DOI: 10.1090/conm/338/06077.

[22] M. Kotani and T. Sunada. Standard realizations of crystal lattices via harmonic maps. *Trans. Amer. Math. Soc.* **353**(1): 1–20, 2001. DOI: 10.1090/S0002-9947-00-02632-5.

[23] K. Lejaeghere et al. Reproducibility in density functional theory calculations of solids. *Science* **351**(6280), 2016. DOI: 10.1126/science.aad3000. pmid: 27013736.

[24] T. Lenosky, X. Gonze, M. Teter, and V. Elser. Energetics of negatively curved graphitic carbon. *Nature* **355**(6358): 333–335, 1992. DOI: 10.1038/355333a0.

[25] A. L. Mackay and H. Terrones. Diamond from graphite. *Nature* **352**(6338): 762–762, 1991. DOI: 10.1038/352762a0.

[26] T. Matsuno, H. Naito, S. Hitosugi, S. Sato, M. Kotani, and H. Isobe. Geometric measures of finite carbon nanotube molecules: a proposal for length index and filling indexes. *Pure Appl. Chem.* **86**(4): 489–495, 2014. DOI: 10.1515/pac-2014-5006.

[27] A. Mizuno, Y. Shuku, M. M. Matsushita, M. Tsuchiizu, Y. Hara, N. Wada, Y. Shimizu, and K. Awaga. 3D spin-liquid state in an organic hyperkagome lattice of Mott dimers. *Phys. Rev. Lett.* **119**(5): 057201, 2017. DOI: 10.1103/PhysRevLett.119.057201.

[28] H. Naito. Visualization of standard realized crystal lattices. In: *Spectral analysis in geometry and number theory*. M. Kotani, H. Naito, and T. Tate (Eds.). Vol. 484. Contemp. Math. Providence, RI: Amer. Math. Soc., 2009, 153–164. DOI: 10.1090/conm/484/09472.

[29] H. Naito, Y. Nishiura, and M. Kotani. Construction of negatively curved cubic carbon crystals via standard realizations. In: *Mathematical challenges in a new phase of materials science*. Vol. 166. Springer Proc. Math. Stat. Tokyo: Springer, 2016, 83–100. DOI: 10.1007/978-4-431-56104-0_5.

[30] M. O'Keeffe and B. G. Hyde. Plane nets in crystal chemistry. *Philos. Trans. Roy. Soc. London Ser. A* **295**(1417): 553–618, 1980. DOI: 10.1098/rsta.1980.0150.

[31] T. Omori, H. Naito, and T. Tate. Eigenvalues of the Laplacian on the Goldberg-Coxeter constructions for 3- and 4-valent graphs. *Electron. J. Combin.* **26**(3): Paper 3.7, 31, 2019. DOI: 10.37236/8481.

[32] T. Ozaki. Variationally optimized atomic orbitals for large-scale electronic structures. *Phys. Rev. B* **67**(15): 155108, 2003. DOI: 10.1103/PhysRevB.67.155108.

[33] T. Ozaki and H. Kino. Efficient projector expansion for the ab initio LCAO method. *Phys. Rev. B* **72**(4): 045121, 2005. DOI: 10.1103/PhysRevB.72.045121.

[34] T. Ozaki and H. Kino. Numerical atomic basis orbitals from H to Kr. *Phys. Rev. B* **69**(19): 195113, 2004. DOI: 10.1103/PhysRevB.69.195113.

[35] K. B. Petersen and M. S. Pedersen. The matrix cookbook. URL: https://www.math.uwaterloo.ca/~hwolkowi/matrixcookbook.pdf.

[36] I. M. Singer and J. A. Thorpe. *Lecture notes on elementary topology and geometry*. Glenview, Ill.: Scott, Foresman and Co., 1967. v+214.

[37] T. Sunada. Crystals that nature might miss creating. *Notices Amer. Math. Soc.* **55**(2): 208–215, 2008.

[38] T. Sunada. Lecture on topological crystallography. *Jpn. J. Math.* **7**(1): 1–39, 2012. DOI: 10.1007/s11537-012-1144-4.

[39] T. Sunada. *Topological crystallography.* Vol. 6. Surveys and Tutorials in the Applied Mathematical Sciences. Tokyo: Springer, 2013. xii+229. DOI: 10.1007/978-4-431-54177-6.

[40] M. Tagami, Y. Liang, H. Naito, Y. Kawazoe, and M. Kotani. Negatively curved cubic carbon crystals with octahedral symmetry. *Carbon* **76**: 266–274, 2014. DOI: 10.1016/j.carbon.2014.04.077.

[41] C. Tao. A construction of converging Goldberg-Coxeter subdivisions of a discrete surface. Preprint.

[42] M. Tsuchiizu. Three-dimensional higher-spin Dirac and Weyl dispersions in the strongly isotropic K_4 crystal. *Phys. Rev. B* **94**(19): 195426, 2016. DOI: 10.1103/PhysRevB.94.195426.

[43] S. Zhang, J. Zhou, Q. Wang, X. Chen, Y. Kawazoe, and P. Jena. Penta-graphene: A new carbon allotrope. *PNAS* **112**(8): 2372–2377, 2015. DOI: 10.1073/pnas.1416591112. pmid: 25646451.